

**Rearrangements of Radical Anions
Generated from Cyclopropyl Ketones**

By

Janice Paige Phillips

Dissertation submitted to the Faculty of the Virginia Polytechnic Institute
and State University in partial fulfillment of the requirement for the degree of

Doctor of Philosophy

In

Chemistry

James M. Tanko, Chairman

Karen J. Brewer

Neal Castagnoli, Jr.

Mark R. Anderson

Harry W. Gibson

James F. Wolfe

October, 1998

Blacksburg, Virginia

Key words: Radical anion, Ring opening, Cathodic reduction, Homogeneous catalysis,
Marcus theory, Voltammetry, Cyclopropyl ketones, Reaction mechanism and kinetics

Copyright 1998, Janice Paige Phillips

Rearrangements of Radical Anions Generated from Cyclopropyl Ketones

By

Janice Paige Phillips

James M. Tanko, Chairman

Chemistry

(ABSTRACT)

Cyclopropyl-containing substrates have been frequently utilized as “probes” for the detection of SET pathways in organic and biorganic systems. These reactions are based on the cyclopropylcarbinyl \rightarrow homoallyl rearrangement, which is fast and essentially irreversible. The implicit assumption in such studies is that if a “radical” species is produced, it will undergo ring opening. We have found that there are two important factors to consider in the design of SET probes: 1) ring strain, the thermodynamic driving force for the rearrangement, and 2) resonance energy, which may help or hinder rearrangement, depending on the specific system. Delocalization of spin and charge were found to be important factors pertaining to substituent effects on the rates of radical anion rearrangements.

Previous studies from our lab have centered on highly conjugated phenyl cyclopropyl ketones. This work considers a series of compounds varying in their conjugative components from a highly conjugated spiro[2.5]octa-4,7-dien-6-one and derivatives to simple aliphatic ketones. Utilizing cyclic, linear sweep voltammetry, and preparative electrolysis techniques, it was discovered that all substrates yielded ring

opened products with rates and selectivities that will prove useful and informative in the design of mechanistic probes based on the cyclopropylcarbinyl \rightarrow homoallyl rearrangement. Rates of homogeneous electron transfer from a series of hydrocarbon mediators to substrates were measured using homogeneous catalysis techniques. Standard reduction potentials and reorganization energies of substrates were derived using Marcus theory. Conjugative interactions with the cyclopropyl group are discussed.

ACKNOWLEDGEMENTS

I would like to express my sincere gratitude to all those individuals who helped with this manuscript. This is an impossible task. Without the combined efforts and support of an enormous number of people (each present at the precise moment in time that I needed them most) none of this would have been possible.

First, I thank Professor James M. Tanko for his guidance and unwavering support over these past few years. You were my advisor when I needed instruction and direction, and my friend when I needed the strength and support to go on. A warm and heartfelt thanks is extended to Mrs. Linda Tanko for welcoming me into her home on many occasions over the years and the encouraging pep-talks she always provided. I also want to thank my committee members: Professors K. Brewer, N. Castagnoli, J. Wolfe, M. Anderson, and H. Gibson for their essential instruction and critical reviews of my work. I have made many friends at Virginia Tech (Sue, Beth, Jason, Larry, and many more . . .), and I thank you all for helping me to get from day to day.

Secondly, I wish to thank the faculty members of Roanoke College who instilled in me my love of chemistry and desire for excellence. A special thanks is extended to Professors J. Muzyka and V. Miller who provided such interesting undergraduate research projects that it was inevitable that I continue on and pursue graduate research.

Finally, I want to thank my family (mother, father, sisters, brothers, uncles etc . . .) for their spiritual and emotional support. I especially thank my husband, Randy, for his love and understanding. I thank my children, Logan and Mason, for their love and for reminding me of what is truly important in life.

TABLE OF CONTENTS

Chapter 1. Historical	1
1.1 Introduction	1
1.1.1 Overview	1
1.1.2 Generation, reactions, and detection of radical anions from >C=O containing compounds.....	4
1.1.3 Fragmentation probes.....	7
1.1.4 Rearrangement probes.....	10
1.2 Background	13
1.3 Dissertation description.....	16
Chapter 2. Cathodic reduction of 5,7-Di-<i>t</i>-butyl[2.5]octa-4,7-diene-6-one and derivatives (13(a-c)).....	19
2.1 Introduction	19
2.2 Results and discussion	22
2.2.1 Direct electrochemical reduction of 13(a-c)	22
2.2.2 Product analysis from preparative electrolysis of 13(a-c)	29
2.2.3 Indirect electrochemistry of 13(a-c)	34
2.2.4 Estimates of the reduction potentials of 13(a-c) using Marcus theory ...	41
2.2.5 Thermodynamics of ring opening for 13(a-c)^{•-}	48
2.3 Conclusions	51

2.4 Graphical analysis and supplemental plots	52
Chapter 3. Cathodic reduction of cyclic aliphatic ketones: Cyclopropyl methyl ketone (14a), 1-acyl-2,2-dimethyl cyclopropane (14b) and cyclobutyl methyl ketone (29).....	70
3.1 Introduction	70
3.2 Results and discussion	74
3.2.1 Direct electrochemical reduction of 14(a,b)	74
3.2.2 Product analysis from preparative electrolysis of 14(a,b)	75
3.2.3 Indirect electrochemistry of 14(a,b)	79
3.2.4 Estimates of the reduction potentials of 14(a,b) using Marcus theory .	84
3.2.5 Product analysis from preparative electrolysis of 29	91
3.2.6 Indirect electrochemistry of 29	91
3.2.7 Thermodynamics of ring opening for 14(a,b)^{•-} and 29^{•-}	102
3.3 Conclusions	105
3.4 Graphical analysis and supplemental plots	107
Chapter 4. Cathodic reduction of 3-cyclopropyl-cyclohex-2-ene-1-one (15).....	122
4.1 Introduction	122
4.2 Results and discussion	125
4.2.1 Direct electrochemical reduction of 15	125
4.2.2 Product analysis from preparative electrolysis of 15	130
4.2.3 Indirect electrochemistry of 15	132
4.3 Conclusions	138

Chapter 5. Conclusions	140
Chapter 6. Experimental.....	141
6.1 General.....	141
6.1.1 Instrumentation description	141
6.1.2 Electrochemical measurements.....	141
6.1.3 Digital simulations	144
6.1.4 Materials and purification.....	145
6.2 Electrolysis	146
6.2.1 Electrolysis (specific).....	146
6.2.2 Spectroscopic data.....	148
Literature cited.....	151
Vita.....	158

LIST OF FIGURES

Figure 1.1. Generation of $>\text{C}=\text{O}^{\bullet-}$ in solution	4
Figure 1.2. Reactions of $>\text{C}=\text{O}^{\bullet-}$	6
Figure 1.3. Intramolecular rearrangement probes used to detect electron transfer	11
Figure 1.4. Ring opening rearrangements of selected radical anions.....	18
Figure 2.1. Cyclic voltammograms of 13a , 13b , and 13c in DMF.....	22
Figure 2.2. LSV analysis of 13a , $\partial E_p/\partial \log v$	24
Figure 2.3. LSV analysis of 13b , $\partial E_p/\partial \log v$	24
Figure 2.4. LSV analysis of 13c , $\partial E_p/\partial \log v$	24
Figure 2.5. LSV analysis of 13(a-c) , $\partial E_p/\partial \log C_A$	25
Figure 2.6. Significance of α	28
Figure 2.7. Mediated reduction of 13a by 4-cyanopyridine	38
Figure 2.8. Marcus curve for electron transfer.....	43
Figure 2.9. Log k as a function of the reduction potential of the mediator	45
Figure 2.10. E_{AB}° and λ derived from fit of log rate constant data to Eq. 2.11	46
Figure 2.11. Mediated reduction of 13c with 9,10-diphenylanthracene.....	52
Figure 2.12. Non-linear fitting of results for 13c + 9,10-diphenylanthracene.....	52
Figure 2.13. Mediated reduction of 13c with 4-cyanopyridine.....	53
Figure 2.14. Non-linear fitting of results for 13c + 4-cyanopyridine.....	53
Figure 2.15. Mediated reduction of 13c with 1-cyanonaphthalene.....	54
Figure 2.16. Non-linear fitting of results for 13c + 1-cyanonaphthalene.....	54

Figure 2.17. Mediated reduction of 13c with fluoranthene	55
Figure 2.18. Non-linear fitting of results for 13c + fluoranthene.....	55
Figure 2.19. Mediated reduction of 13c with 9-phenylanthracene	56
Figure 2.20. Non-linear fitting of results for 13c + 9-phenylanthracene.....	56
Figure 2.21. Mediated reduction of 13b with 9-phenylanthracene	57
Figure 2.22. Non-linear fitting of results for 13b + 9-phenylanthracene	57
Figure 2.23. Mediated reduction of 13b with 9,10-diphenylanthracene	58
Figure 2.24. Non-linear fitting of results for 13b + 9,10-diphenylanthracene	58
Figure 2.25. Mediated reduction of 13b with anthracene.....	59
Figure 2.26. Non-linear fitting of results for 13b + anthracene.....	59
Figure 2.27. Mediated reduction of 13b with cyanonaphthalene.....	60
Figure 2.28. Non-linear fitting of results for 13b + cyanonaphthalene.....	60
Figure 2.29. Mediated reduction of 13b with 4-cyanopyridine	61
Figure 2.30. Non-linear fitting of results for 13b + 4-cyanopyridine	61
Figure 2.31. Mediated reduction of 13b with fluoranthene.....	62
Figure 2.32. Non-linear fitting of results for 13b + fluoranthene	62
Figure 2.33. Mediated reduction of 13b with 9-methylanthracene.....	63
Figure 2.34. Non-linear fitting of results for 13b + 9-methylanthracene	63
Figure 2.35. Mediated reduction of 13a with 1-cyanonaphthalene.....	64
Figure 2.36. Non-linear fitting of results for 13a + 1-cyanonaphthalene.....	64
Figure 2.37. Mediated reduction of 13a with 9-methylanthracene	65
Figure 2.38. Non-linear fitting of results for 13a + 9-methylanthracene	65
Figure 2.39. Mediated reduction of 13a with 9-phenylanthracene	66

Figure 2.40. Non-linear fitting of results for 13a + 9-phenylanthracene	66
Figure 2.41. Mediated reduction of 13a with 9,10-diphenylanthracene	67
Figure 2.42. Non-linear fitting of results for 13a + 9,10-diphenylanthracene.....	67
Figure 2.43. Mediated reduction of 13a with anthracene	68
Figure 2.44. Non-linear fitting of results for 13a + anthracene	68
Figure 3.1. Walsh orbital overlap for cyclopropyl methyl ketone	71
Figure 3.2. Cyclic voltammogram of 14a in DMF.....	75
Figure 3.3. Catalytic reduction of 14a by biphenyl radical anion.....	80
Figure 3.4. Mediated reduction of 14a by naphthalene	82
Figure 3.5. Log k_1 as a function of the reduction potential of the mediator.....	86
Figure 3.6. $E_{A/B}^{\circ}$ and λ derived from fit of log rate constant data to Eq. 2.11	87
Figure 3.7(a). Mediated reduction of 29 by naphthalene.....	92
Figure 3.7(b). Mediated reduction of 29 by biphenyl.....	93
Figure 3.8. Mediated reduction of 29 by 2-methoxybiphenyl	99
Figure 3.9. Mediated reduction of 29 by 2-methoxybiphenyl (rate limiting ET)	101
Figure 3.10. Apparent rate constant dependence on mediator concentration for the reduction of 29 by 2-methoxybiphenyl	102
Figure 3.11. Mediated reduction of 14a with 3,6-dimethylphenanthrene	107
Figure 3.12. Non-linear fitting of results for 14a + 3,6-dimethylphenanthrene	107
Figure 3.13. Mediated reduction of 14a with 2,7-dimethoxynaphthalene	108
Figure 3.14. Non-linear fitting of results for 14a + 2,7-dimethoxynaphthalene.....	108
Figure 3.15. Mediated reduction of 14a with 1,3-dimethylnaphthalene	109
Figure 3.16. Non-linear fitting of results for 14a + 1,3-dimethylnaphthalene	109

Figure 3.17. Mediated reduction of 14a with 2-methoxybiphenyl.....	110
Figure 3.18. Non-linear fitting results for 14a + 2-methoxybiphenyl.....	110
Figure 3.19. Mediated reduction of 14a with methoxynaphthalene.....	111
Figure 3.20. Non-linear fitting of results for 14a + methoxynaphthalene.....	111
Figure 3.21. Mediated reduction of 14a with biphenyl.....	112
Figure 3.22. Non-linear fitting of results for 14a + biphenyl.....	112
Figure 3.23. Mediated reduction of 14b with 1,3-dimethylnaphthalene.....	113
Figure 3.24. Non-linear fitting results for 14b + 1,3-dimethylnaphthalene.....	113
Figure 3.25. Mediated reduction of 14b with 2,7-dimethoxynaphthalene.....	114
Figure 3.26. Non-linear fitting of results for 14b + 2,7-dimethoxynaphthalene.....	114
Figure 3.27. Mediated reduction of 14b with 3,6-dimethylphenanthrene.....	115
Figure 3.28. Non-linear fitting of results for 14b + 3,6-dimethylphenanthrene.....	115
Figure 3.29. Mediated reduction of 14b with 2-methoxybiphenyl.....	116
Figure 3.30. Non-linear fitting of results for 14b + 2-methoxybiphenyl.....	116
Figure 3.31. Mediated reduction of 14b with methoxynaphthalene.....	117
Figure 3.32. Non-linear fitting of results for 14b + methoxynaphthalene.....	117
Figure 3.33. Mediated reduction of 14b with naphthalene.....	118
Figure 3.34. Non-linear fitting of results for 14b + naphthalene.....	118
Figure 3.35. Mediated reduction of 14b with biphenyl.....	119
Figure 3.36. Non-linear fitting of results for 14b + biphenyl.....	119
Figure 3.37. ¹ H NMR (CHCl ₃) of adduct formation in preparative electrolysis of 14a	120
Figure 3.38. ¹ H NMR (CHCl ₃) of adduct formation in preparative electrolysis	

of 29	121
Figure 4.1 Resonance forms of α,β -unsaturated ketones	122
Figure 4.2. Cyclic voltammogram of 15 in DMF	126
Figure 4.3. LSV analysis of 15 (0.0015 M), $\partial E_p/\partial \log v$	127
Figure 4.4. LSV analysis of 15 (0.0029 M), $\partial E_p/\partial \log v$	127
Figure 4.5. LSV analysis of 15 (0.0059 M), $\partial E_p/\partial \log v$	128
Figure 4.6. LSV analysis of 15 , $\partial E_p/\partial \log C_A$	128
Figure 4.7. Mediated reduction of 15 by anthracene.....	134
Figure 4.8. Mediated reduction of 15 by 9-methylanthracene.....	135

LIST OF TABLES

Table 1.1. Rate constants for β -cleavage of several substituted acetophenones and benzophenones	10
Table 2.1. LSV analysis of 13(a-c)	27
Table 2.2. Rate constants for homogeneous electron transfer between the reduced form of the mediator and 13(a-c)	41
Table 2.3. Reduction potentials and reorganization energies for 13(a-c)	47
Table 2.4. Estimated ΔG° for ring opening of 13(a-c)^{•-}	50
Table 2.5. Comparison of experimental vs. calculated heats of formation of several cyclopropyl-containing compounds	69
Table 2.6. Calculated BDE(C-C) based upon Scheme 2.13	69
Table 3.1 AM1-calculated enthalpies of reaction for the ring opening of 14(a,b) and 29	79
Table 3.2. Rate constants for homogeneous electron transfer between the reduced form of the mediator and 14(a,b)	83
Table 3.3. Comparison of ρ values obtained in this study to literature values for 1° and 3° radicals	83
Table 3.4. Reduction potentials and reorganization energies for 14(a,b) derived from Marcus theory	88
Table 3.5. Rate constants for cyclobutane ring opening of 29	96
Table 3.6. Effect of substituents on the rate of ring opening of cyclopropyl- and cyclobutylcarbinyl radicals and their related radical anions	97

Table 3.7. Calculated BDE(C-C) based upon Scheme 3.7.	104
Table 3.8. Estimated ΔG° for ring opening of 14(a,b) and 29	105
Table 4.1. LSV analysis of 3-cyclopropyl-cyclohex-2-enone (15).....	129
Table 4.2. Rate constants for homogeneous electron transfer between the reduced form of the mediator and 15	136
Table 4.3. Standard reduction potentials of mediators	137

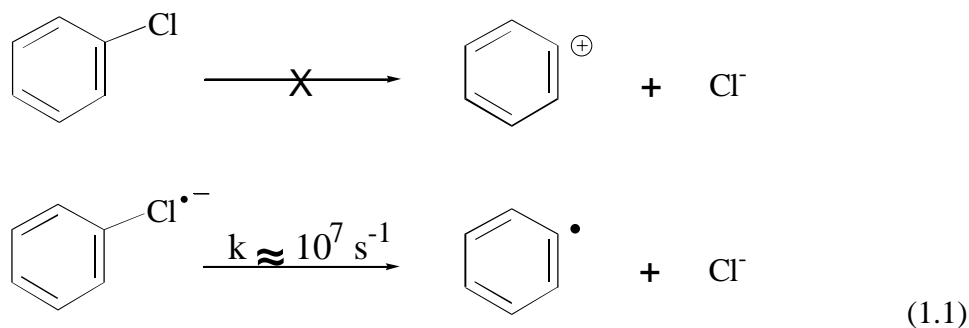
CHAPTER 1: HISTORICAL

1.1 INTRODUCTION

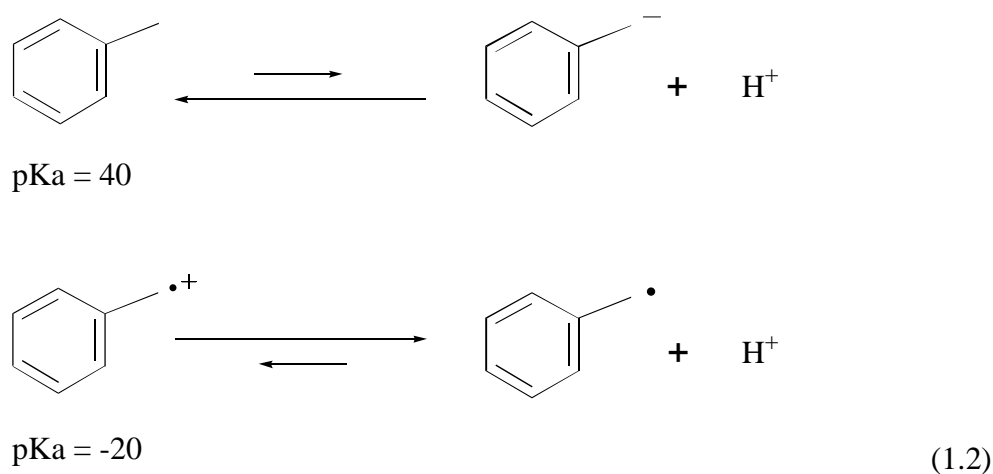
1.1.1 Overview

A tremendous amount of interest in mechanistic organic chemistry has been sparked by the recognition of single electron transfer (SET) as an important reaction pathway. Single electron transfer mechanisms involve paramagnetic intermediates, free radicals, radical cations and radical anions. The chemistry of the neutral free radical is well understood. However, the chemistry of radical ions is not as extensively documented. A radical cation is formed by the removal of an electron from a neutral diamagnetic species (e.g., $M - e^- \rightarrow M^{\bullet+}$). In contrast, a radical anion results from the addition of an electron (e.g., $M + e^- \rightarrow M^{\bullet-}$). Hence, radical ions are formed by oxidation/reduction of neutral closed-shell substrates. This change in oxidation state can drastically affect a substrate's reactivity. Enhanced reactivity stems from the diminution of bond orders in the molecule as a consequence of removing electrons from bonding orbitals or adding electrons to anti-bonding orbitals, and from the introduction of charge.

As a result, radical ions are much more reactive than their corresponding neutral species. For example, neutral chlorobenzene is a stable molecule, which is not prone to homo- or heterolytic C-Cl bond cleavage. However, chlorobenzene decomposes rapidly to phenyl radical and chloride ion when reduced to its radical anion (Equation 1.1).¹



Similarly, neutral toluene is an extremely weak acid with a pKa of ~ 40 .² The radical cation of toluene becomes remarkably more acidic with a pKa of -20 (Equation 1.2).^{3,4}

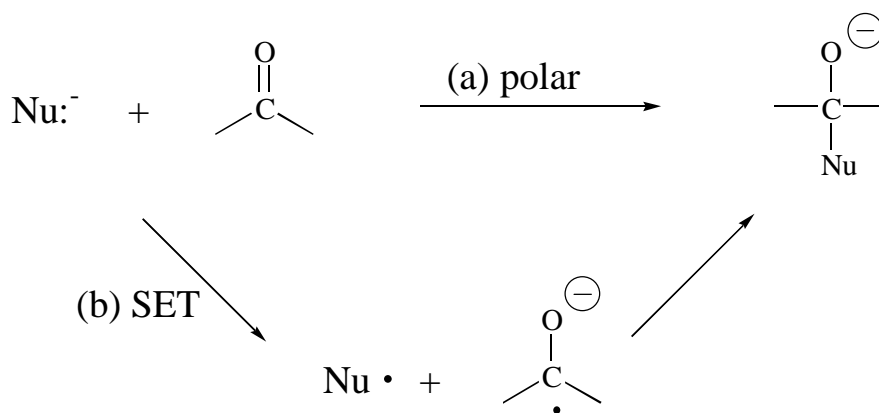


With recognition of the importance of SET mechanisms emerging, reactions previously thought to proceed exclusively through conventional polar intermediates are now thought to involve some component of SET. The role of electron transfer has been extensively examined in a large number of reactions involving aldehydes, ketones, and other carbonyl compounds. As a result, many of these reactions are now currently thought to proceed through radical ion intermediates (*e.g.*, the Grignard reaction⁵, Clemmenson reduction⁶, aldol condensation⁷, Wittig reaction⁸, Meerwein-Ponndorff-

Verley reduction⁹, reactions involving RLi^{10} , $\text{R}_2\text{NLi}^{11}$, NADH analogues¹², complex metal hydrides¹³ and radical mediated reductions involving $\text{R}_3\text{Sn}\bullet^{14}$ and $\text{R}_3\text{Si}\bullet^{15}$.

Consider two possible mechanisms for reaction of a nucleophile (Nu^-) and a carbonyl compound (Scheme 1.1): a) a polar (two electron) process, and b) a single electron transfer process (SET).

Scheme 1.1



Detection of SET pathways (path b) by product analysis is not simple as usually the same products are produced regardless of the pathway taken (polar or SET). The unique characteristic of the SET mechanism is the formation of paramagnetic intermediates (free radicals and radical anions). Consequently, experiments must be designed which exploit this difference.

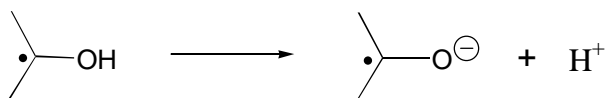
1.1.2 Generation, reactions, and detection of radical anions from >C=O containing compounds.

A radical anion results from the addition of an electron (e.g., $M + e^- \rightarrow M^{\bullet-}$) to a neutral closed-shell molecule. Common methods for generation of ketyl anions are summarized in Figure 1.1.¹⁶

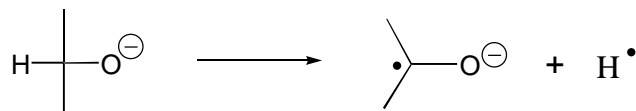
(1) Direct chemical or electrochemical reduction of carbonyl compounds



(2) Deprotonation of ketyl radicals



(3) α -Hydrogen abstraction from alkoxides



(4) Photo-induced electron transfer (PIET)

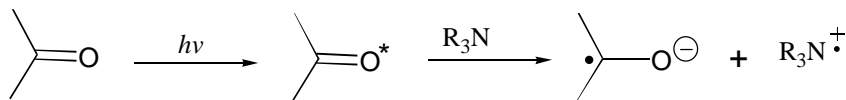


Figure 1.1 Generation of $\text{>C=O}^{\bullet-}$ in solution.

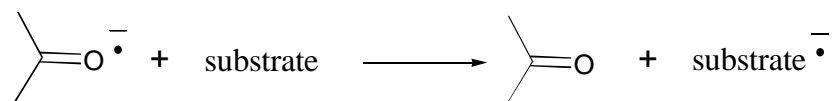
The simplest method of radical anion generation is via direct reduction (Figure 1.1, reaction 1), chemically or electrochemically. A variety of chemical reducing reagents such as alkali metals (*i.e.*, Na/NH₃), stable radical anions, and metals (*i.e.*, R₃Sn[•], SmI₂)

have been employed.^{16,25} Recently, SmI₂ has emerged as a synthetically useful one-electron reducing agent for carbonyl containing compounds.¹⁷

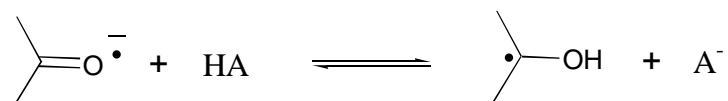
Electrochemical reduction is one of the most important methods to generate radical anions; however, it can be more complicated in terms of the role of the electrode surface, counterion and solvent.¹⁸ Given the proper system, the reduced species is formed at the electrode without the simultaneous formation of the oxidized species in the immediate vicinity. Moreover, because the potential of the electrode can be adjusted precisely, its reducing power can be controlled.

Some examples of the most common reactions of ketyl radical anions are summarized in Figure 1.2.¹⁶ The electron transfer reaction (Figure 1.2, reaction 1) is perhaps the most fundamental and involves electron transfer to another substrate. This mediated reduction has been used extensively in electrochemistry over a wide range of substrates and reactions and is often catalytic. Savéant and Lund are pioneers in this field.¹⁹ Another fundamental reaction of $>C=O^{\bullet-}$ (Figure 1.2, reaction 2) illustrates the basic nature of the radical anion, and can occur when reductions are carried out in protic/acidic media or the radical anion has readily available protons from other substrates in solution (as in PIET). The remaining reactions 3-5 shown in Figure 1.2, represent the bulk of the mechanistic research in the area of radical anions generated from carbonyl containing compounds and an excellent review has appeared.¹⁶

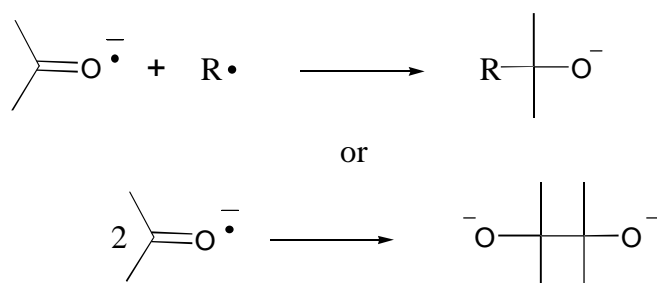
(1) electron transfer



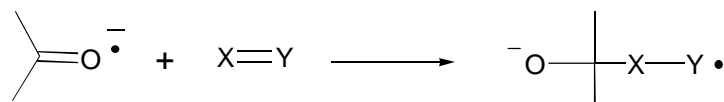
(2) proton transfer



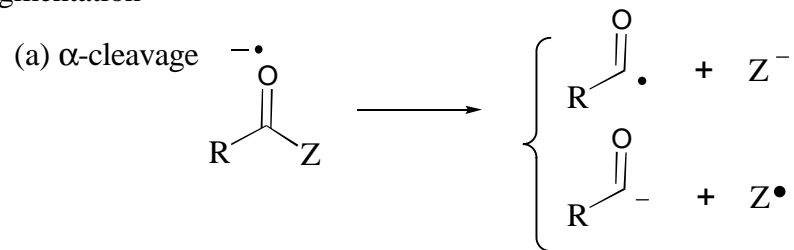
(3) reaction with radicals or radical ions



(4) addition to π -systems



(5) fragmentation



(a) β -cleavage

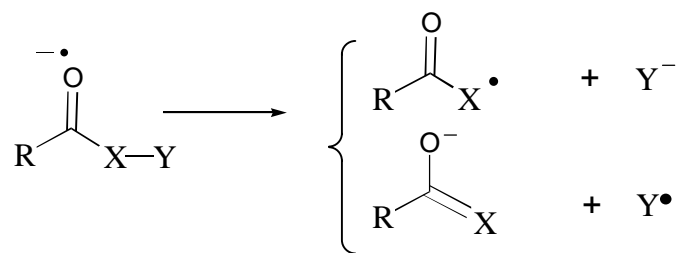


Figure 1.2 Reactions of $>\text{C}=\text{O}^{\bullet-}$

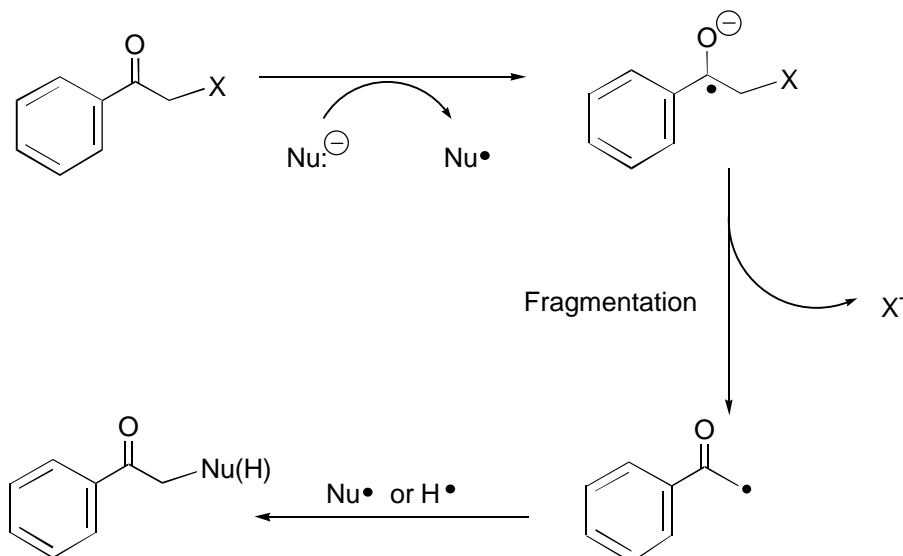
Because of the fleeting nature of radical ions, they can be challenging to detect. Chemically induced dynamic nuclear polarization (CIDNP) has been employed for detection of paramagnetic intermediates in the reactions of alkyl iodides with alkyl lithium reagents.²⁰ Electron paramagnetic resonance spectroscopy (EPR) spectroscopy has proven to be a useful method, and radicals and radical anions can be detected in very low concentrations.^{21,22,23,24} EPR has been used to study SET in additions of hydrides to substituted benzophenones²² and reactions of anions with unsaturated organic molecules.²¹ Other useful methods have included UV absorption,²² trapping by radical scavengers, and kinetic isotope effects.²⁵ Perhaps the most powerful tools for elucidating the mechanisms of radical anion decay are direct and indirect electrochemistry,²⁶ stopped-flow techniques,²⁷ and laser flash photolysis.^{27,28}

Observation of a paramagnetic intermediate does not necessarily mean that the radical/radical anion is involved in product formation.^{7a, 29} To avoid the possibility of monitoring a “blind” pathway, researchers have focused on incorporating mechanistic “probes” into the substrate which will lead to unique products when electron transfer occurs. Mechanistic probes that can be used for detection of SET pathways fall into two main classes, fragmentation and rearrangement probes.

1.1.3 Fragmentation probes.

Fragmentation probes contain substituents which, upon electron transfer, eject stable ions. Identification of SET is then made through product analysis (Scheme 1.2).

Scheme 1.2

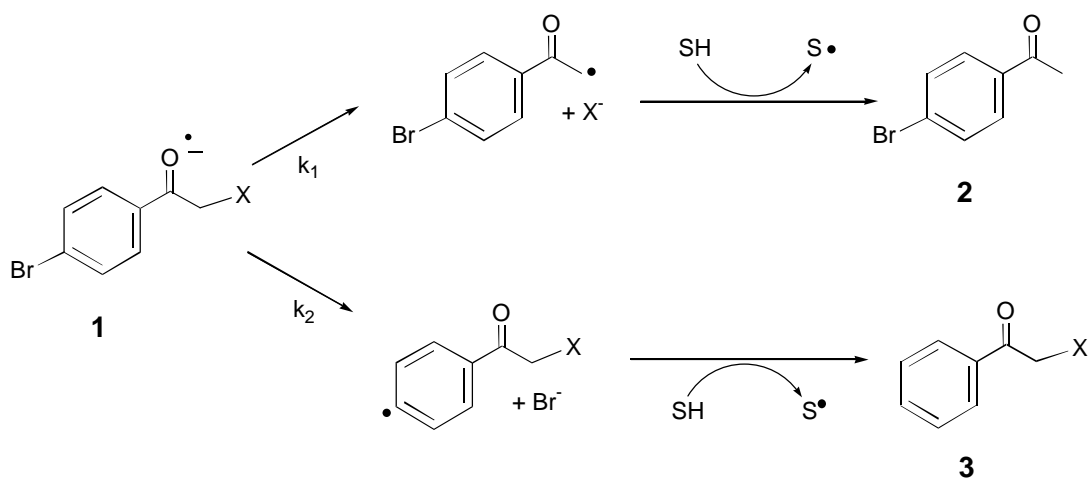


It is presumed that products obtained from a Nu•/neutral radical coupling (ArCOCH₂Nu) or hydrogen atom abstraction (ArCOCH₃) are formed from the radical produced through a SET pathway.^{30,31} However, a direct nucleophilic (S_N2) substitution pathway at the α -carbon can not be discounted as a potential pathway for product (ArCOCH₂Nu) formation. The success of the “fragmentation probe” is dependent on the irreversibility of the fragmentation step and on its rate being faster than any competitive process involving the radical anion.

In an innovative example, Tanner and collaborators have estimated rate constants for fragmentation of a series of α -haloacetophenones.³² Rate constants were determined according to the competition experiment outlined in Scheme 1.3, where radical anion **1** was generated from reaction with 1,3-dimethyl-2-phenylbenzimidazole (DMBI). The rate constant ratio (k_1/k_2) was determined from the relative yields of products **2** and **3**. An

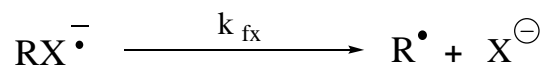
assumption was made that the α -substituent does not affect the magnitude of k_2 , and therefore k_2 could be considered constant and equal to $3 \times 10^7 \text{ s}^{-1}$ (measured earlier by Wipf and Wightman³³).

Scheme 1.3



Pertinent results of these experiments are summarized in Table 1.1. For $\text{X} = \text{Br}$ or Cl , the fragmentation was assumed to occur via dissociative electron transfer (*i.e.*, fragmentation and electron transfer are concerted; the radical anion $\text{Ph}(\text{C}=\text{O}^{\bullet-})\text{CH}_2\text{X}$ does not have a discrete lifetime). Data from this study combined with the findings of other groups have demonstrated that it is possible for a fragmentation probe of this type to identify SET pathways in the reactions of nucleophiles with carbonyl compounds.^{34,35,36,37,38} These fragmentation probes have been successful in detecting SET pathways in reactions of carbonyl compounds with Grignard reagents³⁹ and lithium dialkylcuprates.³⁰

Table 1.1 Rate constants for β -cleavage of several substituted acetophenones and benzophenones.²³



PhCOCH ₂ X ^{•-}		X-C ₆ H ₄ COCH ₃ ^{•-}		X-C ₆ H ₄ COC ₆ H ₅ ^{•-}	
X	k _{fx} (s ⁻¹)	X	k _{fx} (s ⁻¹)	X	k _{fx} (s ⁻¹)
Br	>10 ⁹	<i>m</i> -Cl	15	<i>p</i> -Cl	29
Cl	>10 ⁹	<i>p</i> -Cl	3 x 10 ³	<i>o</i> -Cl	61
F	5.2 x 10 ⁹	<i>o</i> -Cl	3 x 10 ⁵	<i>m</i> -Br	7.9 x 10 ²
PhCO ₂	6.3 x 10 ⁹	<i>m</i> -Br	8 x 10 ³	<i>p</i> -Br	6 x 10 ⁴
CH ₃ CO ₂	9.6 x 10 ⁸	<i>p</i> -Br	3.2 x 10 ⁷	<i>m</i> -I	2.5 x 10 ⁶
PhO	9.5 x 10 ⁶	<i>o</i> -Br	5.1 x 10 ⁹		
PhS	9.3 x 10 ⁶	<i>m</i> -I	1.9 x 10 ⁸		

1.1.4 Rearrangement probes.

A successful rearrangement probe will contain a moiety that upon electron transfer undergoes (ideally) a rapid and irreversible rearrangement. Hence, products obtained from SET vs. polar pathways will be different. Intramolecular rearrangement probes are typically based on geometric (*cis* → *trans*) isomerizations (I), cyclizations involving a remote C=C (II), or the rupture of three- or four-membered rings ((III) in

Figure 1.3).²⁵ Probe substituents (*e.g.*, cyclopropyl groups) have been utilized extensively to detect ketyl and ketyl anion intermediates.^{14,15,30,40}

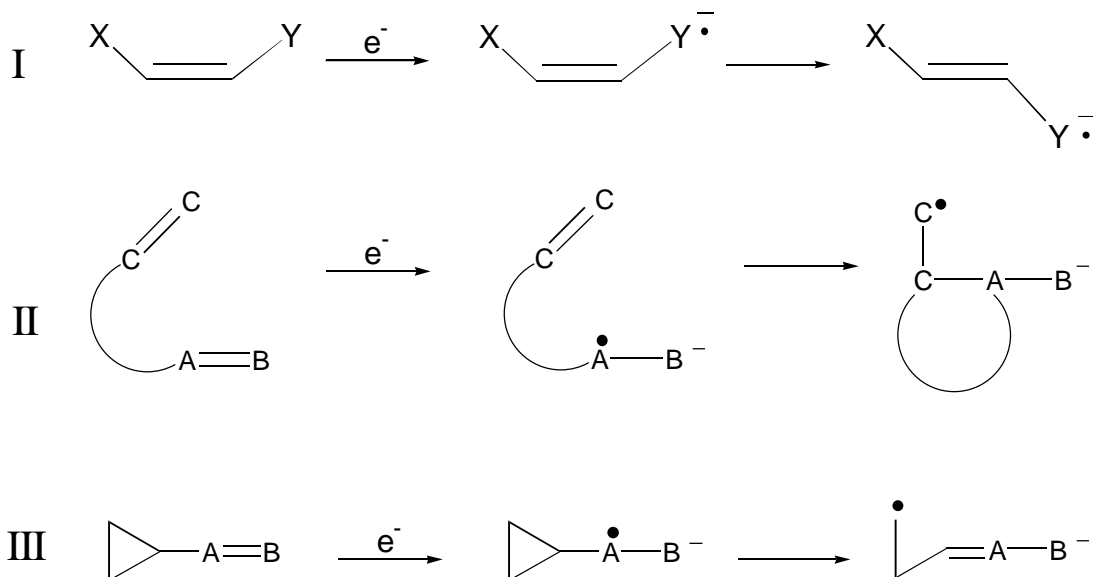


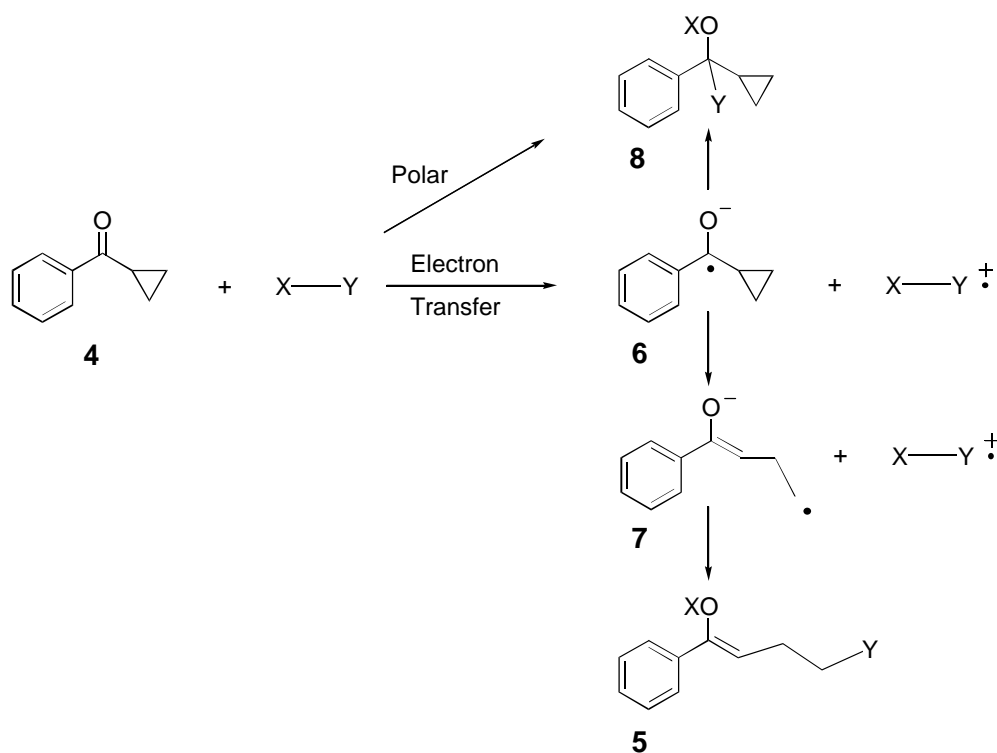
Figure 1.3 Intramolecular rearrangement probes used to detect electron transfer.

In the case of free radicals, rearrangement probes have enjoyed remarkable success because several rearrangements are well-documented,⁴¹ and in some cases their absolute rate constants are known. Griller and Ingold have coined the term “free radical clocks” to describe such rearrangements, because absolute rate constants for competing bimolecular processes can be determined from simple product analyses.⁴²

This level of dependability and sophistication has not yet been attained for radical anion rearrangements. Often it is simply assumed that the same structural features (*e.g.*, relief of cyclopropyl ring strain) which lead to rearrangement of a free radical will (by

analogy) also lead to rearrangement of a radical ion. A case in point involves phenyl cyclopropyl ketone, which has seen extensive use as probe for SET in the reactions of a variety of nucleophiles with carbonyl compounds (Scheme 1.4).^{14,15,30,40(b,c,d,g,i,j,l),43}

Scheme 1.4



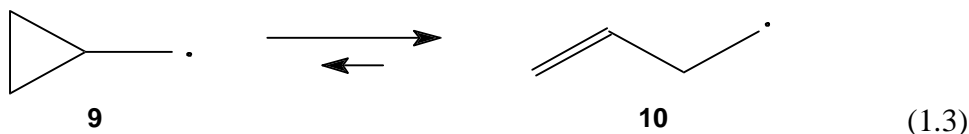
The general procedure is that one takes a reagent (X-Y), which is suspected to undergo SET with carbonyl compounds, and treat it with phenyl cyclopropyl ketone **4**. Ring opened product **5**, if found, supports an electron transfer process through radical anions **6** and **7**. If only ring closed products **8** are obtained, the test is inconclusive, as these products can also be derived: 1) through a traditional polar pathway, or 2) by electron

transfer to give radical anion **6**, and the bimolecular rate of reaction is fast relative to the rate of unimolecular ring opening, **6** → **7**.

1.2 BACKGROUND

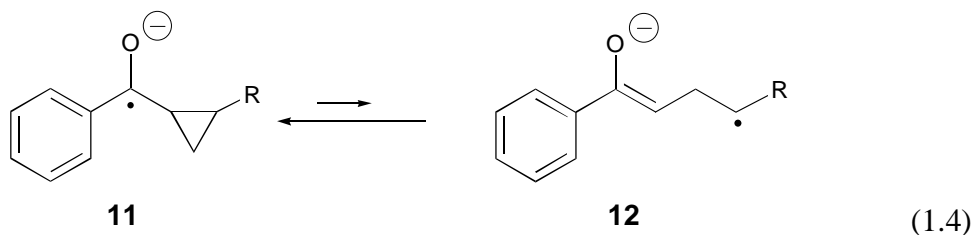
A popular approach for the detection of SET pathways in organic and biorganic systems has been to incorporate functional groups (*i.e.*, probes) into substrates which yield rearranged products that can be uniquely ascribed to a free radical or radical anion. Probe substituents (e.g., cyclopropyl groups) have been utilized extensively to detect ketyl and ketyl anion intermediates.^{14,15,30,40} Incorporation of rearrangeable probes diverts paramagnetic intermediates into different products than would be obtained by a polar pathway, thereby supporting or refuting the contribution of SET to the reaction system.

It is often assumed that the same structural features which lead to rearrangement of a free radical will (by analogy) also lead to rearrangement of a radical anion. In 1990, our lab demonstrated the pitfalls associated with this assumption.⁴⁴ Cyclopropylcarbinyl radical **9** undergoes rapid ($k \approx 10^8 \text{ s}^{-1}$) and irreversible rearrangement to the homoallyl radical **10** (Eq 1.3).⁴⁵



The analogous ring opening of the structurally related phenyl cyclopropyl ketyl anion **11** → **12** (R = H) is nearly eight orders of magnitude slower and reversible with an

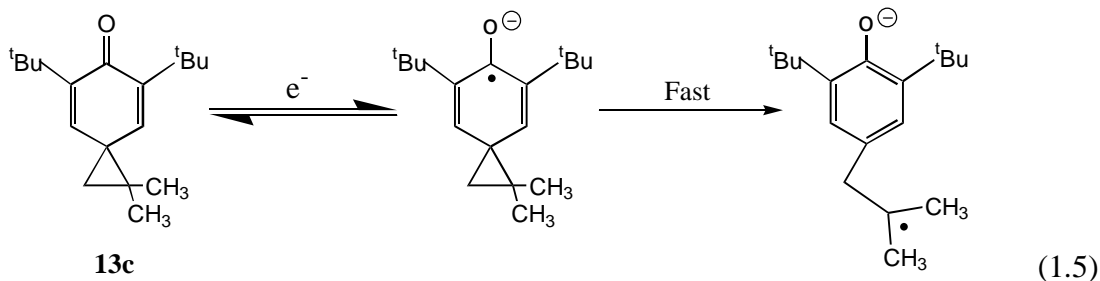
equilibrium constant that favors the ring closed form ($K_{\text{eq}} = 2 \times 10^{-8}$, Eq. 1.4).⁴⁴ As such, phenyl cyclopropyl ketone would fail to detect a *bona fide* SET process.



These findings established that there were two important factors to consider in the design of SET probes based upon the cyclopropylcarbinyl \rightarrow homoallyl rearrangement: a) ring strain, which provides some of the thermodynamic driving force for rearrangement, and b) resonance energy, which may help or hinder rearrangement, depending on the specific system. For the ring opening of **11** ($R = \text{H}$ or alkyl), ring opening is thermodynamically disfavored because there is a loss of resonance energy associated with ring opening which the relief of cyclopropyl ring strain does not compensate for.⁴⁶ Placing radical stabilizing substituents ($R = \text{phenyl}$ or vinyl) on the cyclopropyl group offsets this loss of resonance energy and ring opening becomes more favorable ($k \approx 10^6 - 10^7 \text{ s}^{-1}$ for $R = \text{CH}=\text{CH}_2$ or Ph).^{47,48}

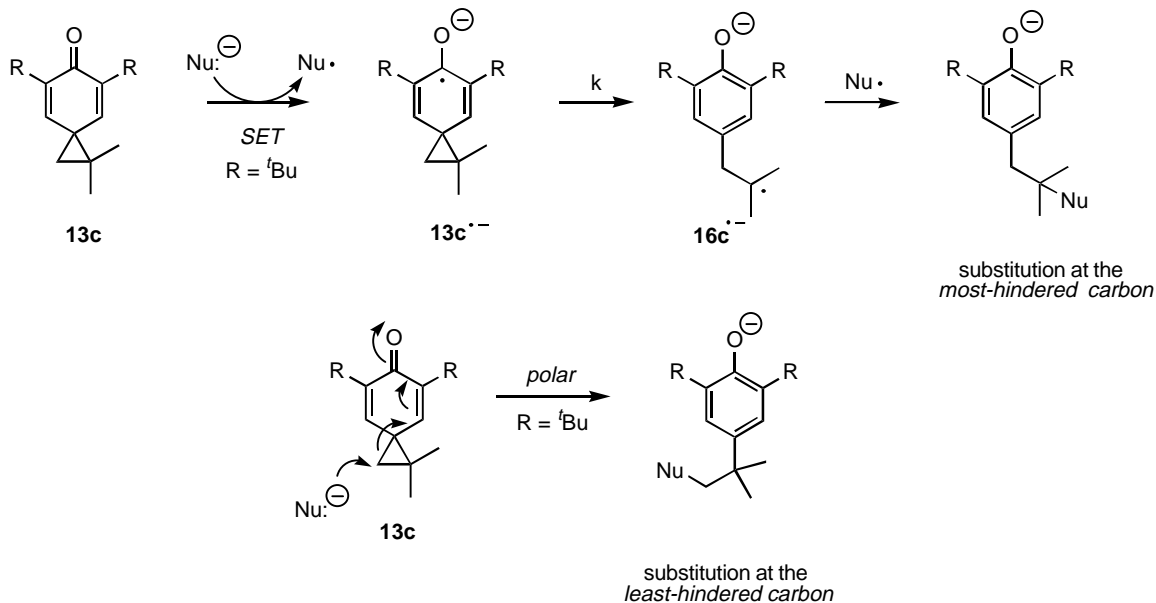
Based on the thermodynamic considerations outlined above, spiro[2.5]octa-4,7-dien-6-one (**13c**) emerged as an excellent candidate for use as a single electron transfer probe. It was envisioned that ring opening of its corresponding radical anion would be especially facile because in addition to the relief of cyclopropane ring strain, ring opening generates an aromatic ring (*i.e.*, the resonance energy of the product is greater than that of the reactant, Eq. 1.5). Considering that relief of cyclopropane ring strain works in

conjunction with resonance stabilization to favor rearrangement, exceptionally high rearrangement rates were anticipated.



In a preliminary report, ring opening of **13c** was found to occur very rapidly ($k > 10^7 \text{ s}^{-1}$).⁴⁹ Moreover, **13c** promises to be an exceptional probe for SET pathways in the reactions of nucleophiles with carbonyl compounds as it may allow clear experimental distinction between SET and polar pathways Scheme 1.5.⁵⁰ If a polar pathway were operating, ring opening would result in products in which the nucleophile was attached to the least hindered carbon. In contrast, an SET mechanism would be expected to yield substitution at the most hindered carbon.

Scheme 1.5



1.3 DISSERTATION DESCRIPTION

Initial interest in the area of radical anion rearrangements was sparked by several contradicting reports in the literature regarding the integrity of the cyclopropyl ring in ketyl radical anions. Dissolving metal reductions of aliphatic cyclopropyl ketones yields ring-opened products ascribed to ketyl anion intermediates.^{51,52,53,54,55} However, dicyclopropyl ketyl anion is apparently stable enough that its ESR spectrum can be recorded with no reported difficulty.⁵⁶

Half-lives of several aryl cyclopropyl ketyl anions were reported to be short and they decay by a ring opening process.³⁰ Exhaustive electrolysis of phenyl cyclopropyl ketone, however, yields the pinacol dimer with the cyclopropane rings still intact.⁵⁷

Alternatively, dissolving metal reduction of phenyl cyclopropyl ketone yields benzyl cyclopropane.^{40c}

Because of the disparity of literature results and the fact that cyclopropyl ketones have been used extensively in mechanistic studies, a thorough investigation into the cyclopropyl rearrangements of several classes of ketyl anions was desired. Previous work has determined that ketyl anions derived from substituted phenyl cyclopropyl ketones would fail to detect an SET mechanism.⁴⁴ Via electrochemical techniques, the rates and products of their ring openings are now well characterized. Preliminary results on spirodienone **13c**, suggests that ring opening is facile and has shown some success in the detection of SET pathways in the reactions of nucleophiles with carbonyl compounds.⁵⁰

These previous studies include highly conjugated phenyl cyclopropyl ketones and spirodienone **13c**. A serious study of the interplay between resonance stabilization and the thermodynamics of ring opening must include less conjugated systems as well (Figure 1.4). The resonance stabilization of the ring closed form of radical anions from groups I, II, and III are quite different. In series II, because little resonance stabilization of the ring closed radical anion exists, relief of cyclopropane ring strain may in fact be able to provide a sufficient thermodynamic driving force for the rearrangement.

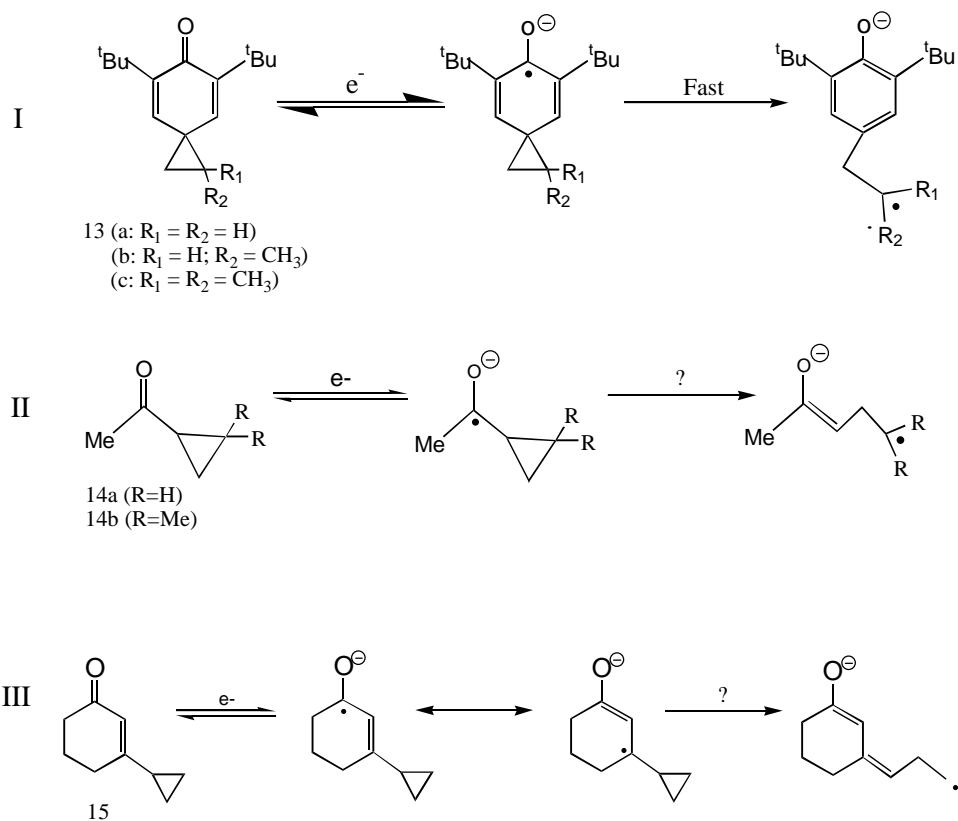


Figure 1.4 Ring opening rearrangements of selected radical anions.

The goal of this project was to identify and fully characterize (where possible), suitable substrates, which upon one electron reduction, undergo rapid and (ideally) irreversible rearrangement. To this end, the substrates in Figure 1.4 were investigated via direct and indirect electrochemical techniques, including cyclic voltammetry (CV), linear sweep voltammetry (LSV), preparative electrolysis (PE), and homogeneous catalysis (HC).

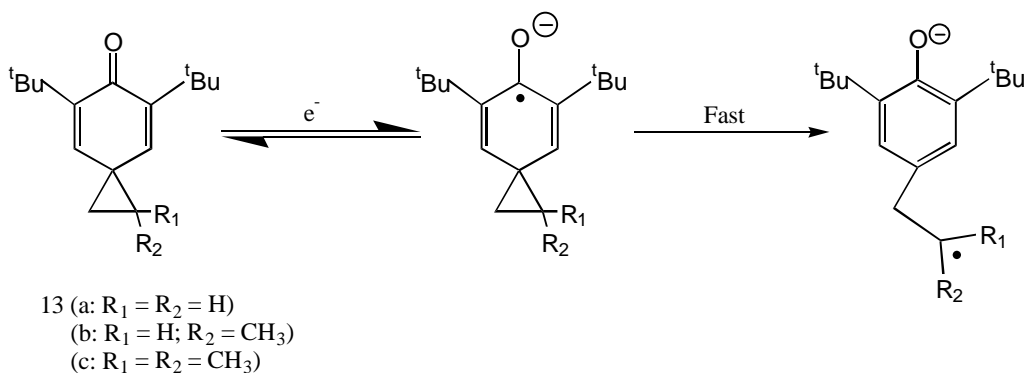
CHAPTER 2. CATHODIC REDUCTION OF 5,7-DI-T-BUTYL

[2.5]OCTA-4,7-DIENE-6-ONE AND DERIVATIVES

2.1 INTRODUCTION

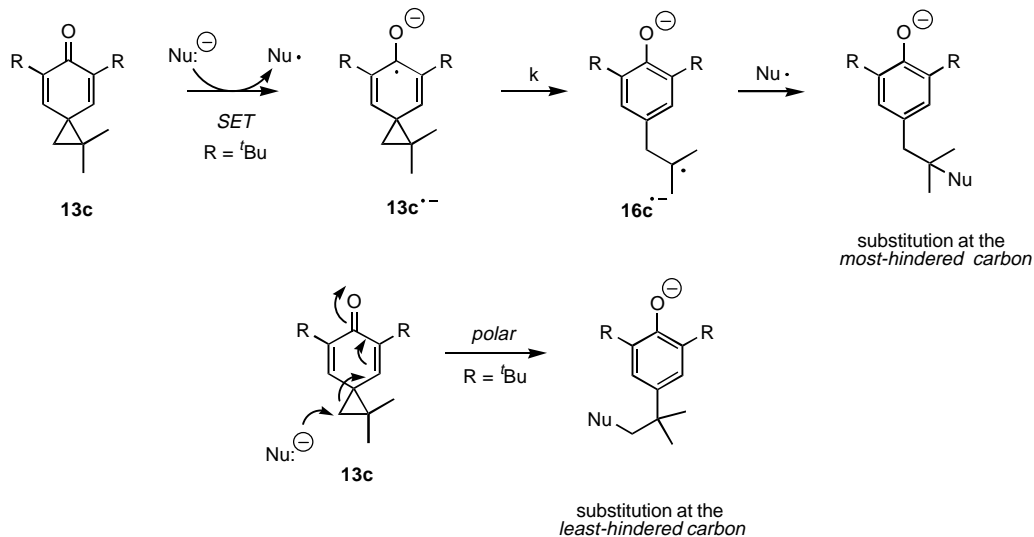
Previous studies dealing with rearrangements of radical anions derived from cyclopropyl ketones identified two factors which influence the rate: a) relief of cyclopropane ring strain (which provides a thermodynamic driving force favoring rearrangement), and b) the difference in resonance energy associated with the ring-opened and ring-closed radical anions (which can help or hinder rearrangement, depending on the specific system).^{44,46,47} Spiro[2.5]octa-4,7-dien-6-ones **13(a→c)** were selected for study because it was envisioned that ring opening of their corresponding radical anions would be especially facile because in addition to the relief of cyclopropane ring strain, ring opening generates an aromatic ring (*i.e.*, the resonance energy of the product is greater than that of the reactant, Scheme 2.1). Considering that relief of cyclopropane ring strain works in conjunction with resonance stabilization to favor rearrangement, exceptionally high rearrangement rates were anticipated.

Scheme 2.1

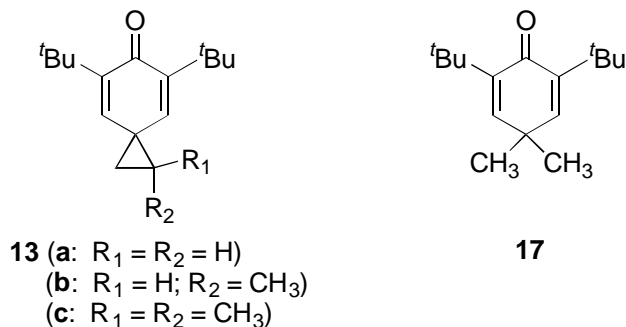


As introduced in section 1.2 and expanded here for clarity, preliminary reports from our lab demonstrated that the radical anion generated electrochemically from 1,1-dimethyl-5,7-di-*tert*-butylspiro[2.5]octa-4,7-dien-6-one (**13c**): 1) undergoes rapid ring opening to yield (preferentially) 3° distonic radical anion **16c^{•-}** with a rate constant estimated to be $\geq 10^6 \text{ s}^{-1}$,⁴⁹ and 2) has proven to be an efficient mechanistic “probe” for distinguishing between SET and conventional polar pathways in reactions of nucleophiles which historically do and do not react with carbonyl compounds via SET (Scheme 2.2).⁵⁰ Relief of cyclopropyl ring strain and the resonance stabilization energy gained in the generation of an aromatic ring provide a tremendous thermodynamic driving force for this rearrangement (AM1 semi-empirical MO theory estimates ΔH° for ring opening of **13a** to be exothermic by 20 kcal/mol).⁴⁹ The distinction in mechanism (SET or polar pathway) is evident in the regiochemistry of the resulting products (Scheme 2.2): an SET mechanism results in nucleophilic substitution at the most hindered position, while a polar pathway would preferentially yield substitution at the least hindered position.

Scheme 2.2



Given the apparent success of **13c** as a mechanistic probe for SET pathways, a complete characterization of the electrochemical behavior of **13c** was desired. Related derivatives **13a**, **13b**, and model compound **17** were also investigated using direct [cyclic voltammetry (CV), linear sweep voltammetry (LSV), and preparative electrolysis (PE)] and indirect [homogeneous catalysis] electrochemical techniques to understand better the chemistry of this intriguing class of compounds.



2.2 RESULTS AND DISCUSSION

2.2.1 Direct electrochemical reduction of **13(a-c)**.

The cyclic voltammograms (CV's) of **13a**, **13b**, and **13c** are all characterized by an irreversible reduction wave at approximately -2.4 V (vs. 0.1 M Ag⁺/Ag at 100 mV/s) and a reversible (or partly reversible) oxidation wave(s) at *ca.* -700 mV (Figure 2.1).

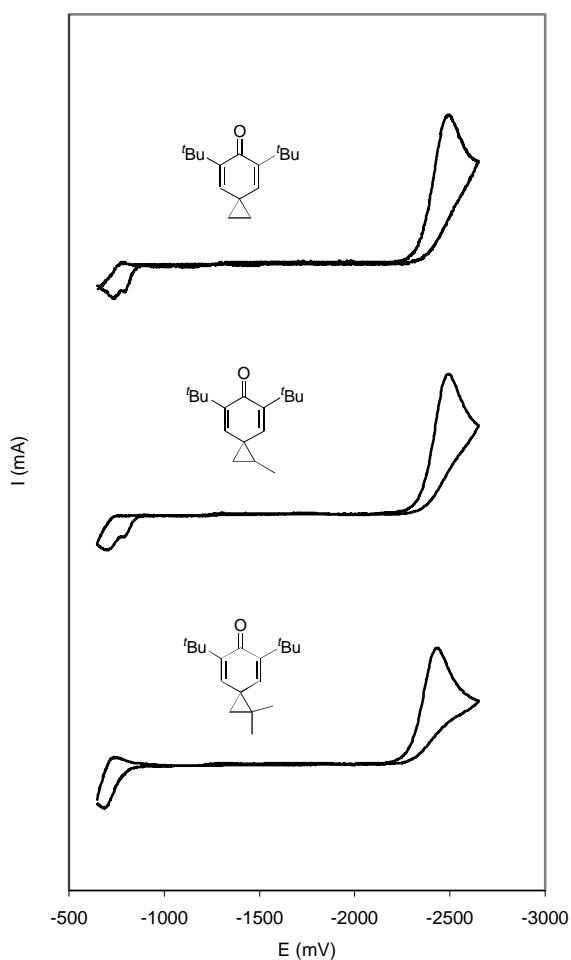


Figure 2.1. Cyclic voltammograms of **13a**, **13b**, and **13c** (0.5 M TBAP in DMF, 0.1 M Ag⁺/Ag reference, $\nu = 100$ mV/s, GCE, 0.003 M in substrate).

A thorough linear sweep voltammetry (LSV)⁵⁸ study was conducted (Figures 2.2, 2.3, 2.4, and 2.5) and for all three compounds: a) the peak potential of the reduction wave (E_p) varied linearly with the log of the sweep rate, b) E_p was *independent* of substrate concentration, and c) the peak width ($E_p - E_{p/2}$, the difference between the peak

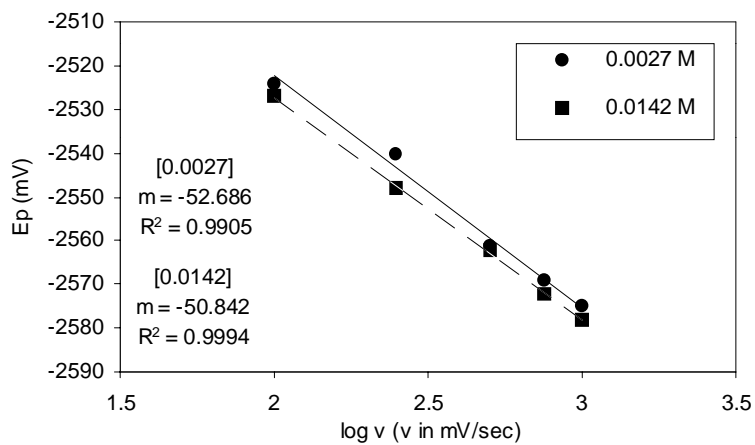


Figure 2.2. LSV analysis of **13a**, $\partial E_p/\partial \log v$. (0.5 M TBAP, DMF, $v = 0.1 - 1.0$ V/s)

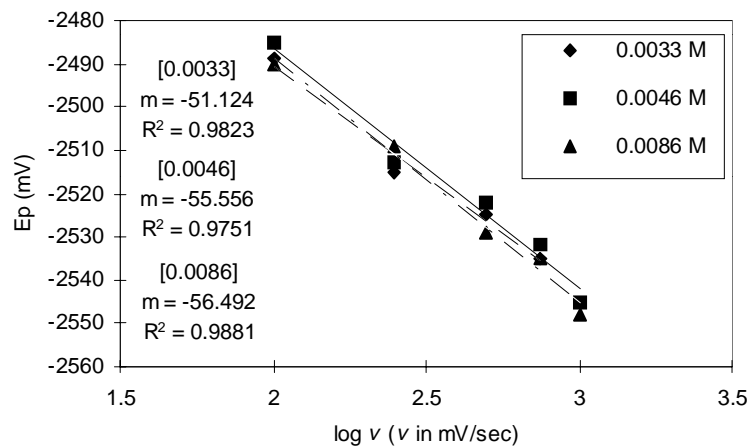


Figure 2.3. LSV analysis of **13b**, $\partial E_p/\partial \log v$. (0.5 M TBAP, DMF, $v = 0.1 - 1.0$ V/s)

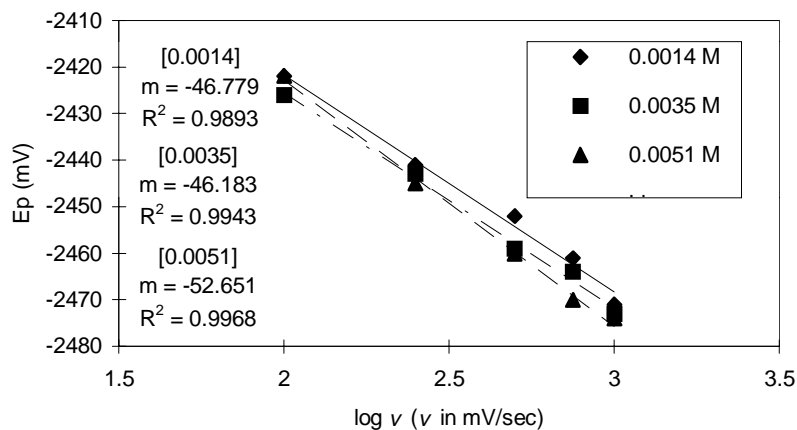


Figure 2.4. LSV analysis of **13c**, $\partial E_p/\partial \log v$. (0.5 M TBAP, DMF, $v = 0.1 - 1.0$ V/s)

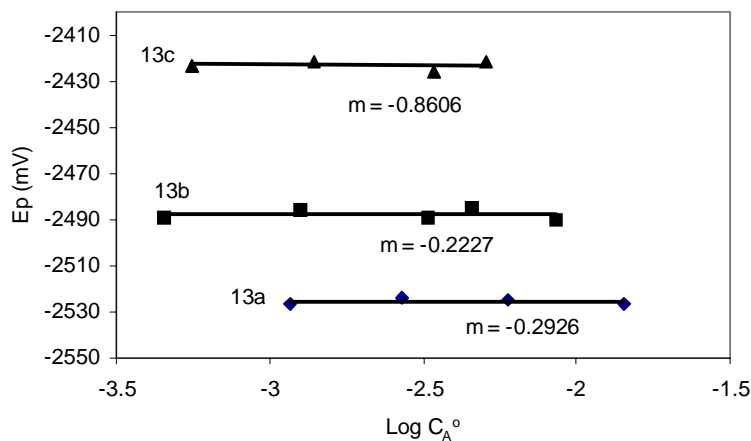


Figure 2.5. LSV analysis of **13a**→**c**, $\partial E_p/\partial \log C_A$. (0.5 M TBAP, DMF, $v = 100$ mV/s)

and half-peak potentials) was broad and did not vary as a function of sweep rate or concentration. Results are summarized in Table 2.1. Combined, the observed variation of E_p with sweep rate and the broadness of the reduction waves are consistent with an EC mechanism exhibiting rate limiting heterogeneous electron transfer (k_s). Scheme 2.3 depicts an EC process, wherein neutral **13(a-c)** is reduced at the electrode surface to give radical anion **13^{•-}** with rate constant k_s (electron transfer, **E**, step). Ring opening of **13^{•-}** yields distonic radical anions **16^{•-}** and **18^{•-}** (chemical, **C**, step).

Under the conditions of rate limiting heterogeneous electron transfer, the transfer coefficient (α) can be of critical importance as a measure of transition state location and criterion for discerning whether the electron transfer step proceeds in a concerted or stepwise fashion. Transfer coefficients (α) were calculated from the slope of E_p vs. $\log(v)$ in accordance with Eq. 1,⁵⁸ and from the peak width according to Eq. 2.⁵⁸ Within experimental error, α values obtained via both procedures were identical (Table 2.1).

Transfer coefficient values of 0.5 support a discrete radical anion intermediate in the reduction of **13a**, **13b** and **13c**. Systems for which electron transfer and bond breaking are concerted (*i.e.*, dissociative electron transfer) are typically characterized by α values significantly less than 0.5 (typically < 0.4).⁵⁹ Saveant has suggested in the reduction of several arylmethyl halides that substrates possessing transfer coefficients ranging from 0.2 – 0.3 exhibited concerted “electron transfer – halogen cleavage” or dissociative electron transfer. While for a similar series of aryl halides, transfer coefficients of ≥ 0.5 were determined and a stepwise mechanism was proposed.

A simple representation of the transition between successive and concerted electron transfer (E) – bond breaking (C) steps is shown in Figure 2.6. In those systems characterized by dissociative electron transfer, $R-X^{\bullet-}$ does not exist as a discrete intermediate ($R-X^{\bullet-}$ exists at a potential energy maximum - point A in Figure 2.6). Therefore, the R-X bond distance is long (partially broken) in the transition state represented by point A in Figure 2.6. In a concerted or stepwise mechanism, the radical anion has a finite lifetime (existing for at least one molecular vibration, and exists at a potential minimum – point B in Figure 2.6) and the transition state would be shifted more reactant like. The R-X bond distance for the concerted mechanism (dotted line) would be shorter in the transition state than its dissociative electron transfer counterpart (solid line).

Scheme 2.3

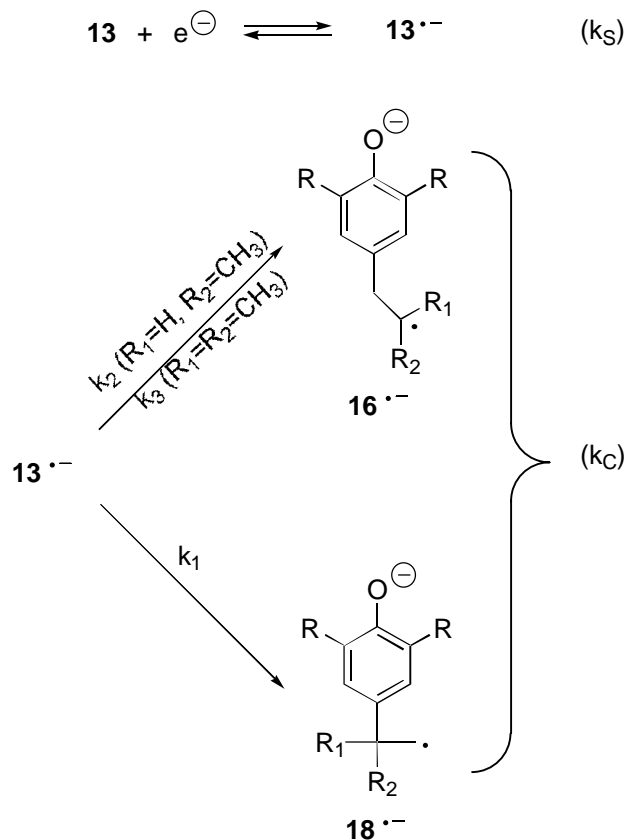


Table 2.1. LSV analysis of **13a**, **13b**, and **13c**^a

Compound	$\partial E_p / \partial \log \nu$ (mV decade ⁻¹)	$\partial E_p / \partial \log C_A$ ^b (mV decade ⁻¹)	$E_p - E_{p/2}$ (mV)	α ^c	α ^c
13a	51.8 ± 4.0	-0.3 ± 2.3	93 ± 5	0.57 ± 0.04	0.51 ± 0.04
13b	54.4 ± 4.0	-0.2 ± 2.5	93 ± 5	0.54 ± 0.04	0.51 ± 0.04
13c	48.5 ± 4.0	-0.9 ± 3.1	90 ± 5	0.61 ± 0.04	0.53 ± 0.04

^aDMF solvent, 0.5 M TBAP, $\nu = 100 - 1000$ mV/s. ^b $\nu = 100$ mV/s ^cCalculated based upon $\partial E_p / \partial \log \nu$ and Eq. 2.1. ^cCalculated based upon $(E_p - E_{p/2})$ and Eq. 2.2.

$$\alpha = \frac{RT}{2F} \frac{\partial \ln v}{\partial E_p} \quad (2.1)$$

$$\alpha = \frac{RT}{F} \frac{1.85}{E_{p/2} - E_p} \quad (2.2)$$

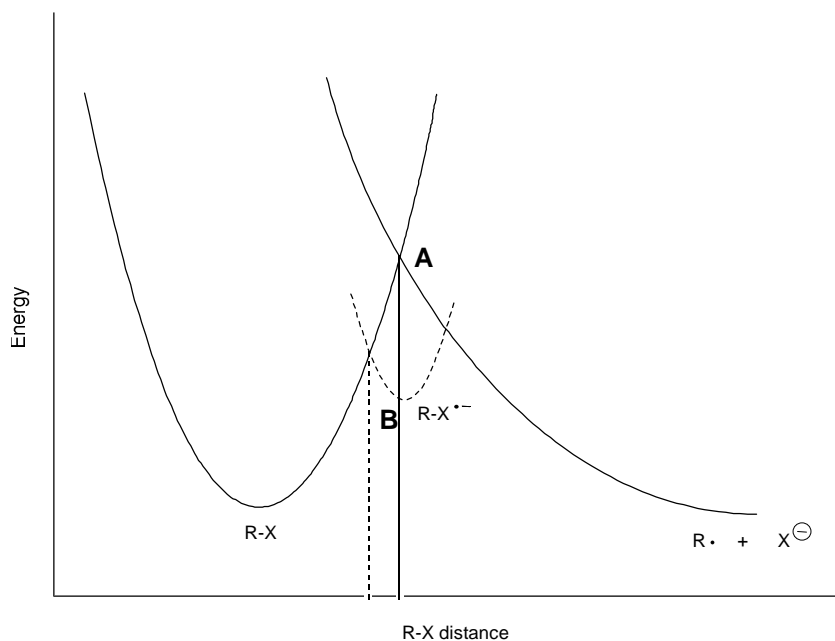


Figure 2.6. Significance of α : A measure of transition state location and criterion for dissociative electron transfer.

Because electron transfer is rate-limiting, neither the reduction potential of these substrates nor the rate constant for ring-opening of their radical anions could be determined by direct electrochemical techniques. However, these experiments help

establish a lower limit for k_c . For an **EC** process, the competition between heterogeneous electron transfer (k_s) and a follow-up chemical step (k_c)⁶⁰ for kinetic control depends upon the parameter p (Eq. 2.3).⁶¹ Making the assumption that for kinetic control by k_s , $\log p \leq -1$,⁶¹ and using a) the median value for the transfer coefficient determined above ($\alpha = 0.54$) and b) typical values for k_s and D (e.g., the literatures value for benzoquinone determined under similar experimental conditions: $D = 1.2 \times 10^{-5} \text{ cm}^2 \text{ s}^{-1}$; $k_s = 0.18 \text{ cm s}^{-1}$)⁶², we estimate that $k_c \geq 10^6 \text{ s}^{-1}$ for ring opening of **13a**, **13b**, and **13c**. It should be noted however that this estimate of a lower limit for k_c depends strongly on the heterogeneous rate constant, k_s .

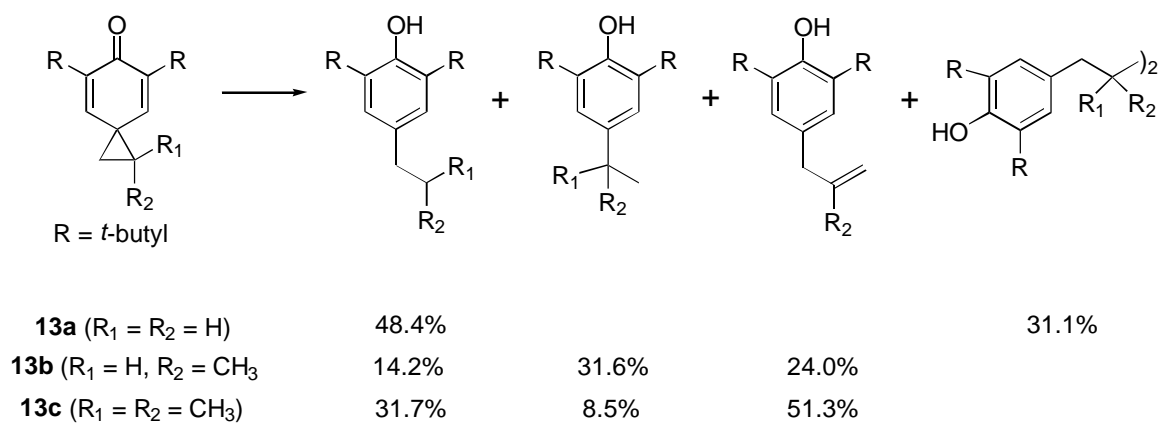
$$p = [\alpha n F v / RT]^{(\alpha-1)/2\alpha} \left[k_s^{1/\alpha} k_c^{1/2} \right] D^{-\frac{1}{2}\alpha} \quad (2.3)$$

2.2.2 Product analysis from preparative electrolysis of **13(a-c)**.

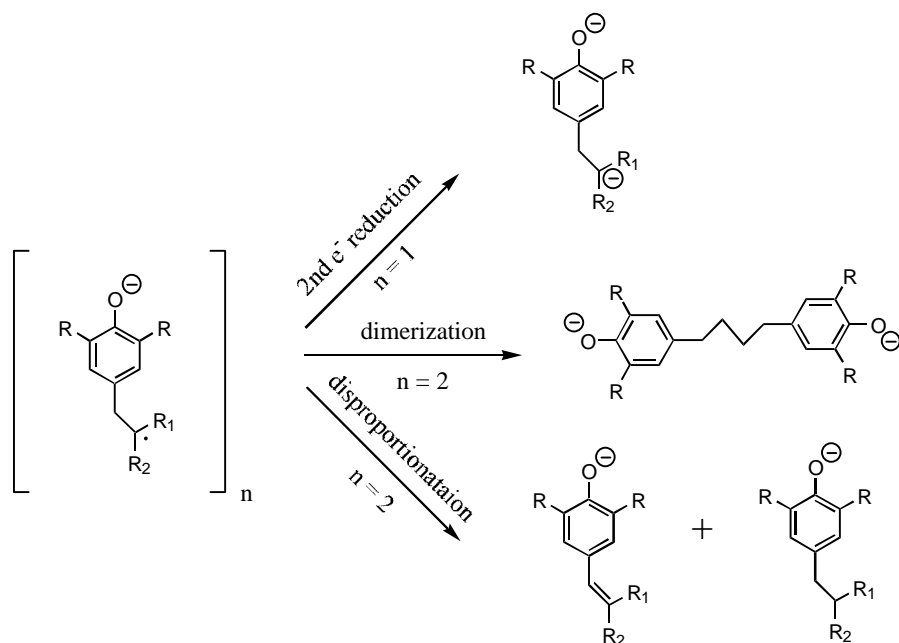
Preparative scale (constant current, DMF, 0.2 M TBAP) electrolysis of all substrates, **13(a-c)**, leads to cyclopropane ring-opened products. Preparative electrolysis of **13b** and **13c** were performed by Larry E. Brammer Jr. and Jason Gillmore. The presence of solely ring cleaved products validates the assumption that the kinetic information obtained in cyclic voltammetry experiments reflects a ring-opening process (Scheme 2.4; Note: Yields are based on consumed starting material). Preparative electrolysis experiments provide additional support for the **EC** mechanism described in Scheme 2.3, in which radical anions **16^{•-}** and **18^{•-}** undergo a second reduction, dimerization or disproportionation (Scheme 2.5) to yield, after acidic workup, the final products. (The

oxidation wave at -700 mV, Figure 2.1, is assigned to the oxidation of the phenolate ions)⁶³ A typical reduction of **13a** ($R_1 = R_2 = H$) gave 48.4% alkane and 31.1% dimer after the transfer of 2 equivalents of electrons. The alkene product from disproportionation of the primary radical ion was not detected.

Scheme 2.4



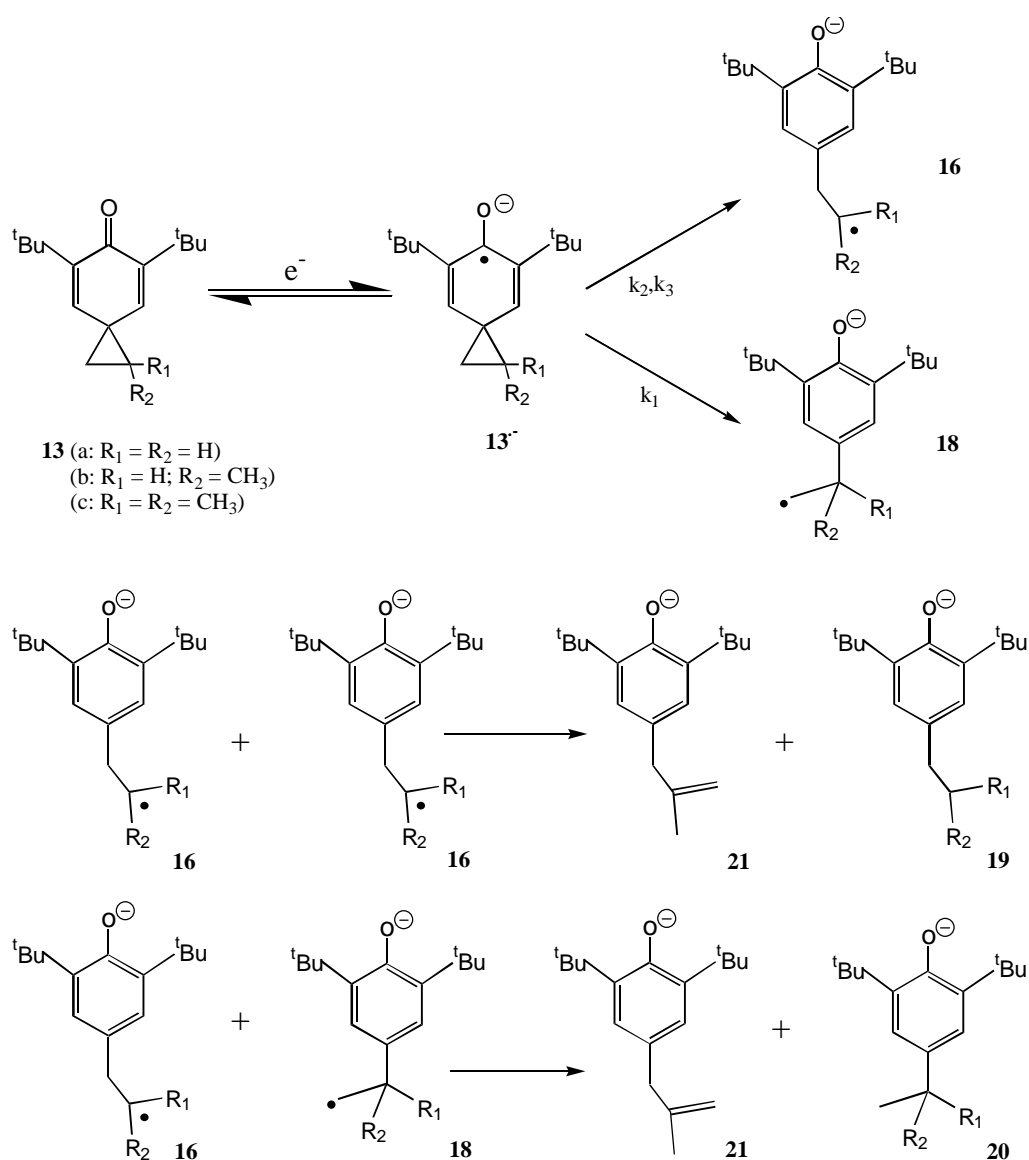
Scheme 2.5



For unsymmetrical radical anions $\mathbf{13b}^{\bullet-}$ and $\mathbf{13c}^{\bullet-}$, ring opening occurs with modest selectivity, favoring the more-substituted (stable) distonic radical anion. Based upon the yield of products observed in the preparative scale electrolyses, $k_3/k_1 = 9.7$ (for $\mathbf{13c}^{\bullet-}$) and $k_2/k_1 = 1.2$ (for $\mathbf{13b}^{\bullet-}$) (Scheme 2.3). Product ratios for k_3/k_1 and k_2/k_1 were determined as follows in Scheme 2.6. After reduction, ring opening can occur to the more stable radical anion (k_2, k_3) or the primary radical anion (k_1). Alkane products (**20** and **19**) arise from 1° and $2^\circ/3^\circ$ radical anions **18** and **16**, while alkene product **21** arises from the disproportionation reaction of radical anion **16** as shown in Scheme 2.6. Product ratios reflect the relative rate constant ratios, and as such k_3/k_1 and k_2/k_1 can be determined. Consistent with the Hammond postulate, this low selectivity suggests an early (reactant-like) transition state for these ring openings, which is anticipated given their highly exothermic nature.

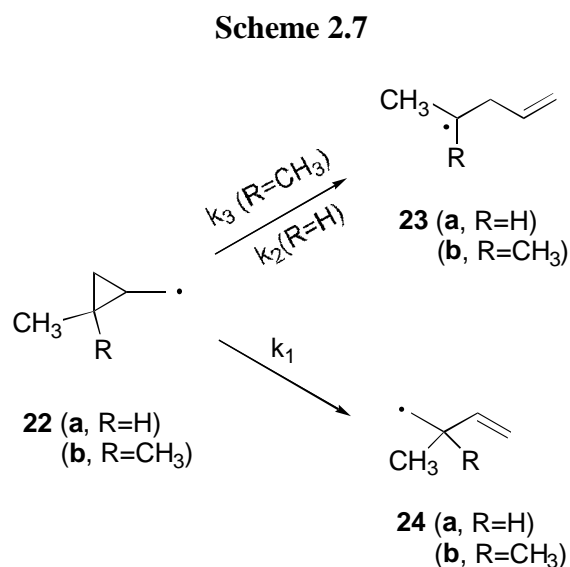
AM1 calculations suggest that ring opening of **13c^{•-}** is exothermic by as much as 20 kcal/mol.⁵⁸ This estimate was based upon the difference in ΔH_f° 's for the ring-opened and ring-closed forms of the radical anion, and of course, refers to the gas phase. A vastly superior procedure for addressing the thermodynamics of ring opening is presented in section 2.2.5. These calculations are based partly on experimental solution-phase measurements for the charged species and avoid the need to calculate any ΔH_f° 's for odd-electron species using MO theory.

Scheme 2.6



Notably, the selectivity observed for ring opening of these radical anions is remarkably similar to the ring-substituted cyclopropylcarbinyl (neutral) free radicals. For example, ring opening of *trans*-**22a** leads to 2° and 1° radicals **23a** and **24a** in a 1.2:1

ratio (Scheme 2.7),⁶⁴ a value identical to that observed for **13b**^{•-}. Dimethyl-substituted radical **22b** leads to 3° and 1° radicals **23b** and **24b** in a 6.7:1 ratio (Scheme 2.7),⁶⁴ vs. 9.7:1 observed for **13c**^{•-}. Ring opening of neutral radicals **22a** and **22b** occurs with rate constants greater than 10⁸ s⁻¹. We anticipate that the similar selectivity observed for of **13b**^{•-} and **13c**^{•-} will be reflected in rate constants for ring opening of the same order of magnitude.

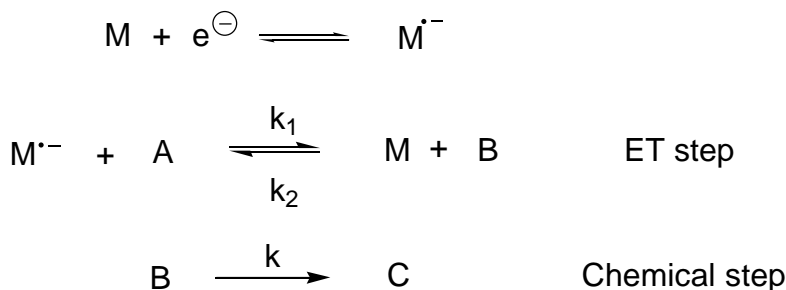


2.2.3 Indirect electrochemistry of **13(a-c)**.

Homogeneous redox catalysis⁶⁵ is a powerful technique for studying the chemistry of highly reactive intermediates produced via electron transfer. Consider the reactions depicted in Scheme 2.8. Rather than the substrate **A**, an electron-transfer mediator or catalyst **M** is reduced at the electrode surface. (In order for this condition to be met, the

mediator must be more easily reduced than the substrate, i.e., $E_{A/B}^{\circ} < E_{M/M^{\bullet-}}^{\circ}$). Reduction of the substrate occurs via electron transfer from the reduced form of the mediator ($M^{\bullet-}$).

Scheme 2.8



In this manner, the reference is taken away from the electrode and placed on the reversible $1e^{-}$ reduction of a compound with a known E° . Effects of substrate addition on this reversible electron transfer are manifested experimentally by an increase in peak current and a loss of reversibility (if catalysis is occurring). The key experimental observable is the current ratio i_p/i_{pd} , where i_p and i_{pd} are the voltammetric peak currents of the mediator in the presence and absence of the substrate, respectively, at a particular value of γ (the ratio of the substrate to mediator concentrations, C_A°/C_M°).

Savéant *et al.* introduced the dimensionless rate constants λ_1 , λ_2 , and λ defined below (Eqs. 2.4 \rightarrow 2.6, where v is the sweep rate in $V s^{-1}$ and R, T and F have their usual meanings).⁶⁵ Published working curves are available which depict the current ratio i_p/i_{pd} a) as a function of $\log(\lambda_1)$ when the electron transfer step (k_1) is rate limiting, or b) as a function of $\log(\lambda\lambda_1/\lambda_2)$ when the chemical step (k_2) is rate limiting.⁶⁵

$$\lambda_1 = (k_1 C_M^0 / \nu)(RT/F) \quad (2.4)$$

$$\lambda_2 = (k_2 C_M^0 / \nu)(RT/F) \quad (2.5)$$

$$\lambda = (k/\nu)(RT/F) \quad (2.6)$$

As noted above, kinetic control may be governed by either the homogeneous electron transfer step (k_1) or the chemical step (k , Scheme 2.8). If the rate of the chemical step is faster than back electron transfer ($k > k_2 [\mathbf{M}]$), then the electron transfer step is rate limiting and k_1 can be determined experimentally. If the chemical step is slow relative to back electron transfer ($k < k_2 [\mathbf{M}]$), the chemical step is rate limiting with the electron transfer step as a rapid pre-equilibrium. Under these conditions the composite rate constant kk_1/k_2 can be determined. (Because $\log(k_1/k_2) = 2.303F/RT(E_{M/M^{\bullet-}}^{\circ} - E_{A/B}^{\circ})$, k can be extracted if the reduction potential of the substrate is known).

Though similar in appearance, different working curves pertain to these two conditions, and it is critical to accurately assess whether the kinetics are governed by the electron transfer or chemical step. For rate limiting electron transfer, the current ratio is a function of γ and λ_1 , the latter of which is related to the mediator concentration (Eq. 2.4). For rate limiting chemical step, i_p/i_{pd} is a function of γ and $\lambda\lambda_1/\lambda_2$, and is *concentration independent* at constant γ (Eqs. 2.4 \rightarrow 2.6). Thus, the distinguishing characteristic between these two rate limiting conditions is the effect of mediator concentration (C_M^0) on i_p/i_{pd} at constant γ and ν . Peak current ratio varies as a function of mediator concentration only when the electron transfer step is rate limiting.

The reduction of **13a**, **13b**, and **13c** by several mediators was studied. Because of the limited quantity of these substrates available (they are not commercially available), it was more economical to examine the current ratio i_p/i_{pd} as a function of sweep rate and mediator concentration at constant excess factor γ (rather than by varying γ and keeping sweep rate constant). As can be seen from Eqs. 2.7 and 2.8, at constant γ , i_p/i_{pd} is a function of $\log(C_M^0/v)$ (when electron transfer is rate limiting) or $\log(1/v)$ when the chemical step is rate limiting. Our approach was to obtain the voltammograms of several mediators in the absence and presence of **13a**, **13b**, and **13c**. By comparing plots of $[i_p/i_{pd} \text{ vs. } \log(1/v)]$ and $[i_p/i_{pd} \text{ vs. } \log(C_M^0/v)]$ obtained at different concentrations of mediator (γ constant), any concentration dependence is readily apparent. In Figure 2.7, the plot of $[i_p/i_{pd} \text{ vs. } \log(1/v)]$ contains 3 sets of data illustrated as 3 discrete curves. When the concentration of each experiment is removed as represented in the plot of $[i_p/i_{pd} \text{ vs. } \log(C_M^0/v)]$, the 3 separate curves converge on 1 data set, indicating there was a concentration dependence on i_p/i_{pd} . The remainder of experimental data is presented in section 2.4. For **13a**, **13b**, and **13c**, over the range of mediators examined, i_p/i_{pd} was found to vary as a function of mediator concentration (at constant γ). For all these substrates, electron transfer was determined to be the rate limiting step. Therefore, conditions must exist where $k > k_2[M]$. A lower limit on the rate constant k can be established by estimating the quantity $k_2[M]$. The reverse electron transfer rate constant k_2 (Scheme 2.8) is closely approximated by the diffusion rate constant 1×10^{10} of a bimolecular reaction in DMF, especially in those electron transfers that are sufficiently endergonic in the forward electron transfer. The mediator concentration limit in this

series of experiments is $\cong 0.001$ M. The product of these is 1×10^7 and suggests that the rate constant for the chemical step (ring opening) must be greater than 10^7 s $^{-1}$.

$$\log \lambda_1 = \log \left(\frac{k_1 RT}{F} \right) + \log \left(\frac{C_M^o}{\nu} \right) \quad (2.7)$$

$$\log \left(\frac{\lambda \lambda_1}{\lambda_2} \right) = \log \left(\frac{k k_1 RT}{k_2 F} \right) + \log(1/\nu) \quad (2.8)$$

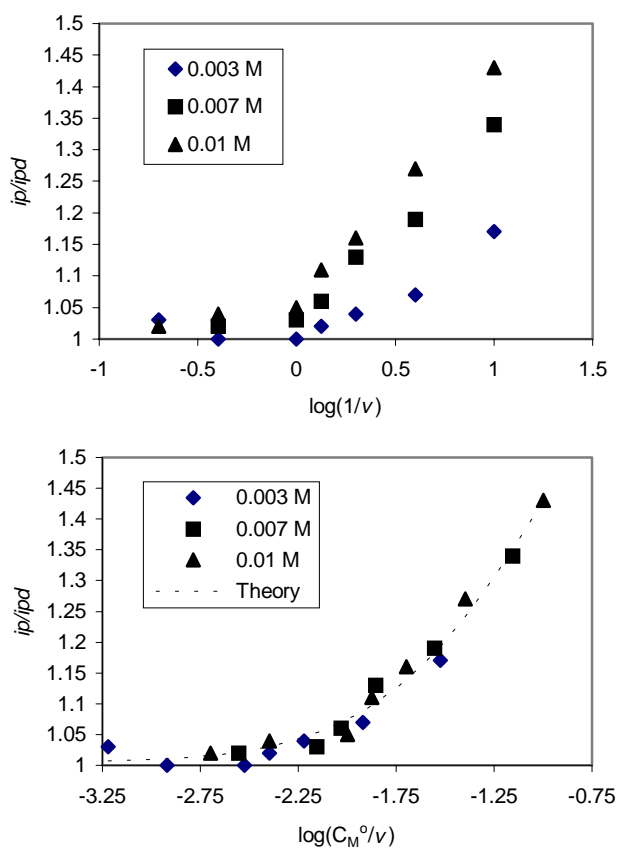
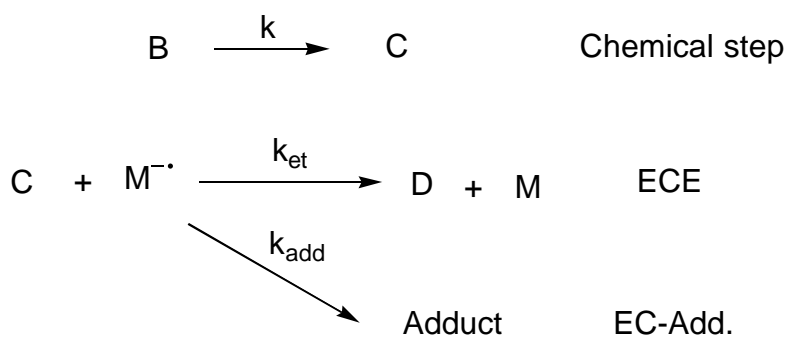


Figure 2.7. Mediated reduction of **13a** by 4-cyanopyridine (DMF, GCE, 0.5 M TBAP, $\nu = 0.1 - 5$ V s $^{-1}$, $\gamma=1.00$; Dashed line is the working curve for rate-limiting ET, $x' = 0.722 \pm 0.017$)

Kinetics of these systems were further complicated by a competing bimolecular reaction between $M^{\bullet-}$ and the product of the chemical step (**C**, i.e., the ring-opened distonic radical anion) as described in Scheme 2.9. Coupling reactions between alkyl radicals and aromatic anion radicals are known to be fast and nearly diffusion-controlled.⁶⁶ For example, the rate constant for the coupling reaction between sodium naphthalene radical anion and the 1-hexenyl radical has been reported by Garst *et al.* To be $2 \times 10^9 \text{ M}^{-1}\text{s}^{-1}$. A similar value of $1 \times 10^9 \text{ M}^{-1}\text{s}^{-1}$ has been obtained by Pederson and Lund in reactions between electrogenerated aromatic anion radicals and ‘radical clocks’ in N,N-dimethylformamide. This competition between addition to the mediator (EC-add step) and the second electron reduction (ECE mechanism) must be considered in the overall reaction profile and introduces a new kinetic parameter ρ , where $\rho = k_{\text{et}}/(k_{\text{add}}+k_{\text{et}})$. The parameter ρ reflects the fraction of **C** which adds to the mediator. A treatment of this problem and the appropriate theoretical working curves have been published by Savéant.⁶⁷

Scheme 2.9



Previously published working curves dealing with addition to the catalyst express i_p/i_{pd} as a function of γ .⁶⁷ In the experiments contained in this dissertation, however, i_p/i_{pd} was measured at various sweep rates at constant γ . It was thus necessary to derive the appropriate working curves (21 plots of i_p/i_{pd} vs $\log(\lambda_1)$ at $\gamma = 1.00$ for $\rho = 0.00$ to 1.00 in 0.05 increments) via digital simulation.⁶⁸ These working curves were subsequently fit to a polynomial of the form $y=(a+cx+ex^2+gx^3+ix^4)/(1+bx+dx^2+fx^3+hx^4+jx^5)$, where the coefficients $a \rightarrow j$ were determined for each working curve.⁶⁹ Via non-linear regression,⁶⁹ the experimental data [i_p/i_{pd} vs $\log(C_M^0/v)$] were fit to the polynomial form of the working curves, $y = f(x + x')$, and the adjustable parameter $x' = \log(k_1RT/F)$ was determined. The parameter ρ was determined by the working curve which gave the best fit to the experimental data and k_1 was determined from x' . A representative fit of the experimental data is provided in Figure 2.7, with the remainder of data treatment provided in section 2.4. Table 2.2 summarizes the values of k_1 obtained for reduction of **13a**, **13b**, and **13c** by a series of mediators. For all mediators examined, $\rho = 0.00 \pm 0.025$, indicating that radical anion/distonic radical anion coupling k_{add} (Scheme 2.11) is fast relative to k_{et} and that our system is decidedly not catalytic. Literature ρ values determined from the reactions of the mediators in Table 2.2 with 1° , 2° , and 3° alkyl halides R-X (X = Cl, Br, I)⁹⁵ give $\rho = 0.0 \pm 0.1$. It is important to note two trends present in the data 1) rate constants increase with increasing reducing power of the mediator radical anion and 2) rate constants increase with alkyl substitution on the cyclopropyl ring.

Table 2.2. Rate constants for homogeneous electron transfer between the reduced form of the mediator and **13a**, **13b**, and **13c** (0.5 M TBAP/DMF)

Mediator	E^0 (V) ^(a)	k_1 (M ⁻¹ s ⁻¹)		
		13a	13b	13c
flouranthene	-2.150	^(b)	2.8 (±0.2) x 10 ²	8.4 (±0.5) x 10 ^{2(c)}
4-cyanopyridine	-2.168	2.1 (±0.1) x 10 ²	4.6 (±0.2) x 10 ^{2(c)}	1.2 (±0.1) x 10 ^{3(c)}
cyanonaphthalene	-2.246	5.6 (±0.3) x 10 ³	7.9 (±0.5) x 10 ³	2.0 (±0.2) x 10 ^{4(c)}
9,10-diphenylanthracene	-2.250	7.2 (±0.5) x 10 ³	9.7 (±0.6) x 10 ³	2.8 (±0.2) x 10 ^{4(c)}
9-phenylanthracene	-2.291	2.4 (±0.1) x 10 ⁴	3.3 (±0.3) x 10 ⁴	1.0 (±0.1) x 10 ⁵
anthracene	-2.337	5.3 (±0.7) x 10 ⁴	3.1 (±0.5) x 10 ⁵	^(b)
9-methylanthracene	-2.359	2.4 (±0.3) x 10 ⁵	3.5 (±0.6) x 10 ⁵	^(b)

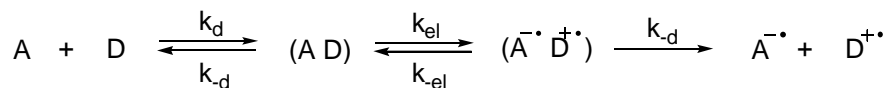
^(a)vs. 0.1 M AgNO₃/Ag, ^(b)these rate constants not available under conditions of $\gamma=1$, either the system is not sufficiently catalytic or $E^0_{M/M\cdot-} \cong E^0_{A/B}$ ^(c)performed by P. Swartz and D. Berger and published in Phillips, J.P.; Gillmore, J.G.; Swartz, P.; Brammer, L.E.Jr.; Berger, D.J. and Tanko, J.M., *J. Am. Chem. Soc.* **1998**, *120*, 195.

2.2.4. Estimates of the reduction potentials of **13a**, **13b**, and **13c** using Marcus theory

Several theories which relate the rate constant for electron transfer to the driving force exist, the preminent of which is Marcus theory⁷⁰. The physical model of the Marcus approach is represented by two spheres **A** and **D** (radii r_1 and r_2 , charges Z_1 and Z_2 , in a dielectric medium, D) which first must diffuse together to form an encounter (or

precursor) complex. After electron transfer, the products diffuse from the successor complex ($A^{\bullet-} D^{\bullet+}$, Scheme 2.10).

Scheme 2.10



The Franck-Condon principle states that electron transfer is faster than any nuclear movement. Therefore, the donor and acceptor energy levels must be made equal to $\pm RT$ prior to electron transfer. This barrier to electron transfer, or reorganization energy, is represented by λ and has an internal and external component. The internal contribution is described by a harmonic oscillator model (bond stretching/compression, angle deformation, and torsional movements) and the external portion can be represented by a dielectric continuum model for solvents (solvent reorganization, electrostatic changes around the reactants). The Marcus equation (2.9) represents the free energy of

$$\Delta G^\ddagger = \frac{Z_1 Z_2 e^2 f}{D r_{12}} + \frac{\lambda}{4} \left(1 + \frac{\Delta G^{o'}}{\lambda} \right)^2 \quad (2.9)$$

activation/intrinsic barrier of the transition state. The first term is a work term, W , and represents the loss or gain in electrostatic free energy in forming the precursor complex.

$$k_{el} = Z \exp(-\Delta G^\ddagger / RT) \quad (2.10)$$

In systems where one reactant is neutral, $W = 0$. And, $\Delta G^\ddagger = \Delta G^\circ$ in cases where $Z_1 = Z_2 + 1$. Equation 2.9 is related to an experimentally derived quantity through the Eyring equation 2.10, assuming adiabatic conditions. By combining equations 2.9 and 2.10 and substituting into the kinetic expression derived for the formation of products in Scheme 2.12, the final form of the Marcus equation used in data analysis is presented as equation 2.11. (Assuming $k_d = 1 \times 10^{10} \text{ M}^{-1}\text{s}^{-1}$ (the diffusion-controlled rate constant in DMF), $K_d = 0.16 \text{ M}^{-1}$,⁷² and the frequency factor $Z = 6 \times 10^{11}\text{s}^{-1}$).

$$\frac{1}{k_{obs}} = \frac{1}{k_d} + \frac{1}{K_d Z \exp\left(\frac{-\lambda}{4RT} (1 + \Delta G^\circ / \lambda)^2\right)} + \frac{1}{k_d \exp(-\Delta G^\circ / RT)} \quad (2.11)$$

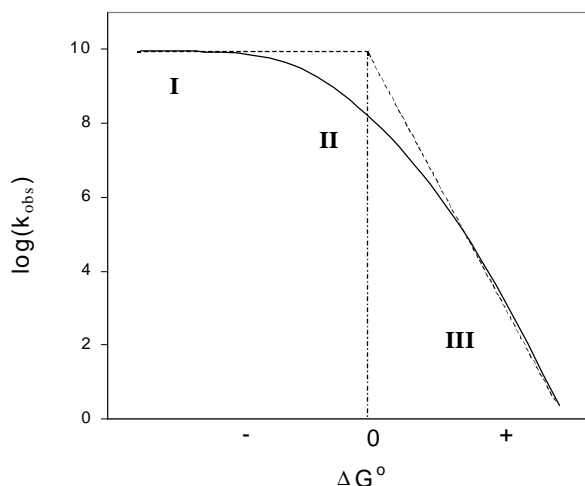


Figure 2.8: Marcus curve for electron transfer ($\Delta G^\circ = F (E^\circ_{A/B} - E^\circ_{M/M^\cdot})$).

Eq. 2.11 relates the rate constant for electron transfer (k_{obs}) to the free energy of the reaction ($\Delta G^\circ = F(E_{M/M\bullet-} - E_{A/B})$) and the reorganization energy (λ).^{71,72} From left to right, the three terms in Eq. 2.11 represent different kinetic regimes (Figure 2.8): diffusion-controlled (**I**), activation-controlled (**II**), and equilibrium (or counter-diffusion-controlled) (**III**), for which the slopes of the $\log(k_{\text{obs}})$ vs. $E_{M/M\bullet-}$ plots are zero, $-\alpha F/(2.303RT) = -8.5 \text{ V}^{-1}$ for $\alpha = 0.5$, and $-F/(2.303RT) = -16.8 \text{ V}^{-1}$, respectively. Plateau regime **I** represents slightly endergonic reactions where k_d predominates. k_{el} controls k_{obs} in regime **II**. The linear portion **III** contributes significantly only when k_{el} is competitive with k_d .

In Figure 2.9, the log of rate constants for electron transfer (k_1) determined for the reactions of **13a**, **13b** and **13c** with a series of mediators are plotted against the reduction potentials of the mediators ($E^\circ_{P/Q}$). For **13a**, **13b**, and **13c**, the slopes are -14.8 , -15.5 , and -15.2 V^{-1} respectively, suggesting mixed kinetic control from regions **II** and **III**. Equation 2.12⁷² allows an estimation of the borderline between region **II** and **III**. Using $\lambda = 16 \text{ kcal/mol}$ (average for series **13a**→**c**, vide infra), $k_d = 1 \times 10^{10} \text{ s}^{-1}$, and $Z = 6 \times 10^{11} \text{ s}^{-1}$, a $\Delta G^\circ \leq 0.17 \text{ V}$ is obtained. Catalysts with E° values more positive than the substrate by 0.17 V (-2.387 V vs AgNO_3/Ag) would be largely under the influence of regime **III**. Clearly, this covers the majority of the catalysts used in this study. However, based on the fact that the most negatively reduced of these catalysts fall near this border and the slope of the $[\log k \text{ vs } E^\circ_{MM\bullet-}]$ plot, the possible contribution from region **II** cannot be ignored.

$$\Delta G^\circ \leq \lambda \left(1 - \left[9.2 RT (11.78 - \log k_{-d}) / \lambda \right]^{1/2} \right) \quad (2.12)$$

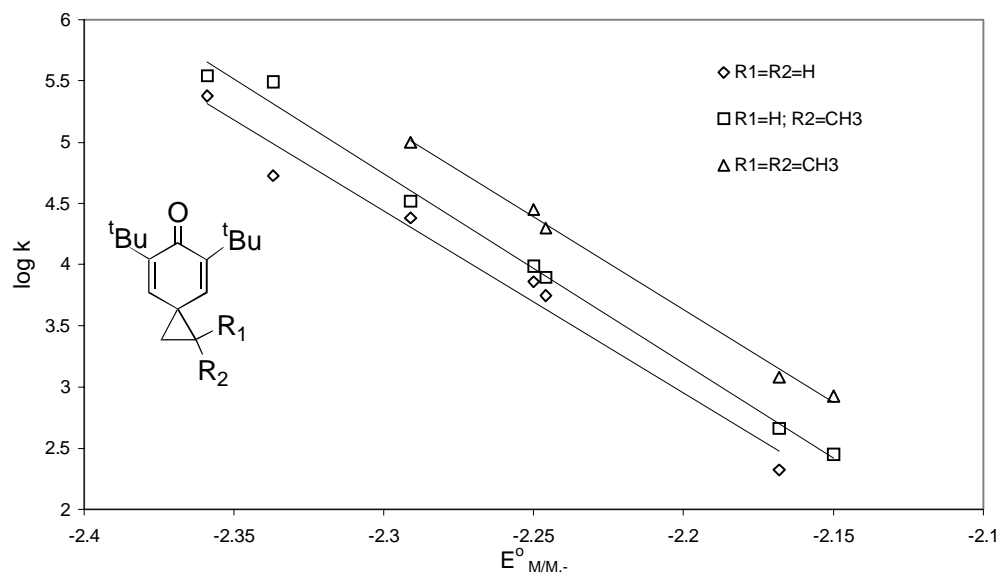


Figure 2.9. Log k as a function of the reduction potential of the mediator M/M^\bullet .

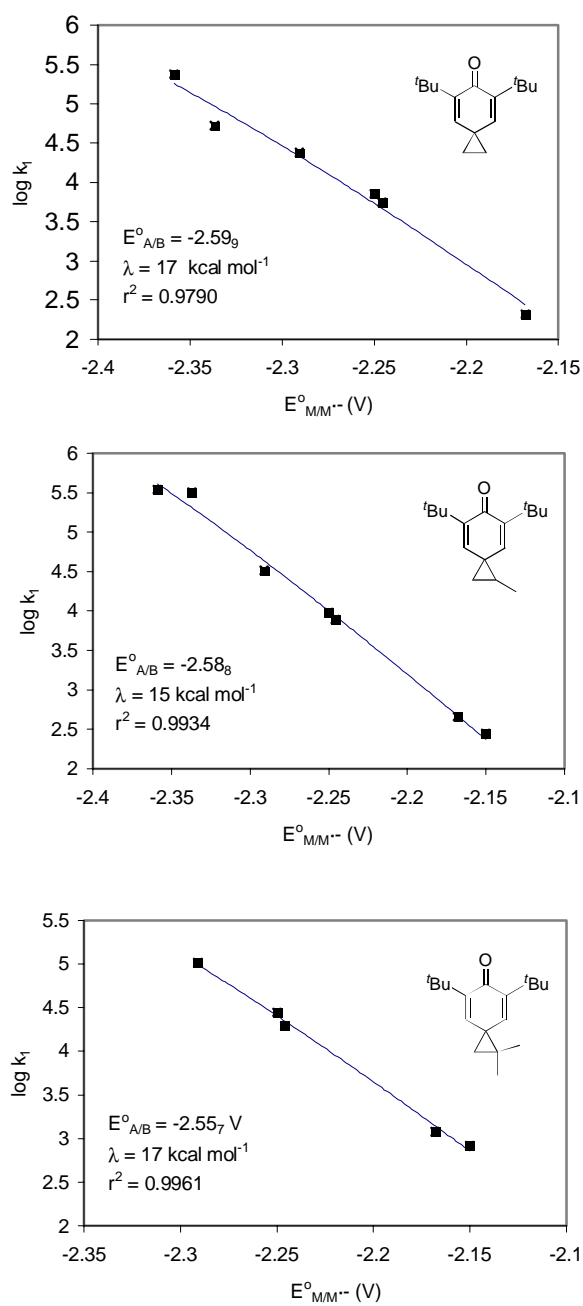


Figure 2.10. $E^{\circ}_{A/B}$ and λ derived from fit of \log rate constant data to Eq. 2.11, see text.

The rate constants in Table 2.2 were fit to Eq. 2.11 via non-linear regression analysis,⁶⁹ with $E^{\circ}_{A/B}$ and λ as the only adjustable parameters. An excellent fit was

achieved in all cases (the dotted lines in Figure 2.10 represent the predicted values based upon this treatment), and E° 's and λ values were obtained (Table 2.3).

Table 2.3. Reduction potentials and reorganization energies for **13a**, **13b**, and **13c**

Compound	E° (V) ^a	λ (kcal/mol)
13a	$-2.59_9 \pm 0.011$	17 ± 2
13b	$-2.58_8 \pm 0.005$	15 ± 1
13c	$-2.55_7 \pm 0.005$	17 ± 1
17	-2.574 ± 0.004	---

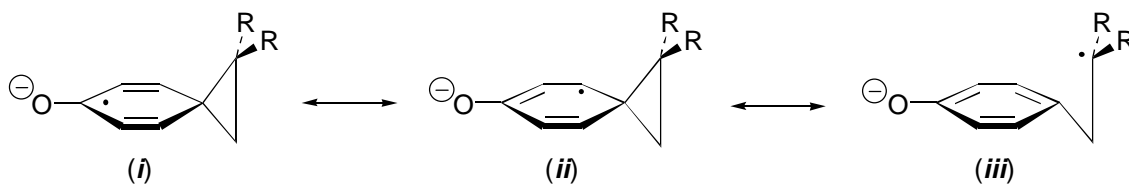
^avs. 0.1 M Ag^+/Ag

Reorganization energy (λ) values derived for **13a**, **13b**, and **13c** are reasonable, considering the molecular functionality involved in these reactions (*i.e.*, electron transfer from an aromatic hydrocarbon to a conjugated ketone) suggesting that there is not an additional contributor (such as bond lengthening or bond angle changes) to the overall reorganization energy associated with these electron transfers. This provides additional indication that ring opening occurs *after* electron transfer and these radical anions exist as discrete intermediates.

E° values derived from this analysis warrant further discussion. It is especially noteworthy that the derived E° 's for **13(a-c)** compare favorably to model compound **17**. The CV of **17** (experiment performed by Dan Berger) is characterized by a fully reversible, one-electron reduction wave from which $E^\circ_{17/17\bullet-}$ was determined directly ($E^\circ_{17/17\bullet-} = -2.574$ V vs. 0.1 M Ag^+/Ag).⁷³ This agreement suggests that the assumptions

of this analysis are correct (*i.e.*, electron transfer is under mixed kinetic control), and thus provides additional evidence that electron transfer is stepwise, not concerted). Within experimental and statistical error, the E° values obtained for **13a**, **13b**, and **13c** are different. This same difference is also reflected in the individual rate constants obtained for any mediator (Table 2.2). With increased alkyl substitution on the cyclopropyl group, electron transfer becomes kinetically and thermodynamically more favorable. These observations can be nicely explained in light of the conjugative properties of the cyclopropyl group,⁷⁴ depicted using resonance structures in Scheme 2.11, which stabilize the radical anion. Contribution of resonance form (iii) to the resonance hybrid is expected to be important because of its aromatic character,⁷⁵ and should be greater for R = CH₃ compared to R = H.

Scheme 2.11

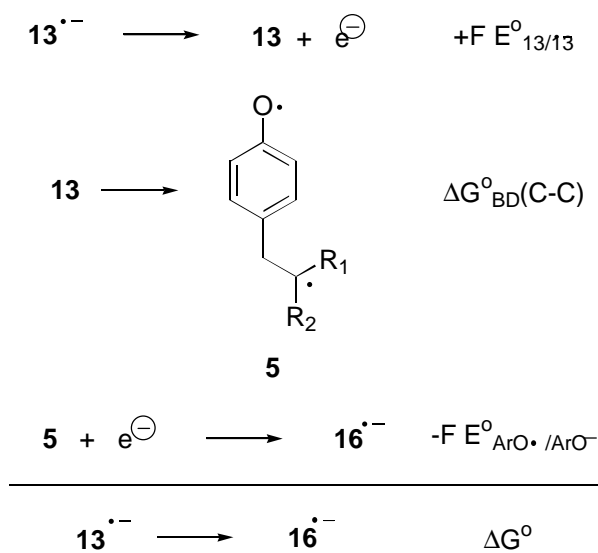


2.2.5 Thermodynamics of ring opening for **13a^{•-}**, **13b^{•-}**, and **13c^{•-}**

ΔG° for ring opening of **13a^{•-}**, **13b^{•-}**, and **13c^{•-}** can be determined utilizing the thermochemical cycle depicted in Scheme 2.12 ($\Delta G^{\circ} = \Delta G^{\circ}_{\text{BD(C-C)}} + F(E^{\circ}_{13/13^{\bullet-}} - E^{\circ}_{\text{ArO}^{\bullet}/\text{ArO}^-})$). Three thermodynamic values are needed to solve for ΔG° 1) the standard potential of the spiro[2.5]octa-4,7-dien-6-one ($E^{\circ}_{\text{A/B}}$ obtained in this study, Table 2.3), 2)

the standard potential of the $\text{ArO}\bullet/\text{ArO}^-$ couple (estimated to be -0.680 V based upon the cyclic voltammogram of 2,4,6-tri-*t*-butyl phenoxide anion),⁶³ and 3) the strength of the C-C bond of the cyclopropyl group ($\Delta G^\circ_{\text{BD}}(\text{C-C})$). It is assumed that ΔS for this unimolecular process is small and $\Delta G^\circ_{\text{BD}}(\text{C-C}) \approx \text{BDE}_{\text{C-C}}$. This procedure for estimating ΔG° for ring opening is especially attractive because the pertinent reduction potentials used in this analysis were obtained in this laboratory and should adequately account for any effect of solvent and/or electrolyte.

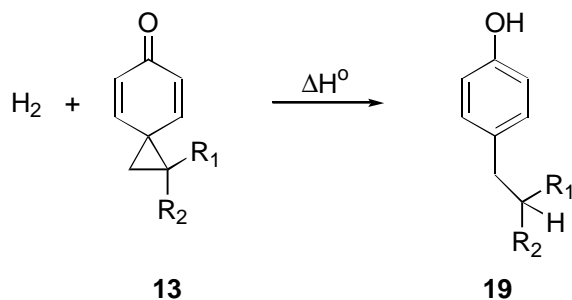
Scheme 2.12



The strength of the cyclopropyl C-C in **13a**, **13b**, and **13c** was estimated according to Scheme 2.13, where ΔH_f° 's for the pertinent species were obtained using semi-empirical molecular orbital theory (PM3, details are provided in section 2.4),⁷⁶ and literature values for the bond dissociation energies: $\text{BDE}(\text{PhO-H}) = 90.4\text{ kcal/mol}$,⁷⁷

BDE(1°C-H) = 100.0 kcal/mol, BDE(2°C-H) = 98.5 kcal/mol, and BDE(3°C-H) = 95.6 kcal/mol.⁷⁸ We assume that these calculated values for BDE(C-C) are the same in the gas phase and in solution.⁷⁹ Results of this analysis are summarized in Table 2.4.

Scheme 2.13



$$\begin{aligned} \Delta H^\circ &= \Delta H_f^\circ(19) - \Delta H_f^\circ(13) \\ &= \text{BDE}(\text{H}_2) + \text{BDE}(\text{C-C}) - \text{BDE}(\text{OH}) - \text{BDE}(\text{C-H}) \end{aligned}$$

Table 2.4. Estimated ΔG° for ring opening of **13a^{•-}**, **13b^{•-}**, and **13c^{•-}**

Reaction	ΔG° (kcal/mol)
13a^{•-} → 18a^{•-}	-11.2
13b^{•-} → 16b^{•-}	-13.2
13b^{•-} → 18b^{•-}	-10.0
13c^{•-} → 16c^{•-}	-13.3
13c^{•-} → 18c^{•-}	-5.3

2.3 CONCLUSIONS

Radical anions derived from **13a**, **13b**, and **13c** undergo facile ring opening, with rate constants $\geq 10^7 \text{ s}^{-1}$. Based upon the values of α observed in the direct electrochemistry of these compounds, the reorganization energy (λ) derived from the mediated reductions, and the fact that the derived E^{01} 's closely match model compound **17**, we conclude that these radical anions have a finite lifetime (*i.e.*, electron transfer and ring opening are not concerted). For unsymmetrical radical anions **13b^{•-}** and **13c^{•-}**, ring opening yielded preferentially the more substituted (stabilized) distonic radical anion. These results also provide evidence for stabilization of these radical anions via conjugative interactions with the cyclopropyl group, decreasing in the order **13c^{•-}** > **13b^{•-}** > **13a^{•-}**. Both the rapid rate and selectivity associated with the ring opening of these radical anions can be exploited in the utilization of these substrates as "probes" for single electron transfer.

2.4 GRAPHICAL ANALYSIS AND SUPPLEMENTAL PLOTS

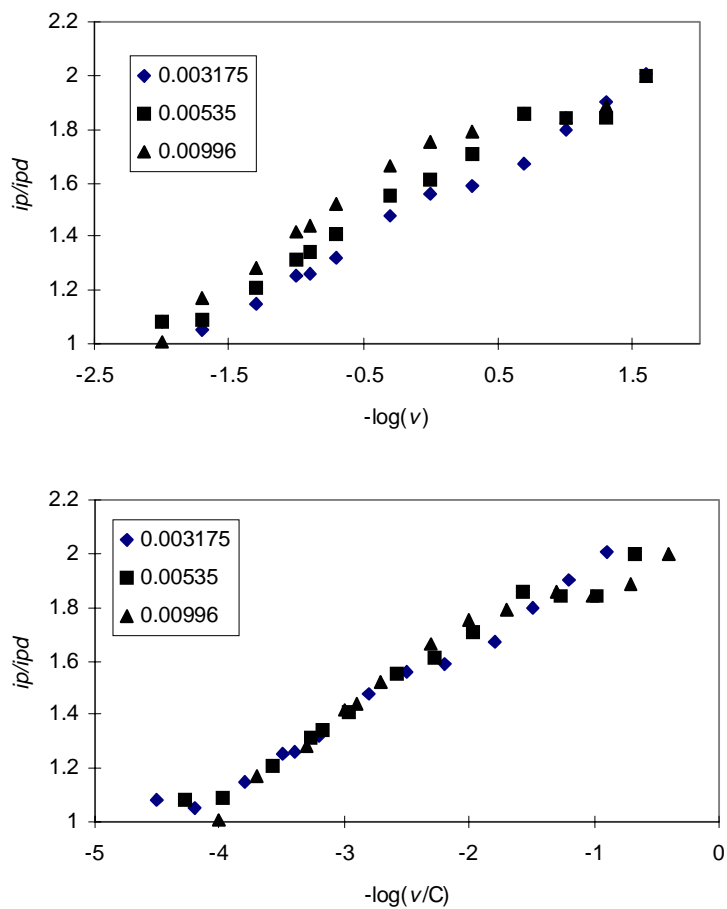


Figure 2.11. Mediated reduction of **13c** with 9,10-diphenylanthracene. (DMF, GCE, TBAP, $v = 0.025 - 10$ V/s)

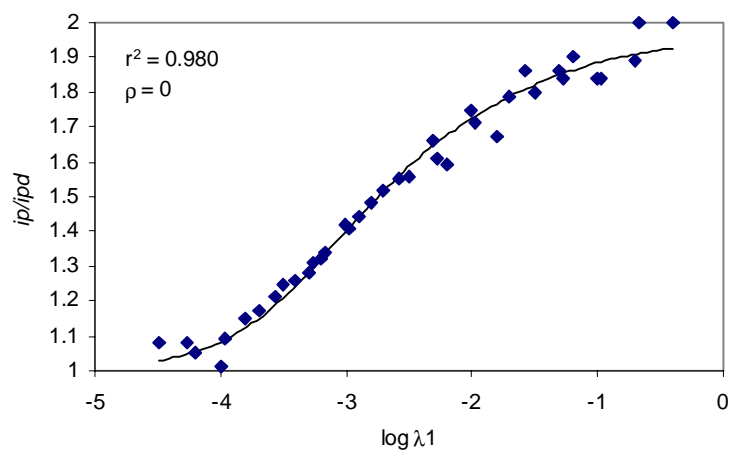


Figure 2.12. Non-linear fitting of results for **13c** + 9,10-diphenylanthracene ($x' = 2.855 \pm 0.026$)

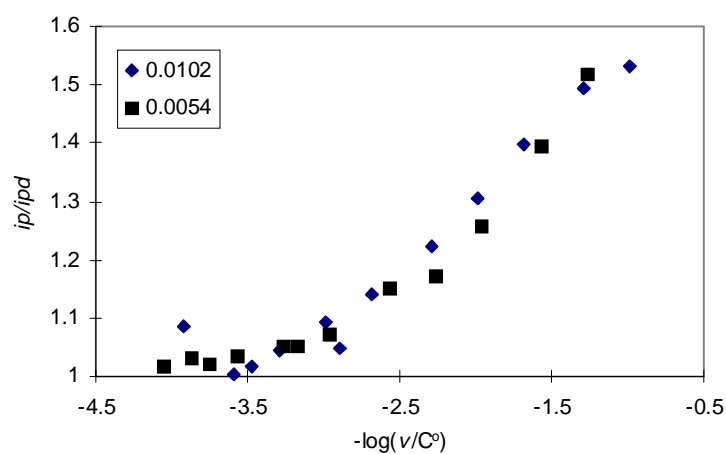
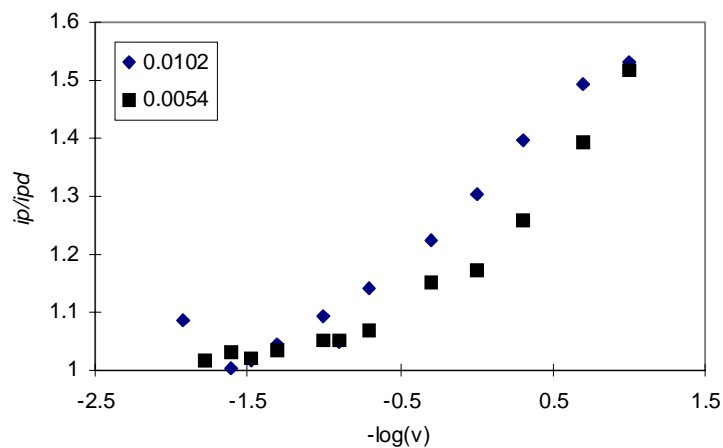


Figure 2.13. Mediated reduction of **13c** with 4-cyanopyridine. (DMF, GCE, TBAP, $v = 0.1 - 85$ V/s)

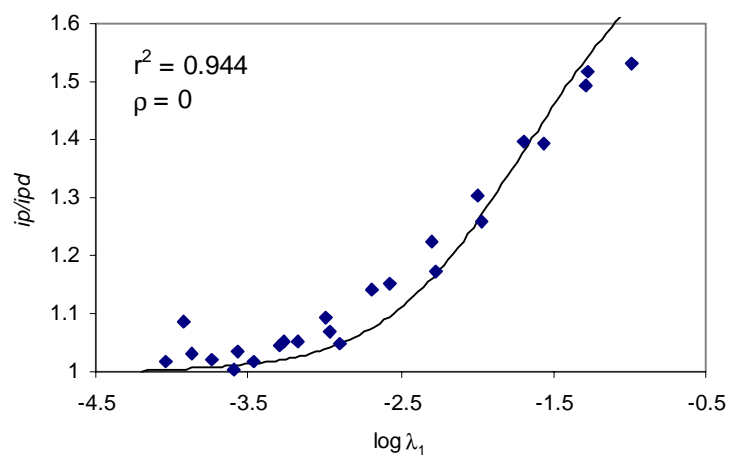


Figure 2.14. Non-linear fitting of results for **13c** + 4-cyanopyridine ($x' = 1.494 \pm 0.037$)

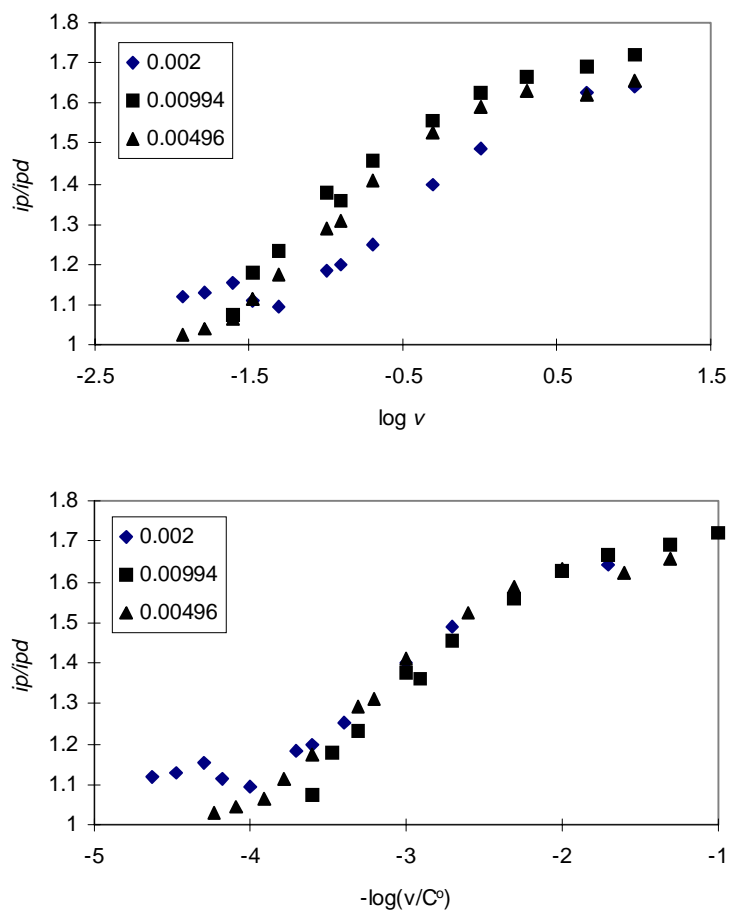


Figure 2.15. Mediated reduction of **13c** with 1-cyanonaphthalene. (DMF, GCE, TBAP, $v = 0.10 - 40$ V/s)

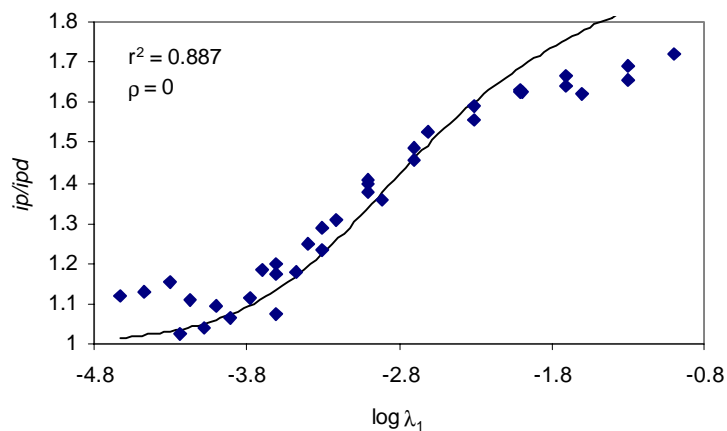


Figure 2.16. Non-linear fitting of results for **13c** + cyanonaphthalene ($x' = 2.701 \pm 0.048$)

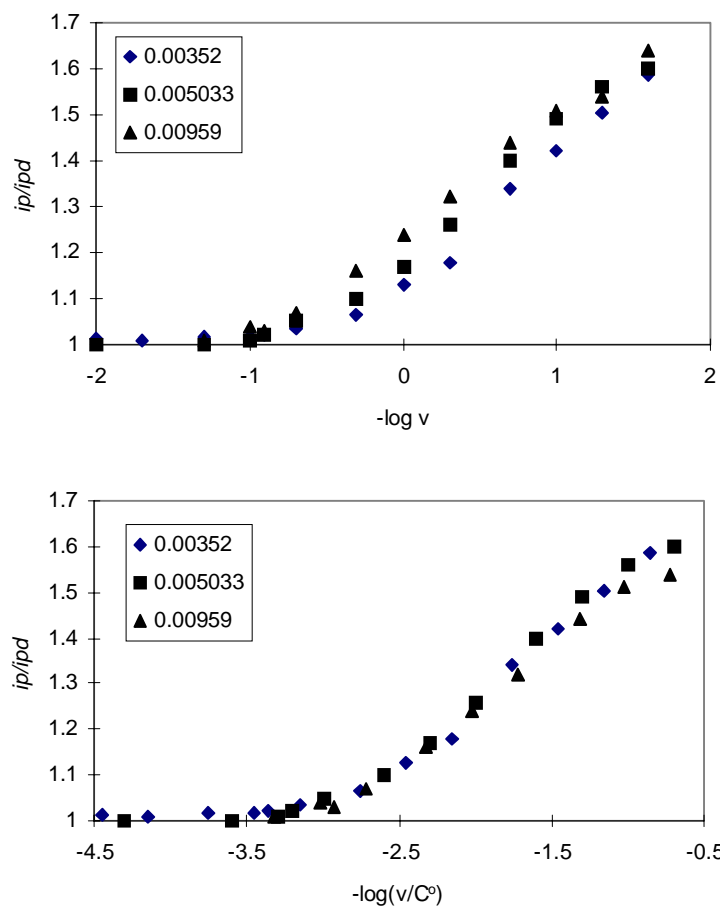


Figure 2.17. Mediated reduction of **13c** with fluoranthene. (DMF, GCE, TBAP, $v = 0.025 - 100$ V/s)

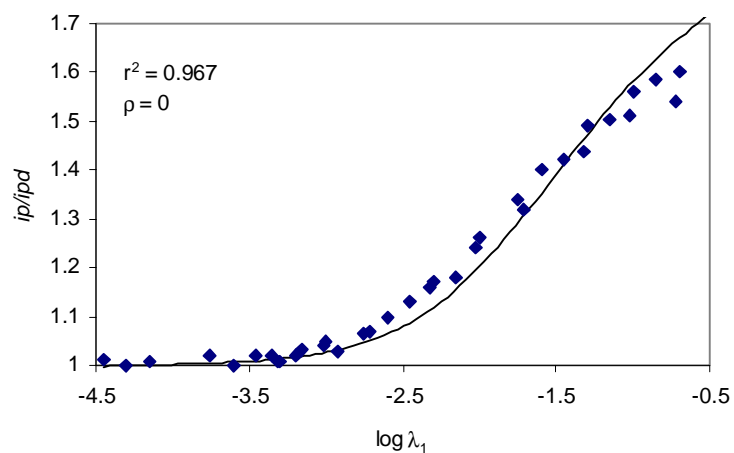


Figure 2.18. Non-linear fitting of results for **13c** + fluoranthene ($x' = 1.333 \pm 0.028$)

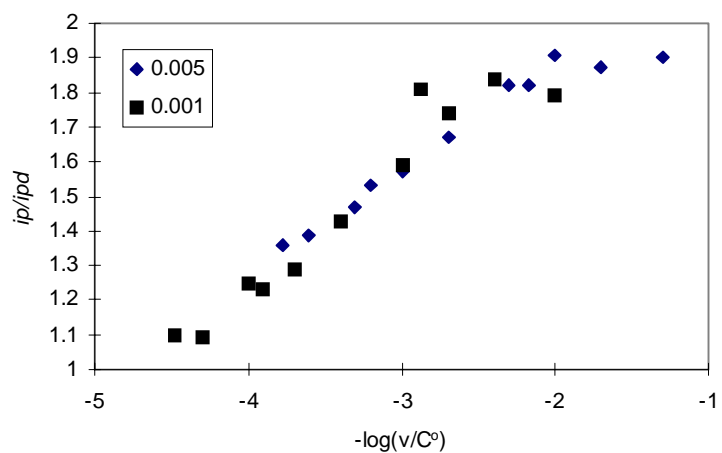
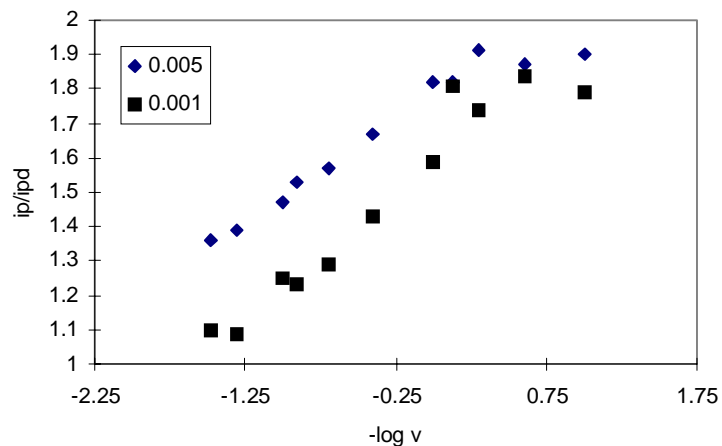


Figure 2.19. Mediated reduction of **13c** with 9-phenylanthracene. (DMF, GCE, TBAP, $v = 0.1 - 30$ V/s)

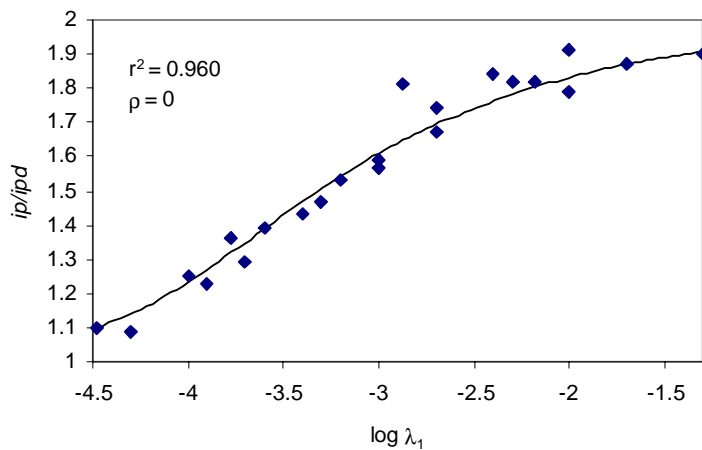


Figure 2.20. Non-linear fitting of results for **13c** + 9-phenylanthracene ($x' = 3.424 \pm 0.039$)

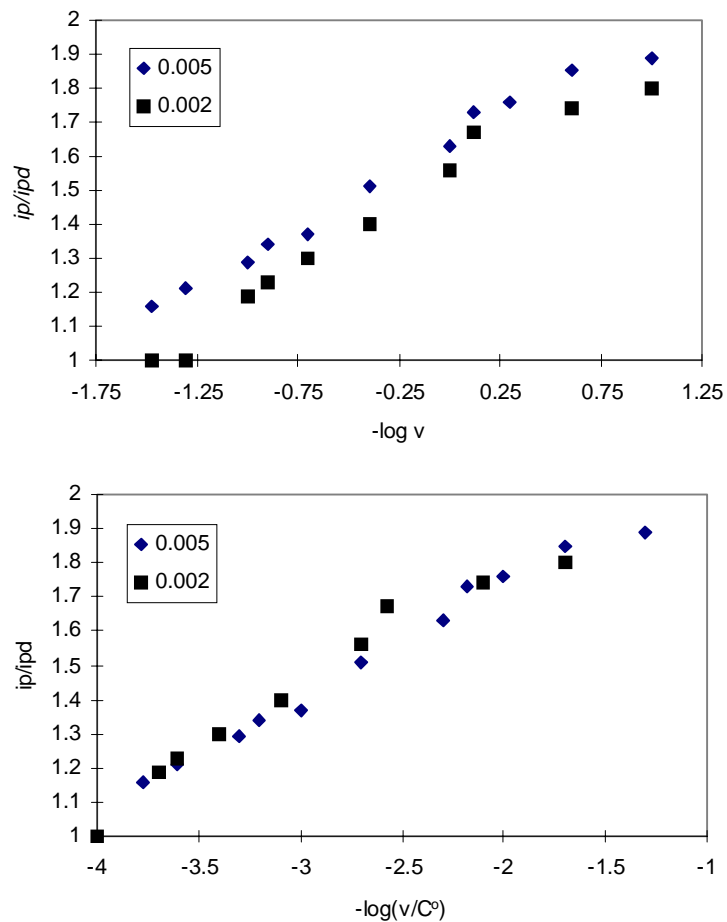


Figure 2.21. Mediated reduction of **13b** with 9-phenylanthracene. (DMF, GCE, TBAP, $v = 0.1 - 30 \text{ Vs}^{-1}$)

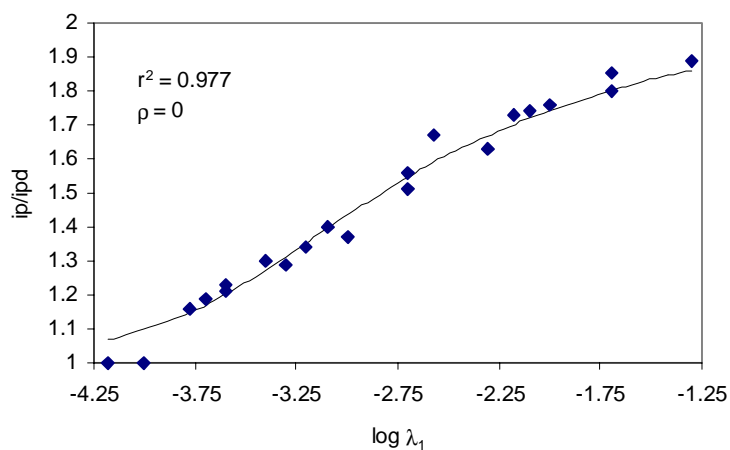


Figure 2.22. Non-linear fitting of results for **13b** + 9-phenylanthracene ($x' = 2.932 \pm 0.031$)

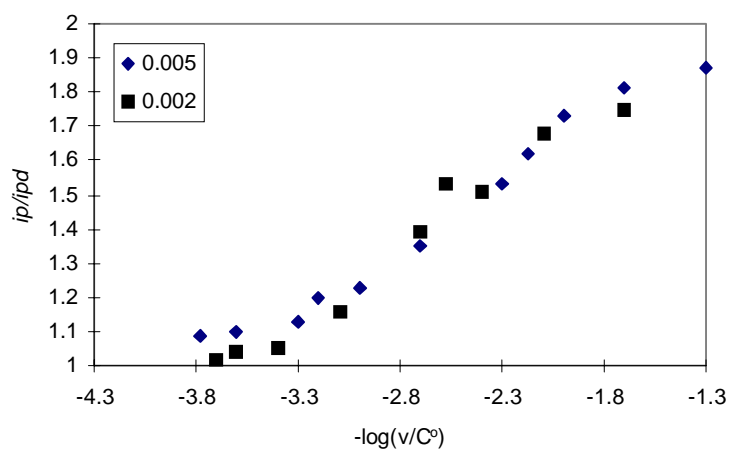
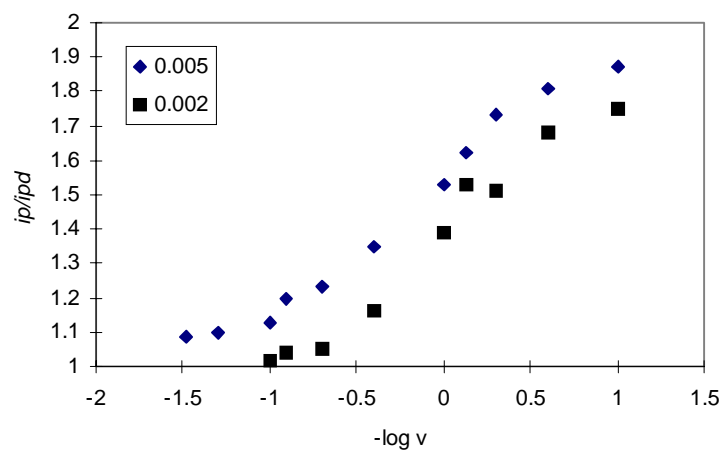


Figure 2.23. Mediated reduction of **13b** with 9,10-diphenylanthracene. (DMF, GCE, TBAP, $v = 0.1 - 30$ V/s)

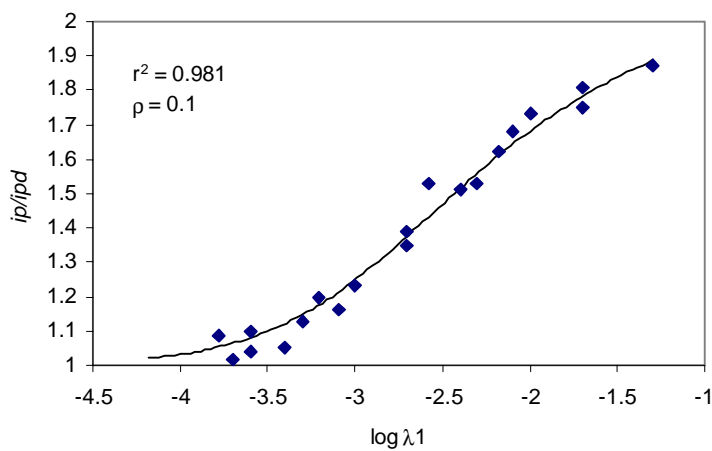


Figure 2.24. Non-linear fitting of results for **13b** + 9,10-diphenylanthracene ($x' = 2.398 \pm 0.027$)

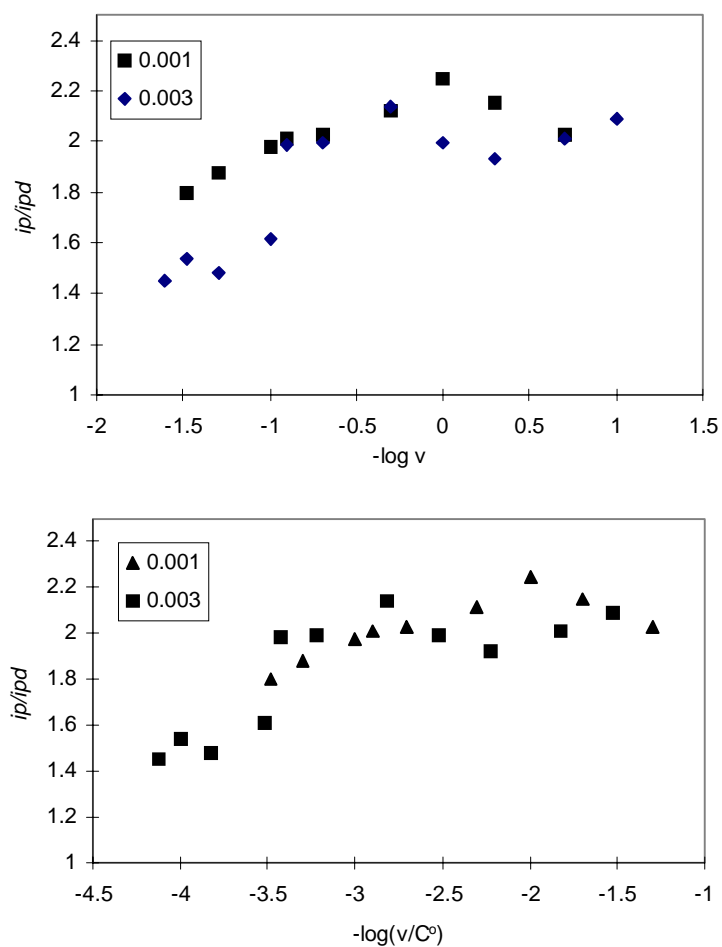


Figure 2.25. Mediated reduction of **13b** with anthracene. (DMF, GCE, TBAP, $v = 0.025 - 20$ V/s)

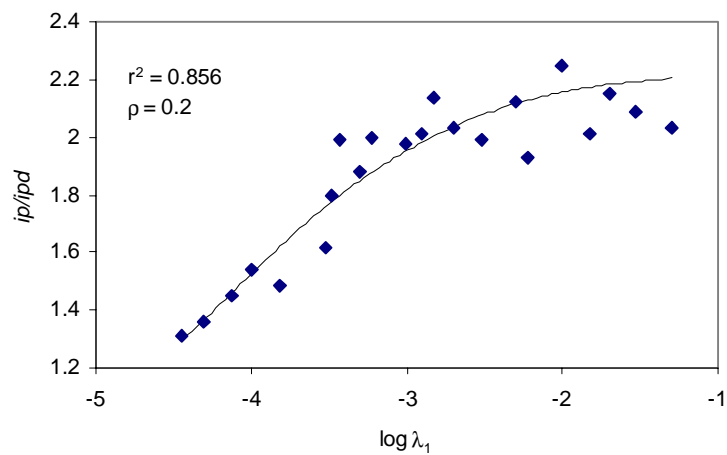


Figure 2.26. Non-linear fitting of results for **13b** + anthracene ($x' = 3.904 \pm 0.067$)

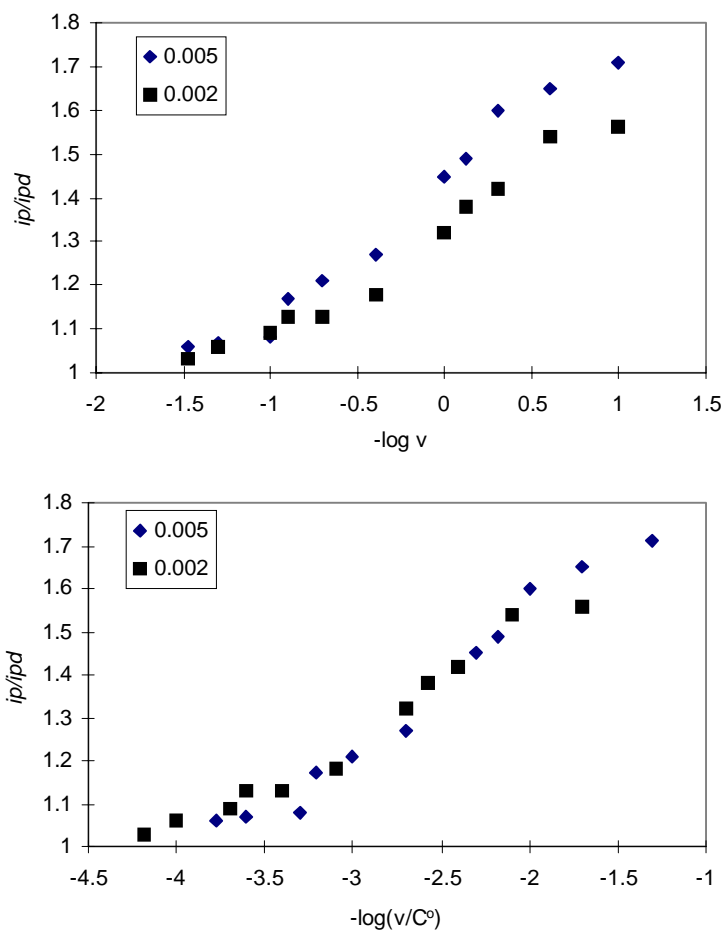


Figure 2.27. Mediated reduction of **13b** with cyanonaphthalene. (DMF, GCE, TBAP, $v = 0.1 - 30$ V/s)

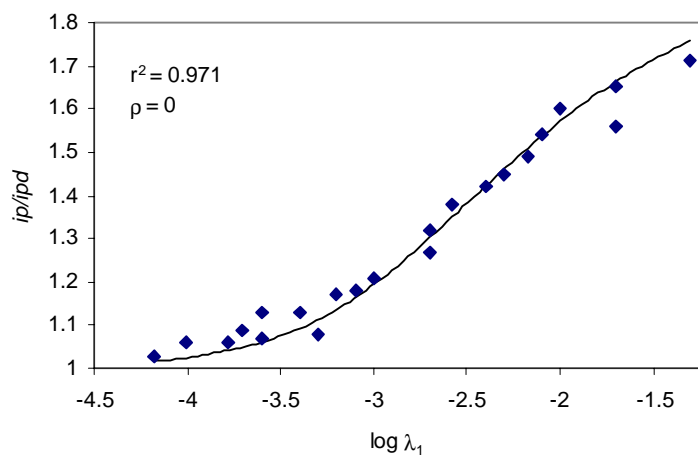


Figure 2.28. Non-linear fitting of results for **13b** + cyanonaphthalene ($x' = 2.305 \pm 0.028$)

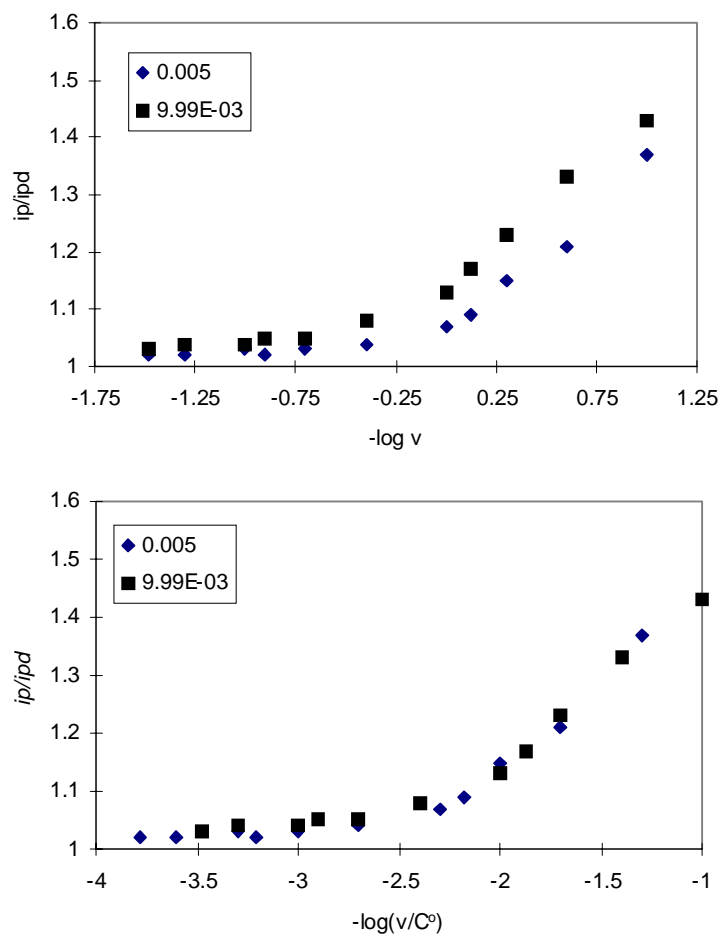


Figure 2.29. Mediated reduction of **13b** with 4-cyanopyridine. (DMF, GCE, TBAP, $v = 0.1 - 30$ V/s)

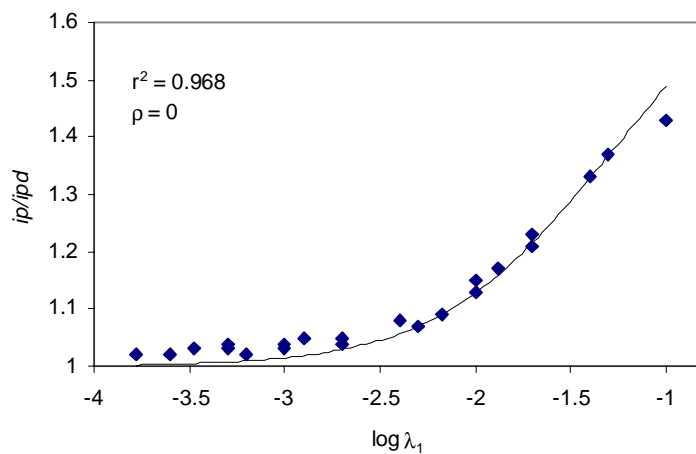


Figure 2.30. Non-linear fitting of results for **13b** + 4-cyanopyridine ($x' = 1.072 \pm 0.022$)

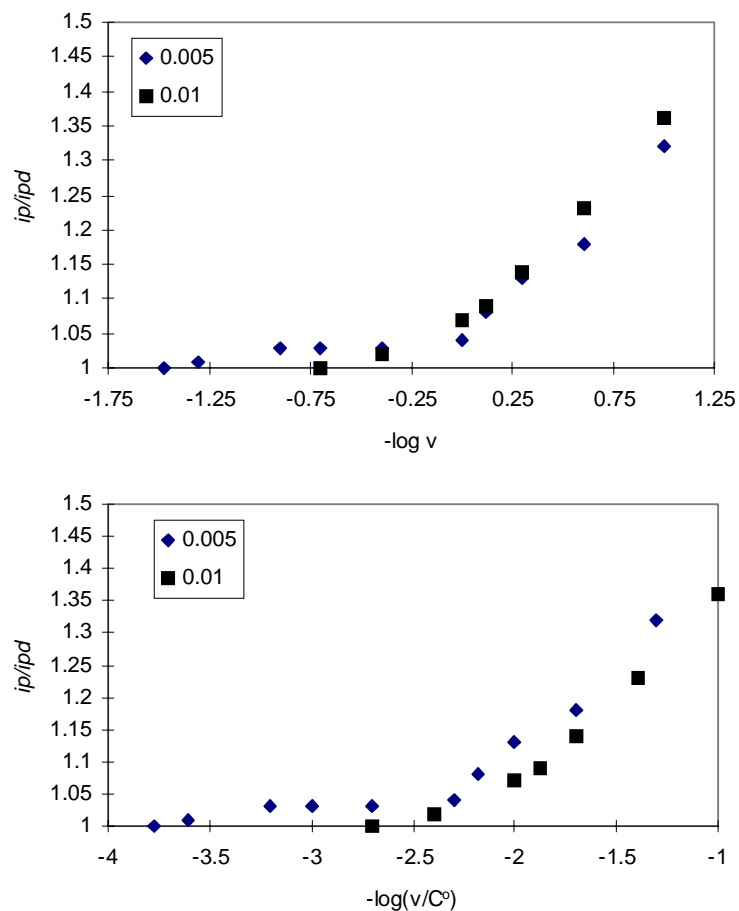


Figure 2.31. Mediated reduction of **13b** with fluoranthene. (DMF, GCE, TBAP, $v = 0.1 - 30$ V/s)

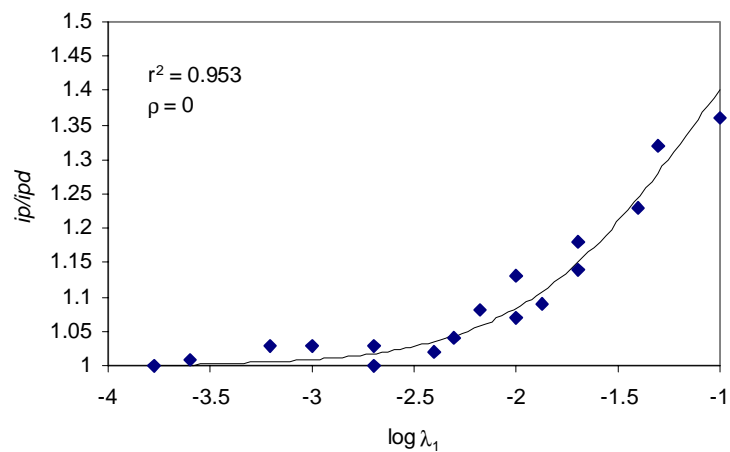


Figure 2.32. Non-linear fitting of results for **13b** + fluoranthene ($x' = 0.855 \pm 0.028$)

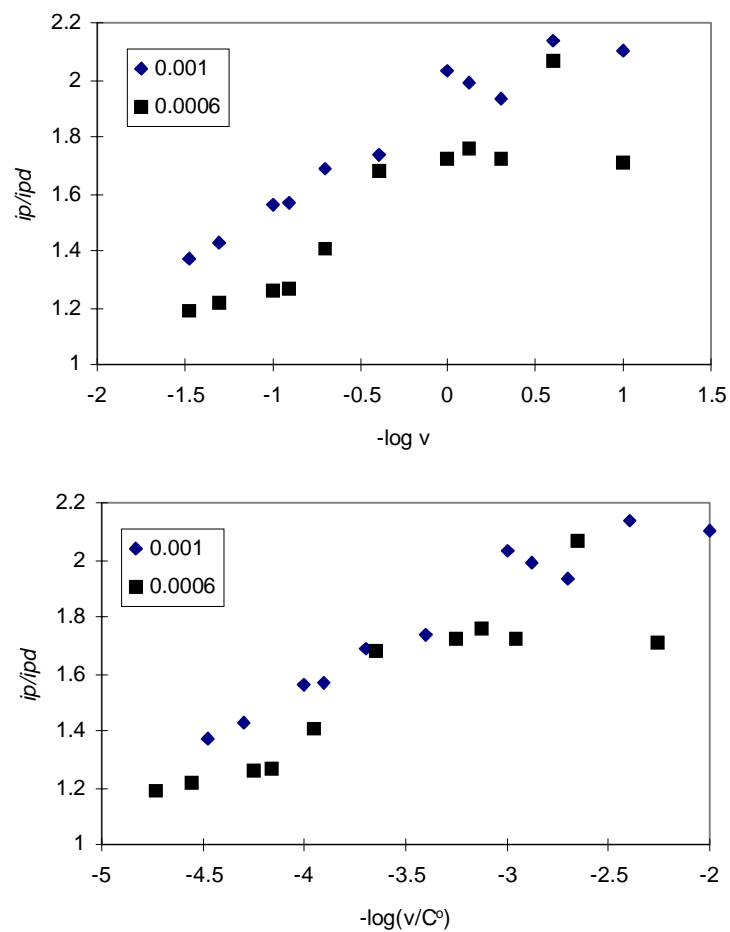


Figure 2.33. Mediated reduction of **13b** with 9-methylantracene. (DMF, GCE, TBAP, $v = 0.1 - 30$ V/s)

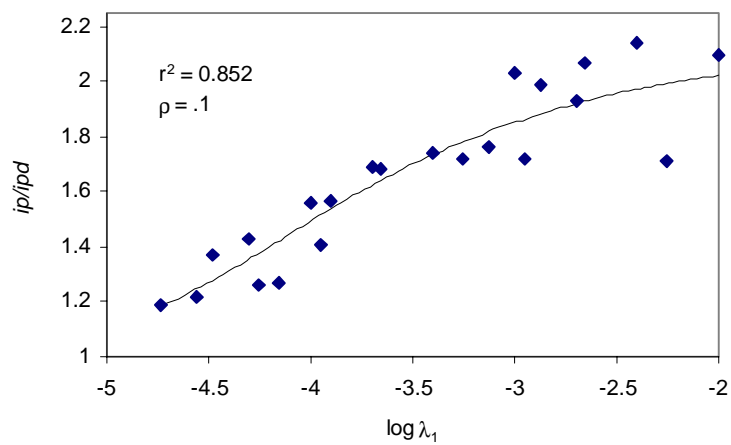


Figure 2.34. Non-linear fitting of results for **13b** + 9-methylantracene ($x' = 3.952 \pm 0.072$)

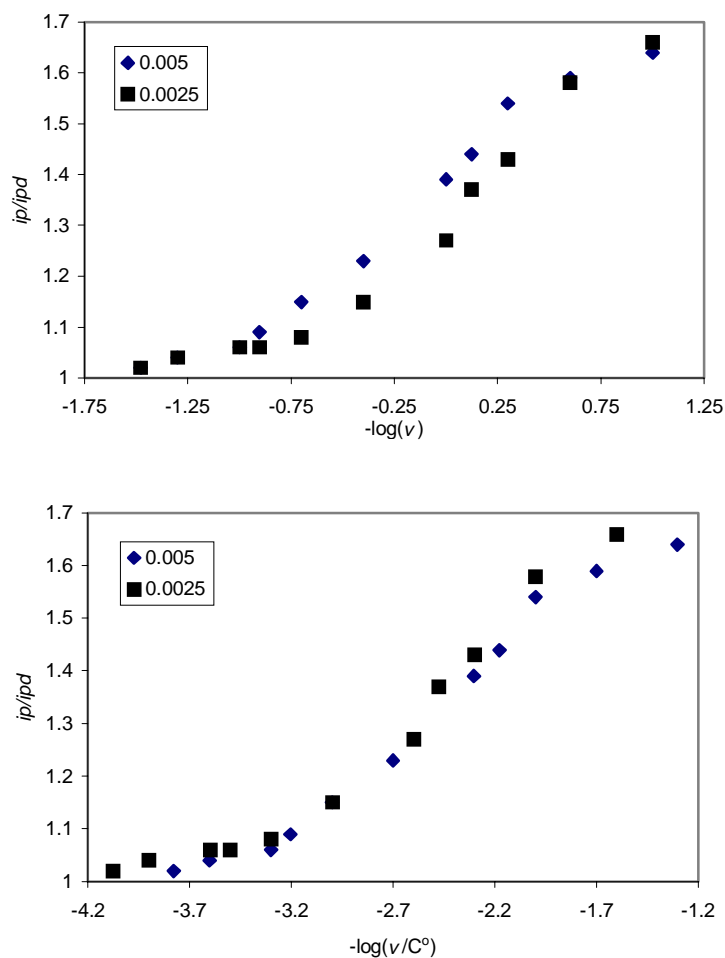


Figure 2.35. Mediated reduction of **13a** with 1-cyanonaphthalene. (DMF, GCE, TBAP, $v = 0.1 - 30$ V/s)

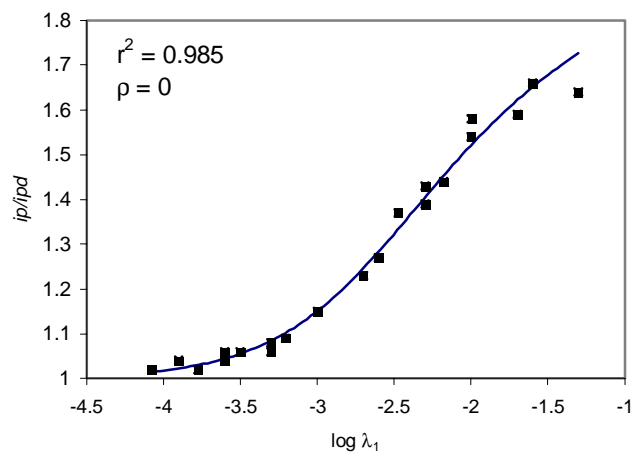


Figure 2.36. Non-linear fitting of results for **13a** + 1-cyanonaphthalene ($x' = 2.159 \pm 0.022$)

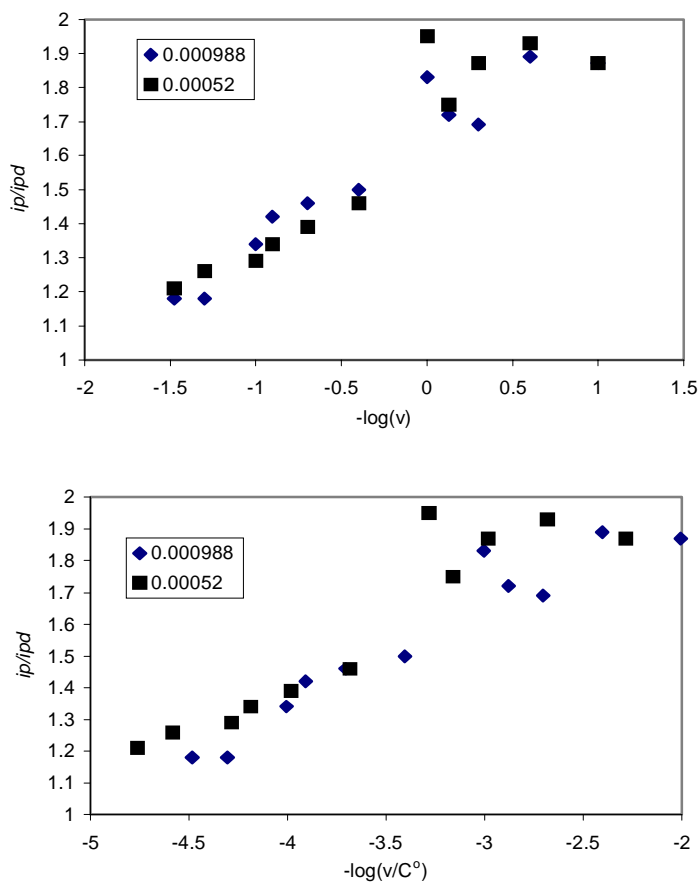


Figure 2.37. Mediated reduction of **13a** with 9-methylantracene. (DMF, GCE, TBAP, $v = 0.1 - 30$ V/s)

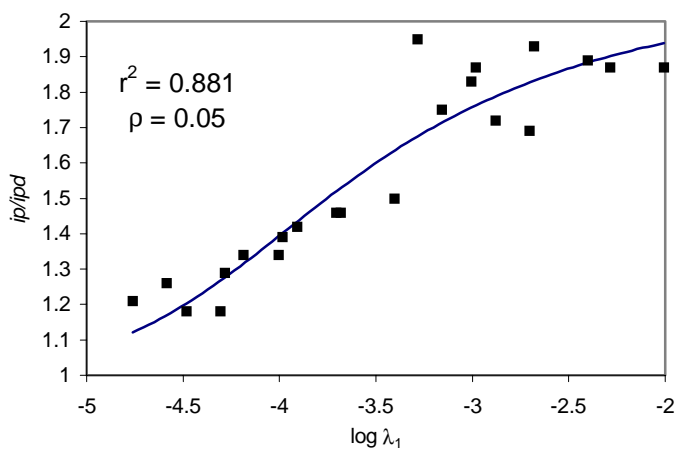


Figure 2.38. Non-linear fitting of results for **13a** and 9-methylantracene ($x' = 3.783 \pm 0.062$)

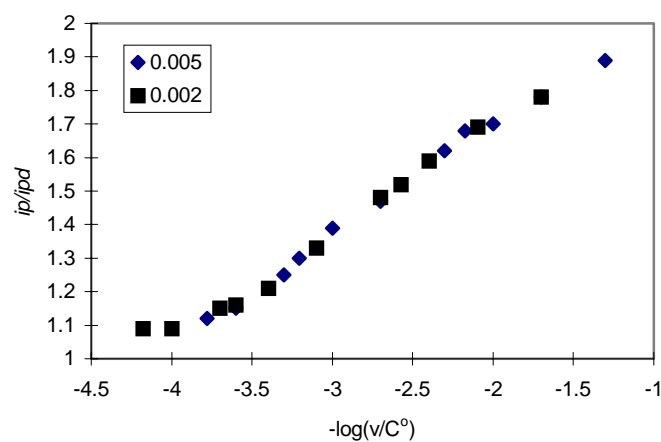
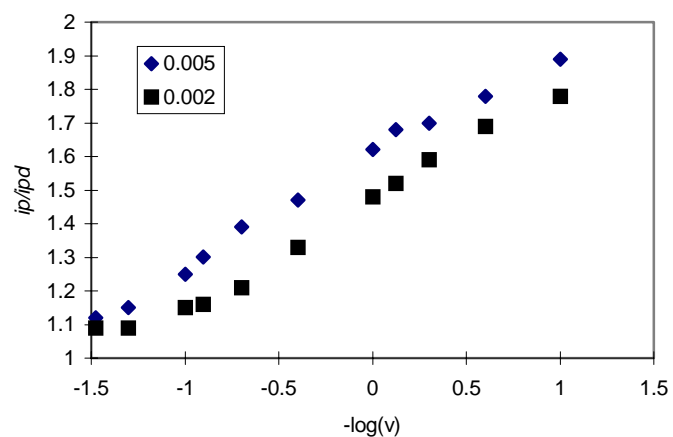


Figure 2.39. Mediated reduction of **13a** with 9-phenylanthracene. (DMF, GCE, TBAP, $v = 0.1 - 30$ V/s)

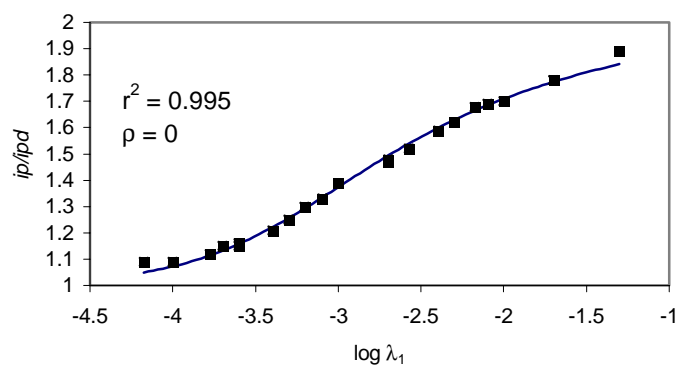


Figure 2.40. Non-linear fitting of results for **13a** and 9-phenylanthracene ($x' = 2.786 \pm 0.013$)

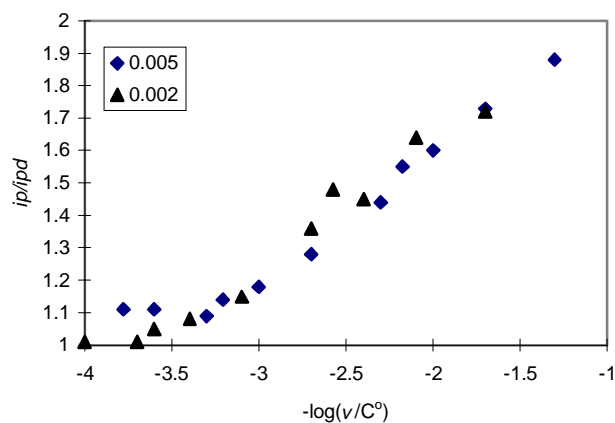
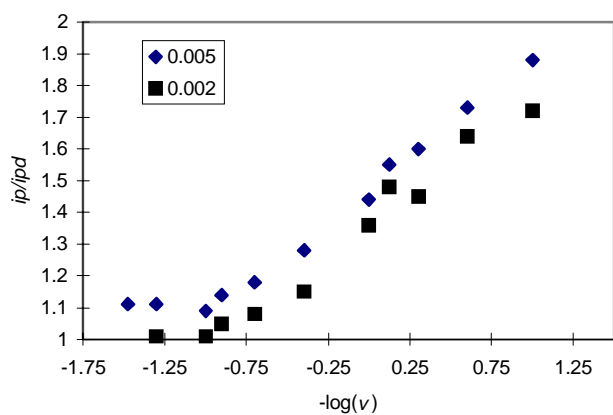


Figure 2.41. Mediated reduction of **13a** with 9,10-diphenylanthracene. (DMF, GCE, TBAP, $v = 0.1 - 30$ V/s)

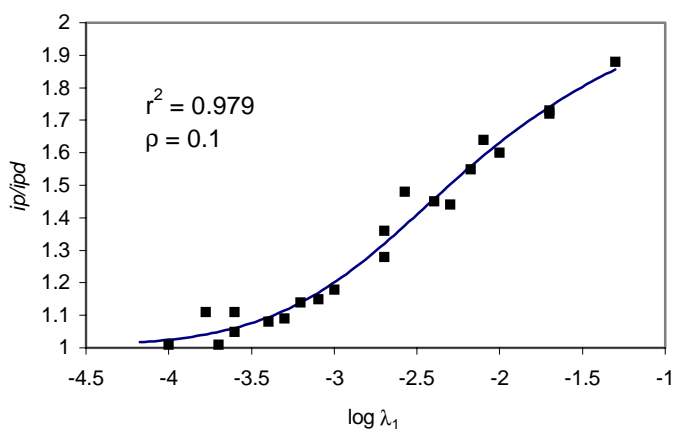


Figure 2.42. Non-linear fitting of results for **13a** and 9,10-diphenylanthracene ($x' = 2.269 \pm 0.027$)

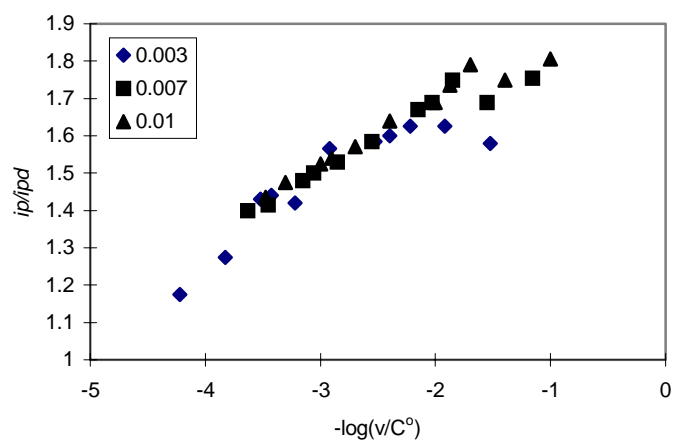
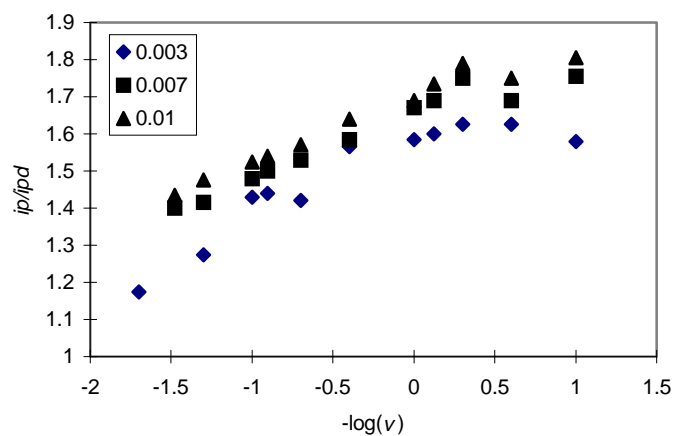


Figure 2.43. Mediated reduction of **13a** with anthracene. (DMF, GCE, TBAP, $v = 0.1 - 30$ V/s)

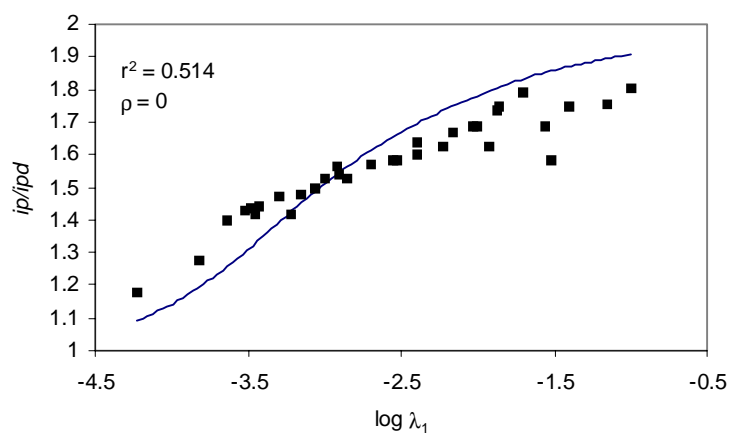


Figure 2.44. Non-linear fitting of results for **13a** + anthracene ($x' = 3.129 \pm 0.062$)

Table 2.5. Comparison of experimental vs. calculated heats of formation of several cyclopropyl-containing compounds

Compound	ΔH_f° (expt.) ^a	ΔH_f° (AM1) ^a	ΔH_f° (PM3) ^a
phenylcyclopropane	36.02 ^b	44.02	42.55
cyclopropane	9.392 ^c 12.74 ^d	17.78	16.27
1,1-dimethylcyclopropane	-1.97 ^e	5.68	0.775
cyclopropyl methyl ketone	-27.56 ^f	-20.16	-25.01
vinylcyclopropane	30.4 ^g	34.95	33.84
spiro[2.4]hepta-4,6-diene	56.8 ^g	69.02	59.29
1,1-divinylcyclopropane	48.2 ^g	53.13	52.46
average error	---	7.1	3.6

^akcal/mol. ^bReference 80. ^cReference 81. ^dReference 82. ^eReference 83. ^fReference 84.
^gReference 85

Table 2.6. Calculated BDE(C-C) based upon Scheme 2.13

Compound	$\Delta H_f^\circ(1)$ ^a	$\Delta H_f^\circ(5)$ ^a	$\Delta H_f^\circ(5')$ ^a	BDE(C ₁ -C ₃) ^a	BDE(C ₂ -C ₃) ^a
1a (R ₁ =R ₂ =H)	17.58	-35.59	---	33.9	33.9
1b (R ₁ =H, R ₂ =CH ₃)	11.03	-41.05	-40.27	32.6	35.8
1c (R ₁ =R ₂ =CH ₃)	3.71	-46.23	-4.49	31.9	39.9

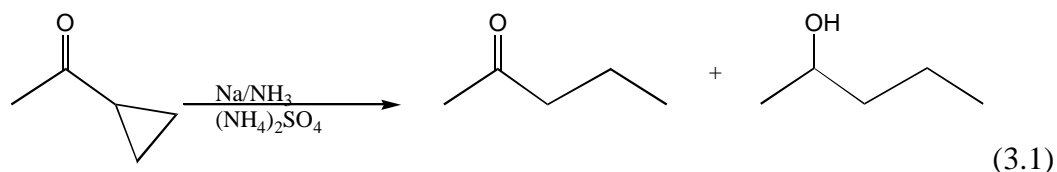
^akcal/mol.

**CHAPTER 3: CATHODIC REDUCTION OF CYCLIC ALIPHATIC KETONES:
CYCLOPROPYL METHYL KETONE, 1-ACYL-2,2-DIMETHYL
CYCLOPROPANE AND CYCLOBUTYL METHYL KETONE**

3.1 INTRODUCTION

A second facet of this research focused on the cathodic reduction of aliphatic cyclopropyl ketones. There are conflicting reports in the literature regarding the integrity of the cyclopropyl ring in aliphatic ketyl radical anions. The ketyl anion generated from dicyclopropyl ketone is reported to be sufficiently stable such that its ESR spectrum can be recorded without any difficulty.⁵⁶ However, other reports indicate that radical anions produced from dissolving metal reductions of aliphatic cyclopropyl ketones yield ring-opened products, which are ascribed to the rearrangement of ketyl anions.^{51,52,53,54,55}

Reduction of methyl cyclopropyl ketone by sodium in liquid ammonia with ammonium sulfate was reported to give a mixture of 2-pentanone



and 2-pentanol (Equation 3.1)⁸⁶. In a detailed analysis, Norin showed that for dissolving metal reductions the ring-opening of aliphatic cyclopropyl ketones occurs in a highly stereospecific manner.⁸⁷ The cyclopropane bond that it cleaved is the one that has the maximum overlap of the Walsh orbitals with the π orbital of the carbonyl group.

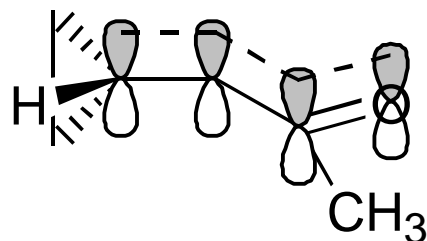
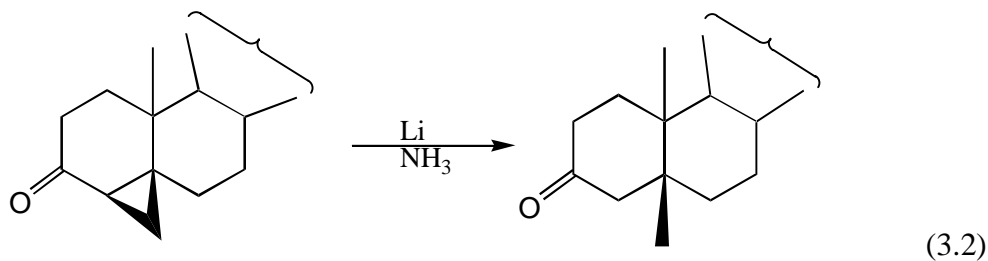
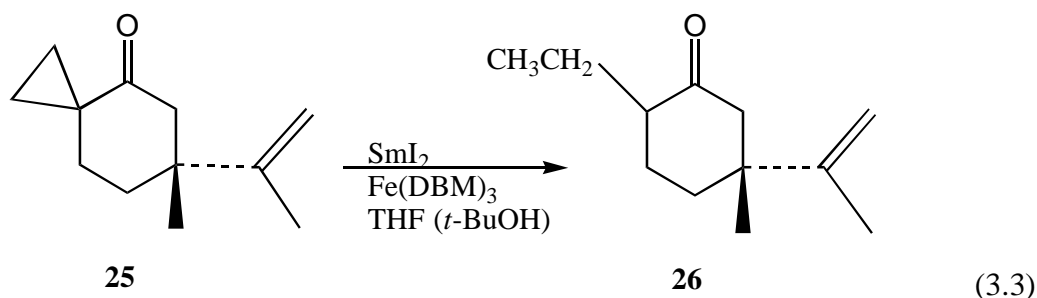


Figure 3.1 Walsh orbital overlap for cyclopropyl methyl ketone

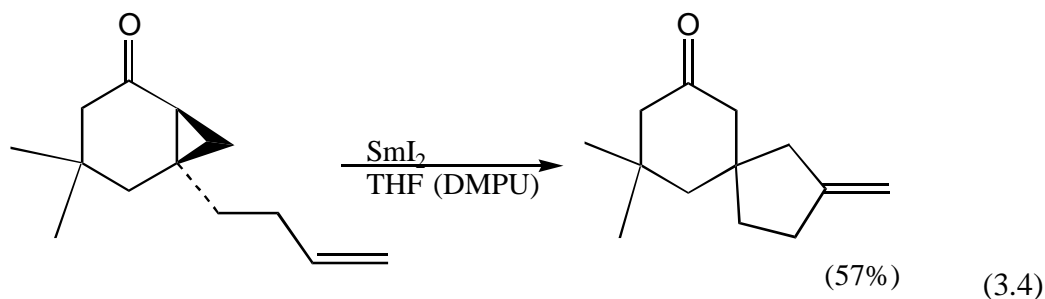
In cyclopropyl rearrangements, geometric requirements of rigid systems have been confirmed, and the importance of electronic vs. steric factors were investigated.⁸⁸ In fact, dissolving metal (Li/NH₃) reduction of aliphatic cyclopropyl ketones is now a classic procedure for introducing angular methyl groups in steroid synthesis (Equation 3.2).⁸⁸



Samarium iodide (SmI₂) has emerged as an efficient reagent for ketyl anion generation from aliphatic cyclopropyl ketones ($E^{\circ} = -1.55$ V vs. SCE for $\text{Sm}^{+3} + e^{-} \rightarrow \text{Sm}^{+2}$).¹⁷ Molander reported in 1991 that reduction of ketone **25** with SmI₂ yields ring-opened product **26** in 81% overall yield (Equation 3.3).⁸⁹



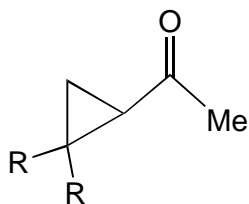
Bately and Motherwell have reported other interesting SmI_2 reductions of aliphatic cyclopropyl ketones.⁹⁰ These reductions involve subsequent addition of the ring-opened radical anion onto a remote $\text{C}=\text{C}$ or $\text{C}\equiv\text{C}$, forming a new cyclic (*e.g.*, Equation 3.4). Interestingly, researchers were also able to alkylate ring-opened enolate anion intermediates with electrophilic reagents. Analogous SmI_2 induced ring openings of cyclopropyl esters were reported in 1994 by Imamoto, Hatajima, and Yoshizawa.⁹¹ In summary, ring-opening reactions involving $\text{C}=\text{O}$ are sensitive to stereoelectronic factors (*i.e.*, the rupturing $\text{C}-\text{C}$ bond must properly overlap with the π system of $\text{C}=\text{O}$) and they are reported to involve ketyl anion intermediates.



Cathodic reduction of aliphatic ketones can be more complex. Reduction of

aliphatic ketones in aprotic organic solvents occurs at potentials that are too negative to exhibit meaningful (if any) voltammetric waves, and therefore standard reduction potentials are unknown. In addition, the effects of counter ion/electrolyte and solvent on radical anion rearrangements are not well understood.

Mairanovskii and coworkers reported that the preparative polarographic reduction of cyclopropyl methyl ketone yields 2-pentanone, exclusively.⁹² These findings support the notion that radical anion intermediates generated electrochemically, instead of chemically, can be equally reliable at yielding ring-opened products. The wealth of information regarding the reliability of cyclopropyl ring openings in aliphatic cyclopropyl ketones suggested that without extended conjugation in the ring-closed radical anion, relief of cyclopropane ring strain may in fact be able to provide a sufficient thermodynamic driving force for the rearrangement. (AM1 semi-empirical MO theory estimates ΔH° for ring-opening of methyl cyclopropyl ketone radical anion to be exothermic by 15 kcal/mol, and to increase with methyl substitution on the cyclopropyl ring, see Table 3.1)⁹³ One of the goals of this project was to develop and characterize suitable substrates which upon one electron reduction undergo rapid and irreversible rearrangement. Compounds **14a** and **14b** appeared promising and a full mechanistic profile of their cathodic reduction was pursued.



14a (R=H)
14b (R=Me)

3.2 RESULTS AND DISCUSSION

3.2.1 Direct electrochemical reduction of **14a** and **14b**.

Cyclic voltammetry of aliphatic cyclopropyl ketones is problematic at best. Reduction occurs at the solvent limit, the point at which the cell solution becomes susceptible to cathodic reduction resulting in a significant amount of background current. The cyclic voltammogram of cyclopropyl methyl ketone shown in Figure 3.2 is characterized by a small wave attributable to the reduction of substrate superimposed on a large background current attributable to solvent/electrolyte decomposition. At low concentrations and slow sweep rates it is possible to generate the small voltammetric response shown. As concentration or sweep rate is increased, the peak potential is quickly shifted into the background response. Because of these complications, a thorough linear sweep voltammetry study could not be conducted.

A gross estimation of peak width was made (~106 mV) and kinetics for this system, analogous to that observed for spiro series **13(a-c)**, were projected to be controlled by the heterogeneous electron transfer step. An α value was determined ($\alpha = 0.45$) based upon the peak width in accordance with Equation 2.2 (For a detailed discussion of the significance of α see Chapter 2). A value of 0.45 suggests that although the radical anion may be found to rearrange rapidly, it does have a discrete lifetime. The linear sweep voltammetry of 1-acyl-2,2-dimethyl-cyclopropane was not attempted. Given the complications associated with the direct electrochemical reduction of aliphatic ketones, neither the reduction potentials of these substrates nor the rate

constants for ring-opening of their radical anions could be determined from direct electrochemical analysis.

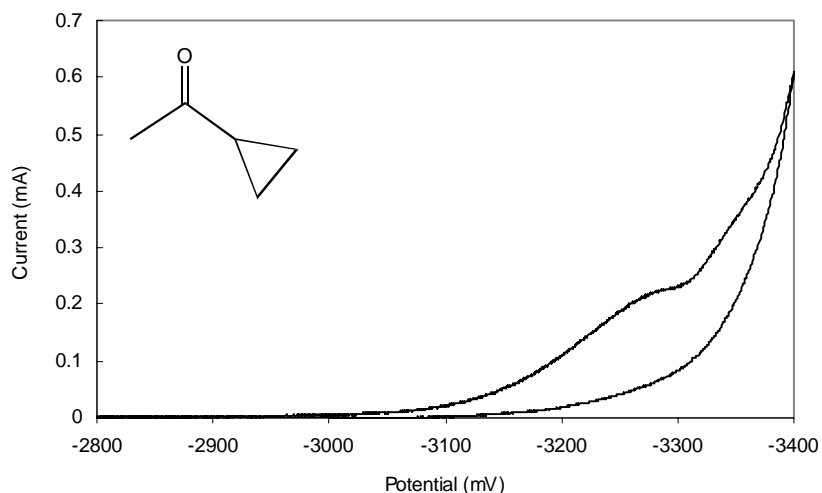
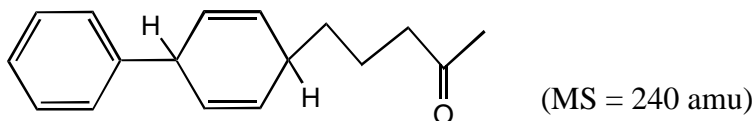
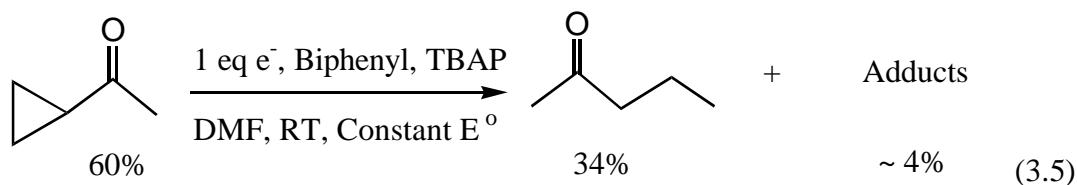


Figure 3.2 Cyclic voltammogram of **14a**. (0.5 M TBAP in DMF, 0.1 M Ag^+/Ag reference, $v = 100$ mV/s, GCE, 0.003 M in substrate)

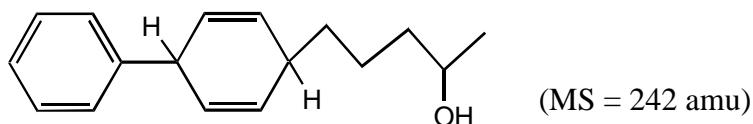
3.2.2 Product analysis from preparative electrolysis of **14a** and **14b**.

Miller and Mahachi demonstrated that functional groups which do not exhibit voltammetric waves can, nevertheless, be preparatively reduced (employing very negative potentials, large excess of charge, tetralkylammonium electrolytes, and a mercury cathode).⁹⁴ However, for this study a mediated reduction using biphenyl radical anion was attempted for cyclopropyl methyl ketone **14a** (Equation 3.5). After passage of 1 eq. of electrons (E^0 constant = -3V vs. AgNO_3/Ag) and acidification, 2-pentanone was obtained in 34% yield, with 60% unreacted starting material. A small amount of addition products (1 major) were detected (^1H NMR, GC/MS; included in section 3.4) but were

not individually isolated. ^1H NMR indicates a substituted biphenyl and a cleaved cyclopropane ring. Potential structures are offered, (**27(a, b)**), but no effort was made to completely discern adduct connectivity. In summary, preparative electrolysis results collaborate previous reports of Mairanovskii and coworkers and support the notion that in a mediated reduction adduct formation (to some defined extent) is expected.

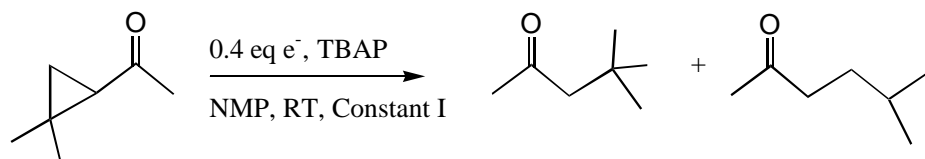


27a



27b

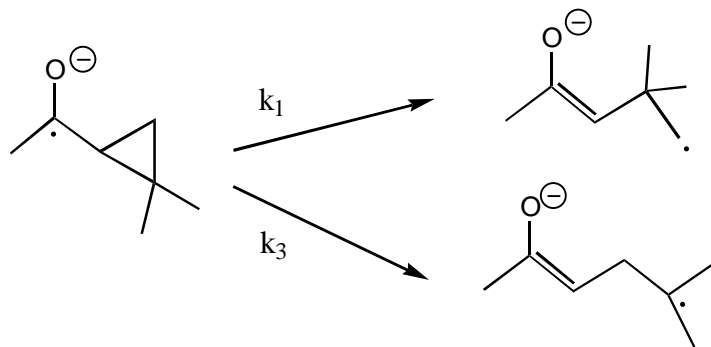
Preparative reduction of 1-acyl-2,2-dimethylcyclopropane (**14b**) (Equation 3.6) gave a mixture of 4,4-dimethyl-2-pentanone and 5-methyl-2-hexanone after 0.4 eq of



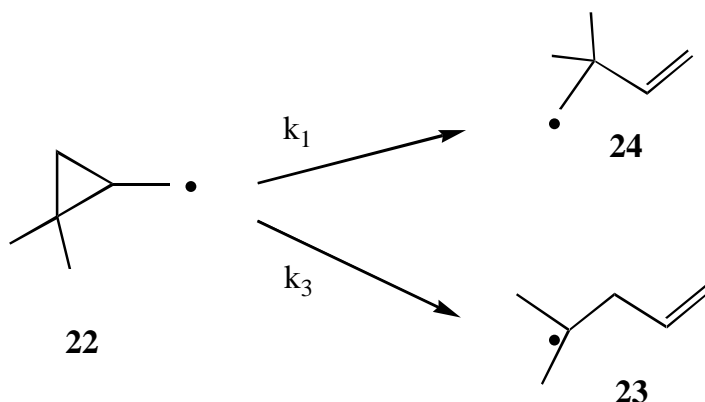
Experiment 1	91%	3%	7%	
Experiment 2	80%	3%	8%	(3.6)

electrons. A mediated reduction, as in the case of **14a**, was not attempted due to the likelihood of an increased amount of adduct formation. The radical anion of **14b** has the potential to rearrange to the primary (k_1) or tertiary (k_3) distonic radical anions shown in Scheme 3.1, and tertiary radicals are known to add to the mediator radical anion more readily than primary radicals.^{97,95}

Scheme 3.1



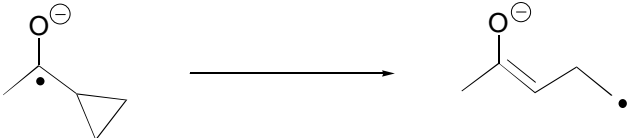
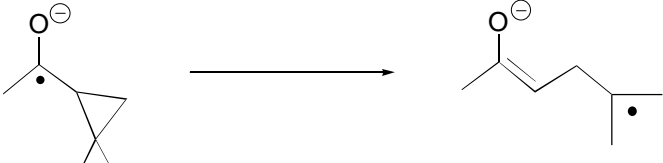
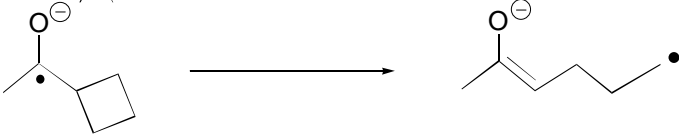
Scheme 3.2



Ring opening occurs with only slight preference for the more-substituted (stable) distonic radical anion. Based upon the yield of products observed in the preparative-scale electrolysis, $k_3/k_1 \cong 2.5$ (Scheme 3.1 and Equation 3.6). Dauben and Wolf obtained similar results ($k_3/k_1 \cong 3.1$) in 1970 with Li/NH_3 as the reducing agent.⁹⁶ For comparison, the dimethyl-substituted radical **22b** leads to 3° and 1° radicals **23b** and **24b** in a 6.7:1 ratio (Scheme 3.2) vs. 2.5:1 for **14b**, and 9.7:1 observed for spiro compound **13c** (Chapter 2). Less selectivity is observed for ring opening of **14b** than for the neutral radical or the spiro compound **13c** from Chapter 2. Invoking the Hammond postulate, this low selectivity suggests a more reactant like transition state for these ring openings. Ring opening of **22** occurs with a rate constant greater than 10^8 s^{-1} . The rate constant for ring opening of **14b** is expected to be of similar magnitude.

AM1 calculations suggest that ring opening of **14a^{•-}** is exothermic by 15 kcal/mol, and increases to 25 kcal/mol for **14b^{•-}** (Table 3.1).

Table 3.1 AM1-calculated enthalpies of reaction for the ring opening of **14a**, **14b**, and **28**.⁹³

Reaction	ΔH_{ro} (kcal/mol)
	-15
	-25
	-1

As in the case of the spiro series **13(a-c)**, these estimates were based upon the difference in ΔH_f° 's for the ring-opened and ring-closed forms of the radical anion, and refer to the gas phase.

3.2.3 Indirect electrochemistry of **14a** and **14b**.

The reduction of **14a** and **14b** by several mediators was studied. As in previous experiments, the current ratio i_p/i_{pd} was examined as a function of sweep rate and mediator concentration at constant excess factor γ ($\gamma = 1$ unless otherwise noted). Figure 3.3 illustrates the effects of added substrate (i_p) to the cyclic voltammogram of biphenyl (i_{pd}). The increased current and loss of reversibility are readily apparent.

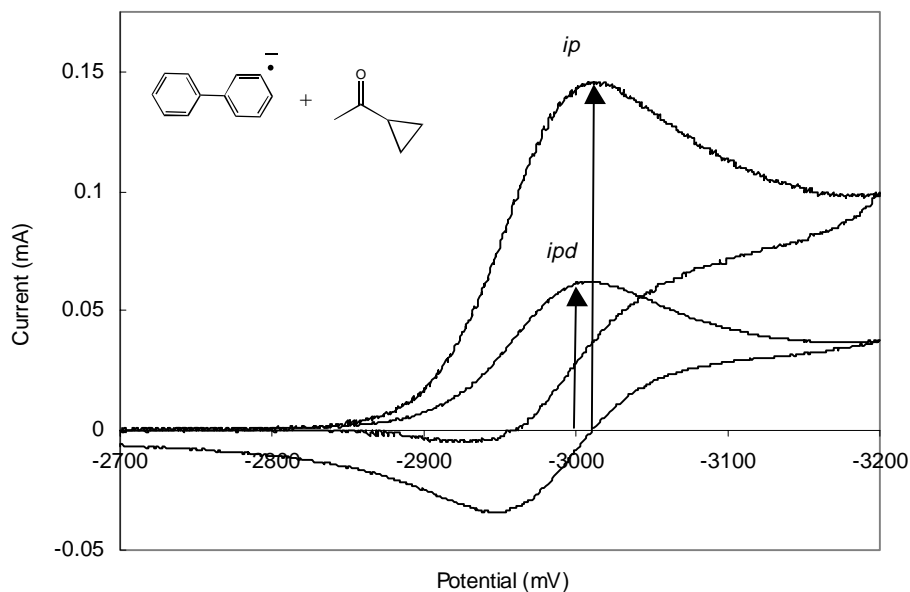
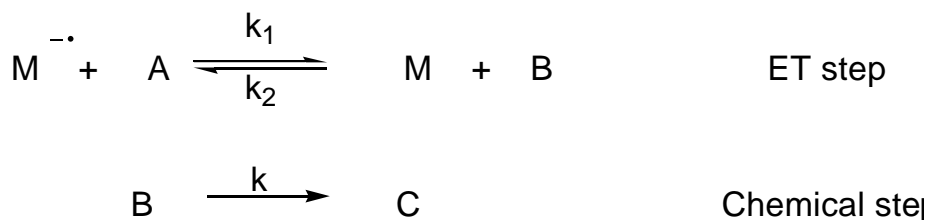


Figure 3.3 Catalytic reduction of cyclopropyl methyl ketone by biphenyl radical anion (DMF, 0.5 M TBAP, 0.1 M Ag^+/Ag reference, GCE working, 0.008 M substrate, $\gamma = 1$, $\nu = 100$ mV/s)

Details of the homogeneous catalysis technique are provided in section 2.2.3.⁶⁵ Only the most pertinent details will be reiterated here. Kinetic control may be governed by either the homogeneous electron transfer step (k_1) or the chemical step (k , Scheme 3.3). The discerning characteristic between these two regimes is the effect of mediator concentration (C_M^0) on i_p/i_{pd} at constant γ and ν . Peak current ratio (i_p/i_{pd}) varies as a function of mediator concentration only when the electron transfer step is rate limiting. Voltammograms of several mediators in the absence and presence of **14a** and **14b** were obtained. By comparing plots of [i_p/i_{pd} vs $\log(1/\nu)$] and [i_p/i_{pd} vs $\log(C_M^0/\nu)$] obtained at different concentrations of mediator (constant γ) any concentration dependence is readily apparent. Representative plots are provided in Figure 3.4; the remainder of

experimental data is presented in section 3.4. For **14a** and **14b**, over the range of mediators examined, i_p/i_{pd} was found to vary as a function mediator concentration. Electron transfer was determined to be the rate limiting step and k_1 rate constants were determined from previously derived working curves (Chapter 2). The parameter ρ was determined by the working curve which gave the best fit to the experimental data and k_1 was determined from x' . A representative fit of the experimental data is provided in Figure 3.4, with the remainder of data treatment provided in section 3.4. Table 3.2 summarizes the values of k_1 and ρ obtained for the reduction of **14a** and **14b** by a series of mediators.

Scheme 3.3



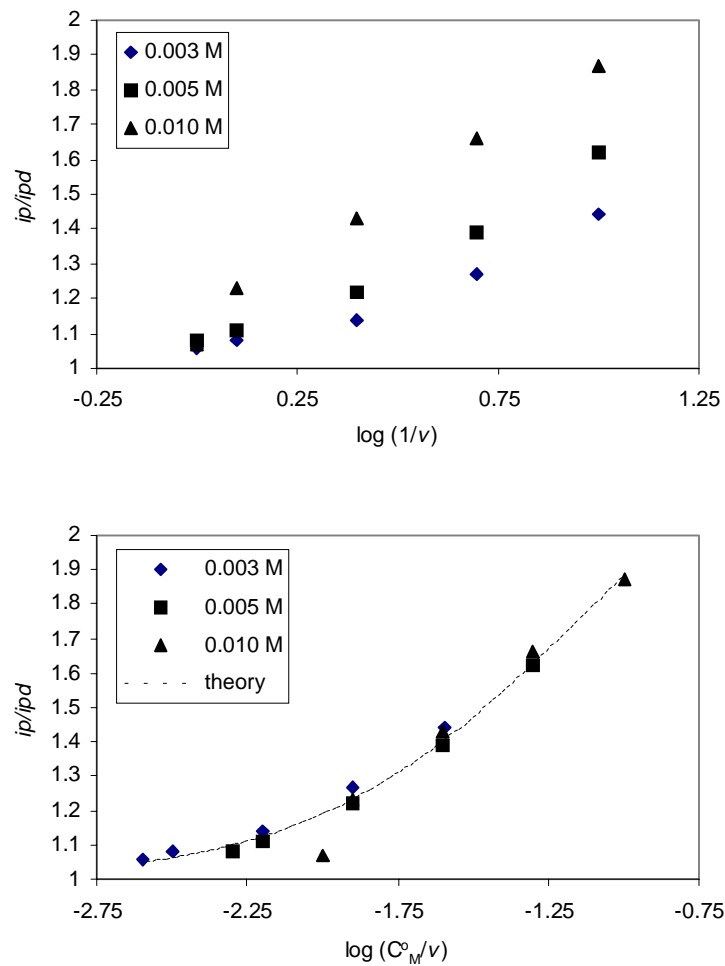


Figure 3.4 Mediated reduction of **14a** by naphthalene (DMF, GCE, 0.5 M TBAP, $v = 0.1-1 \text{ Vs}^{-1}$, $\gamma = 1.00$; Dashed line is the working curve for rate-limiting ET, $x' = 1.030 \pm 0.018$)

Table 3.2. Rate constants for homogeneous electron transfer between the reduced form of the mediator and **14a** and **14b** (0.5 M TBAP/DMF)

Mediator	E° (V) ^a	14a		14b	
		k_1 (M ⁻¹ s ⁻¹)	ρ^b	k_1 (M ⁻¹ s ⁻¹)	ρ
naphthalene	-2.901	4.2 (\pm 0.2) x 10 ²	0.60	5.9 (\pm 0.2) x 10 ²	0.45
3,6-dimethylphenanthrene	-2.937	1.3 (\pm 0.1) x 10 ³	1.00	8.1 (\pm 0.6) x 10 ²	0.90
1,3-dimethylnaphthalene	-2.971	3.5 (\pm 0.2) x 10 ³	0.95	2.2 (\pm 0.1) x 10 ³	0.55
biphenyl	-2.977	2.1 (\pm 0.1) x 10 ³	0.95	2.4 (\pm 0.2) x 10 ³	0.65
methoxynaphthalene	-2.988	5.2 (\pm 0.2) x 10 ³	1.00	2.8 (\pm 0.2) x 10 ³	0.80
2,7-dimethoxynaphthalene	-3.027	9.6 (\pm 0.3) x 10 ³	1.00	8.0 (\pm 0.3) x 10 ³	0.30
o-methoxybiphenyl	-3.086	3.4 (\pm 0.1) x 10 ⁴	0.95	3.6 (\pm 0.1) x 10 ⁴	0.50

^avs. 0.1 M AgNO₃/Ag. ^b(\pm 0.05) for all ρ

Table 3.3. Comparison of ρ values obtained in this study to literature values for 1^o and 3^o radicals.

Mediator	E° (V) ^a	1 ^o		3 ^o	
		ρ^b for 14a	ρ	ρ^b for 14b	ρ^d
naphthalene	-2.901	0.60	0.9 ^c ; 1.0 ^e	0.45	–
biphenyl	-2.977	0.95	0.9 ^c ; 0.95 ^c	0.65	0.6; 0.30
methoxynaphthalene	-2.988	1.00	1.0 ^c	0.80	0.6

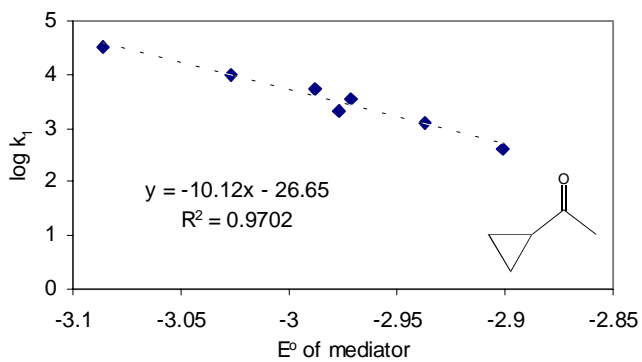
^avs. 0.1 M AgNO₃/Ag. ^b(\pm 0.05) for all ρ ., ^cdetermined from the reaction with *n*-BuCl^{97,98}; ^d *t*-BuCl; ^e1-Chloro-2-methylpropane.

It is important to comment on several points concerning Table 3.2: 1) rate constants increase with increasing reducing power of the mediator radical anion, 2) there appears to be no effect of methyl substitution on rate (*i.e.*, k_1 values obtained for **14a** and **14b** are approximately equal) and 3) ρ values determined for the reduction of **14b** are consistently lower than those determined for the reduction of **14a**. ρ values obtained in this study compare similarly to literature sources (Table 3.3), and the same trend from 1° to 3° radicals is noted. Primary alkyl radicals are easier to reduce than tertiary radicals. Standard reduction potentials for 1° and 3° alkyl radicals have been reported to be -1.62 , and -1.77 V vs. SCE⁹⁷ (another source estimates E° for 1° at $(-1.30$ to $-1.42)$, and 3° at $(-1.48$ to -1.60 V vs SCE)⁹⁵). This order is expected since alkyl groups are considered to be electron donating. Ring opening to 1° radicals results in less addition, as the 1° alkyl radical is more quickly reduced and is therefore less stable.

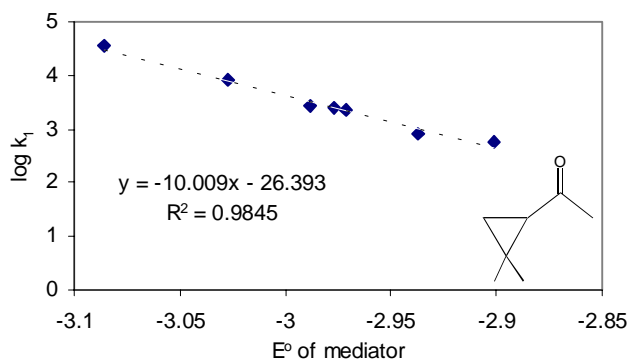
3.2.4 Estimates of the reduction potential of **14a** and **14b** using Marcus theory⁷⁰

In Figure 3.5 (a and b), the log of the rate constants for electron transfer (k_1 , Table 3.2) determined for the reactions of **14a** and **14b** with a series of mediators are plotted against the reduction potential of the mediator ($E^\circ_{M/M\bullet-}$). For **14a** and **14b** the slopes are -10.1 and -10.0 V⁻¹ respectively, suggesting kinetic control from region **II** in the Marcus regimes plot (Figure 2.8). Or more simply, possible contribution from the counter diffusion region may be ignored. Region **III** contributes significantly only when k_{-e1}

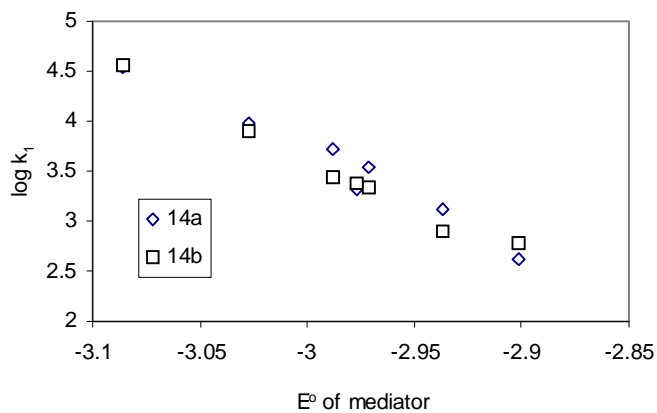
becomes competitive with k_{-d} (Eq 2.11). Using Equation 2.12, $\lambda = 29$ kcal/mol (average value for **14a** and **14b**), and $k_{-d} = 1 \times 10^{10} \text{ s}^{-1}$, an estimation of the borderline between region **II** and **III** behavior was obtained. A value of $\Delta G^{\circ} \leq 13$ kcal/mol was determined, which translates to a maximum allowable difference of 0.56 V vs AgNO₃/Ag before the contribution from region **III** becomes significant. All of the catalysts used in Table 3.2 fall well within this limit.



a.



b.



c.

Figure 3.5. $\log k_1$ as a function of the reduction potential of the mediator $M/M^{\bullet-}$

The rate constants in Table 3.2 were fit to Eq. 2.11 via non-linear regression⁶⁹ analysis, with $E^{\circ}_{A/B}$ and λ as the only adjustable parameters. An excellent fit was

achieved in both cases (the solid lines in Figure 3.6 represent the predicted values based upon this treatment), and E° 's and λ values were obtained (Table 3.4).

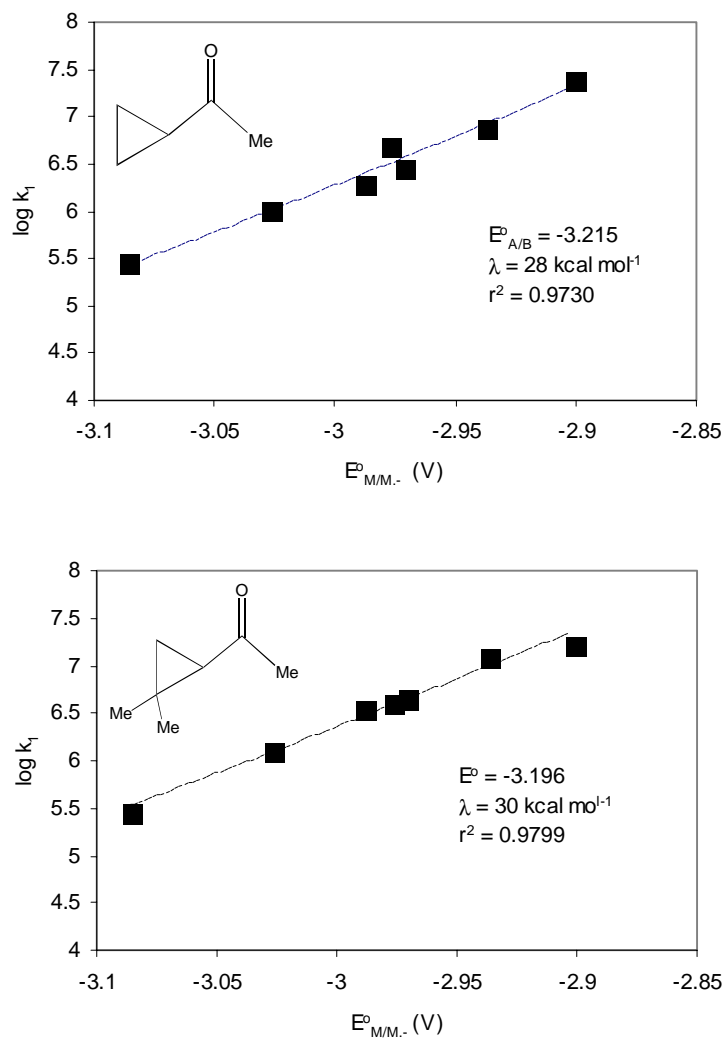


Figure 3.6. $E^{\circ}_{A/B}$ and λ derived from fit of log rate constant data to Eq. 2.11, see text.

Table 3.4. Reduction potentials and reorganization energies for **14a** and **14b** derived from Marcus theory.

Compound	E° (V) ^a	λ (kcal/mol)
14a	-3.215 ± 0.068	28 ± 4
14b	-3.196 ± 0.067	30 ± 4

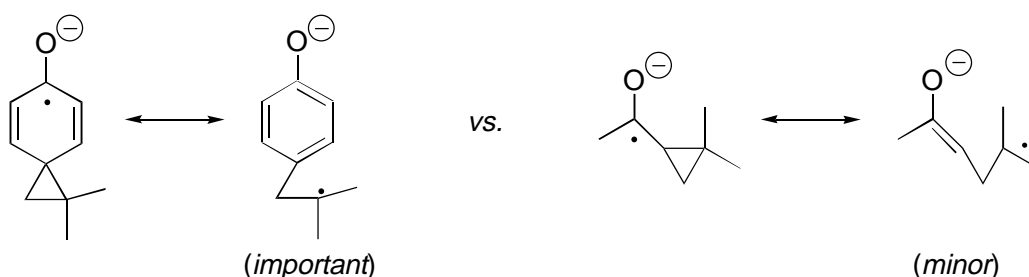
^avs 0.1 M Ag⁺/Ag

Values derived for the reorganization energy (λ) for **14a** and **14b** are consistent with an electron transfer reaction from an aromatic hydrocarbon to an aliphatic ketone, suggesting that there is not an additional contributor (such as bond lengthening or bond angle deformation) to the overall reorganization energy. The λ values in Table 3.4 are substantially different than those obtained for the reduction of spiro series **13(a-c)** by similar aromatic hydrocarbons, and merit further comment. Ebersson has presented a qualitative summary of the structural and environmental effects on λ ²⁵. Spiro compounds **13(a-c)** are highly conjugated substrates and the charge gained in producing the radical anion can be accommodated over a large volume; this results in little reorganization energy to reach the transition state. In the aliphatic cyclopropyl substrates charge is more highly localized in the radical anion than the neutral ketones and a higher solvent reorganization energy would be required.

E° values obtained in this analysis offer an interesting comparison to those obtained in the analysis of spiro series **13(a-c)**. Within experimental and statistical error, the E° values obtained for **14a** and **14b** are identical. This similarity is also reflected in the rate constant values obtained in Table 3.2. There is no increase in rate associated

with methyl substitution on the cyclopropane ring (Figure 3.5.c). For radical ions derived from spiro cyclohexadienones, delocalization of spin onto the carbons of cyclopropyl group yields a resonance form which is aromatic and therefore a major contributor to the overall resonance hybrid (Scheme 3.4). In the case of the aliphatic cyclopropyl ketones, the contribution of the non-bonded resonance structure shown would be minor. Methyl substitution on the cyclopropane ring does not appear to significantly affect the standard reduction potentials of these two substrates.

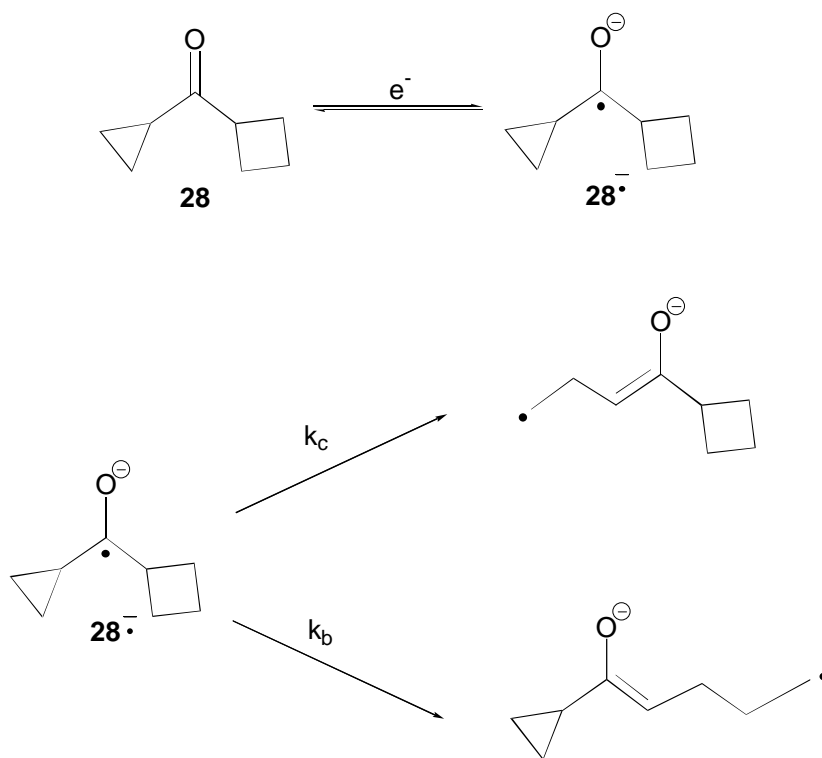
Scheme 3.4



Because the kinetics of both the direct and mediated reduction of **14a** and **14b** involve rate limiting electron transfer, the rate constant for ring opening could not be determined. However, we reasoned that the corresponding cyclobutyl derivative would undergo ring opening at a significantly lower rate, and that ring opening might be the rate limiting step for this system. Ingold⁹⁹ has reported a value of $2.2 \times 10^4 \text{ s}^{-1}$; a slightly different value of $5.0 \times 10^2 \text{ s}^{-1}$ was reported by Beckwith,⁹⁹ for the analogous cyclobutylcarbinyl radical rearrangement. The slower rate of ring opening is also supported by the differences in calculated enthalpies of reaction shown in Table 3.1.

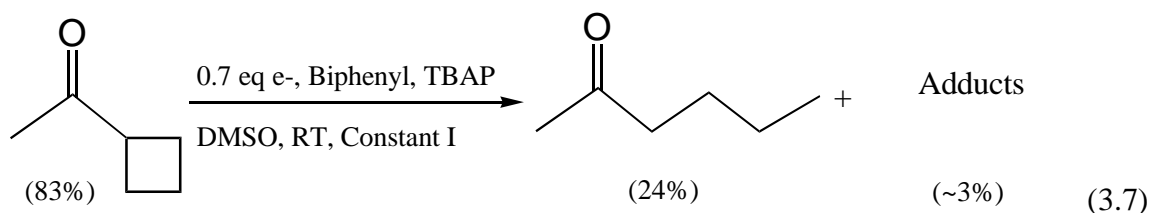
Provided that the rate determining step is found to be the rearrangement in the reduction of cyclobutyl methyl ketone, this rate constant can be used as an intramolecular clock to determine the rate constant for cyclopropyl ring opening via competition experiments. Generation of $28^{\bullet-}$, and from product analyses, determination of the relative amounts of 3- vs 4-membered ring cleavage will give relative rate constants and since k_b is known, k_c can be determined (Scheme 3.5). A detailed electrochemical analysis of cyclobutyl methyl ketone ensued.

Scheme 3.5



3.2.5 Product analysis from preparative electrolysis of cyclobutyl methyl ketone **29**.

A mediated reduction using biphenyl radical anion was chosen for the preparative electrolysis of **29** (Eq. 3.7). After the transfer of 0.7 eq of electrons, 2-hexanone (24%) and a small amount of addition products (~3%) were obtained (note: reaction yields determined by GC).



The extent of adduct formation (¹H NMR and GC/MS in section 3.4) is consistent with the ρ value obtained for the addition of a primary radical to biphenyl radical anion. In this work, the ρ value determined (from homogeneous catalysis experiments) for the addition of the ring opened radical anion generated from cyclopropyl methyl ketone to biphenyl radical anion was found to be $\rho = 0.95 \pm 0.05$. Savéant has also reported $\rho = 0.95$ for the homogeneous reduction of *n*-BuCl with biphenyl.⁹⁸

3.2.6 Indirect electrochemistry of **29**.

The reduction of **29** by three mediators was studied. Naphthalene, biphenyl, and 2-methoxybiphenyl were chosen because they represent the extremes and median values in mediator reduction potentials. As in previous experiments, the current ratio i_p/i_{pd} was examined as a function of sweep rate and mediator concentration at constant excess

factor, $\gamma = 1$. Plots of $[i_p/i_{pd} \text{ vs } \log(1/\nu)]$ and $[i_p/i_{pd} \text{ vs } \log(C_M^0/\nu)]$ for the reduction of **29** by naphthalene and biphenyl radical anions are presented in Figure 3.7(a). and Figure 3.7(b).

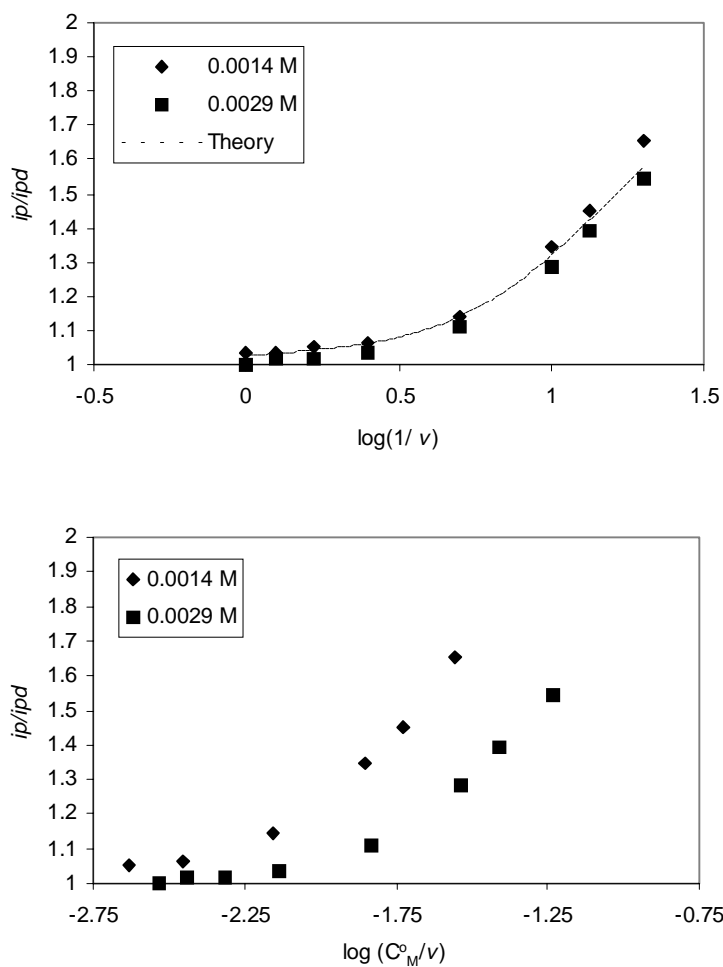


Figure 3.7(a). Mediated reduction of **29** by naphthalene (DMF, GCE, 0.5 M TBAP, $\nu = 0.05 - 1.0 \text{ Vs}^{-1}$, $\gamma = 1.00$; The line is the working curve for rate-limiting chemical step, $x' = -2.267 \pm 0.014$, $\rho = 0.5$).

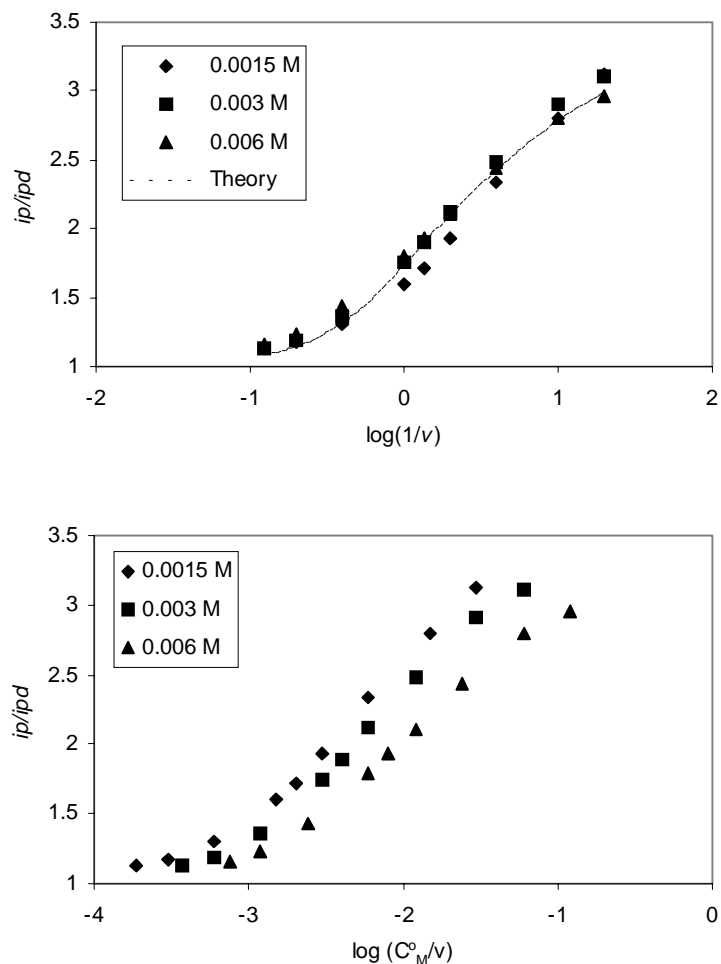


Figure 3.7(b). Mediated reduction of **29** by biphenyl (DMF, GCE, 0.5 M TBAP, $v = 0.05 - 8.0 \text{ Vs}^{-1}$, $\gamma = 1.00$; The line is the working curve for rate-limiting chemical step, $x' = -0.9895 \pm 0.018$, $\rho = 0.9$).

By comparing the plots presented in Figure 3.7(a) and Figure 3.7(b), it is apparent that there is no concentration effect on the peak current ratio. Therefore, it was determined that the chemical step was the rate limiting step. A composite rate constant can be determined from theoretical working curves. Though similar in appearance, different working curves pertain to the two limiting conditions. It was necessary to

derive the appropriate working curves (21 plots of i_p/i_{pd} vs $\log(\lambda\lambda_1/\lambda_2)$ at $\gamma = 1.00$ for $\rho = 0.00$ to 1.00 in 0.05 increments) via digital simulation. Working curves were subsequently fit to a polynomial of the form $y = (a+cx+ex^2+gx^3+ix^4)/(1+bx+dx^2+fx^3+hx^4+jx^5)$, where the coefficients $a \rightarrow j$ were determined for each working curve. Via non-linear regression, experimental data [i_p/i_{pd} vs $\log(1/\nu)$] were fit to the polynomial form of the working curves, $y=f(x+x')$, and the adjustable parameter $x' = \log(RT/F)(kk_1/k_2)$ was determined. The parameter ρ was defined by the working curve which gave the best fit to experimental data and kk_1/k_2 was determined from x' . Fits of experimental data are provided in Figure 3.7(a) and Figure 3.7(b). Making the allowance that $E_{29/29}^{\bullet-} \cong E_{14/14}^{\bullet-}$ (the error associated with this assumption is expected to be small), the ratio k_1/k_2 can be calculated via equation 3.8.

$$\frac{k_1}{k_2} = \exp\left[\frac{F}{2.303RT} (E_{A/B}^{\bullet-} - E_{P/Q}^{\bullet-})\right] \quad (3.8)$$

By combining the composite rate constant determined from experimental data with the k_1/k_2 ratio obtained from equation 3.9, the rate constant for cyclobutane ring opening can be extracted. Table 3.3 summarizes results. An average value of $2.5 \times 10^4 \text{ s}^{-1}$ was obtained for the cyclobutane ring opening of cyclobutyl methyl ketone **29** (AM1 semi-empirical MO theory estimates ΔH° for ring-opening of cyclobutyl methyl ketyl anion to be exothermic by 1 kcal/mol, Table 3.1, and Table 3.6), which is very similar to Ingold's reported value of $2.2 \times 10^4 \text{ s}^{-1}$ ($5.0 \times 10^2 \text{ s}^{-1}$, Beckwith)⁹⁹ for the analogous cyclobutyl carbinyl rearrangement. A very interesting observation was made regarding

the substituent effects on the rate of ring-opening of cyclopropyl- and cyclobutylcarbonyl radicals and their related radical anions (Table 3.6). For the case of the phenyl cyclopropyl ketyl anions, the rate of cyclopropyl ring opening is retarded going from the neutral radical to the radical anion. However, in the case of the aliphatic ketones the opposite seems to hold true. The rate of ring opening of cyclobutyl methyl ketyl anion was faster than for the corresponding neutral radical. Supporting semiempirical molecular orbital calculations⁹³ reveal that for the case of the phenyl cyclopropyl ketyl anions in the ring closed form 62% of the charge is associated with the aromatic ring. Conversely, in the ring opened form 80% of the charge is associated with the oxygen and α -carbon of the enolate anion. Delocalization of charge into the aromatic ring is lost upon ring opening and is an important contributor to the rates of these radical anion rearrangements.

This phenomenon is also evident in the calculated enthalpies for ring opening for these two systems. Ring opening of cyclopropyl methyl ketyl anion is predicted to be favored over the neutral radical. Given that there is less selectivity for the formation of the most stable product in preparative reductions of **14b** than for the structurally related free radical **22**, it is likely that the rate of cyclopropyl ring opening may prove to be faster ($>10^8$) in the case of **14b**.

Table 3.5 Rate constants for cyclobutane ring opening of **29**.

Mediator	E° (V) ^a	k (s ⁻¹)
Naphthalene	-2.901	$3.3 (0.2) \times 10^4$
Biphenyl	-2.977	$3.2 (0.2) \times 10^4$
o-methoxybiphenyl	-3.086	$1.1 (0.9) \times 10^4$
		Avg = 2.5×10^4

^avs. 0.1 M AgNO₃/Ag

Table 3.6 Effect of substituents on the rate of ring opening of cyclopropyl- and cyclobutylcarbinyl radicals and their related radical anions.⁹³

Reaction		k_1 (s ⁻¹)	ΔH_{ro} (kcal/mol)
	\rightleftharpoons		1×10^6 -12.0
	\rightleftharpoons		< 2 +5.5
	\rightleftharpoons		3.6×10^8 -14.1
	\rightleftharpoons		1×10^7 +2.3
	\rightleftharpoons		5.0×10^2 +0.2
	\rightleftharpoons		2.5×10^4 -1.0
	\rightleftharpoons		1.2×10^8 -10.7
	\rightleftharpoons		? -14.5

Homogeneous catalysis experiments with 2-methoxybiphenyl posed new challenges. When plots of $[i_p/i_{pd}]$ vs $\log(1/\nu)$ and $[i_p/i_{pd}]$ vs $\log(C_M^0/\nu)$ in Figure 3.8(a

and b) are compared for the reduction of **29** by 2-methoxybiphenyl, it is not readily apparent which gives a better fit to experimental data. This suggested that the reduction of **29** by 2-methoxybiphenyl was under mixed kinetic control by the ET and chemical steps.

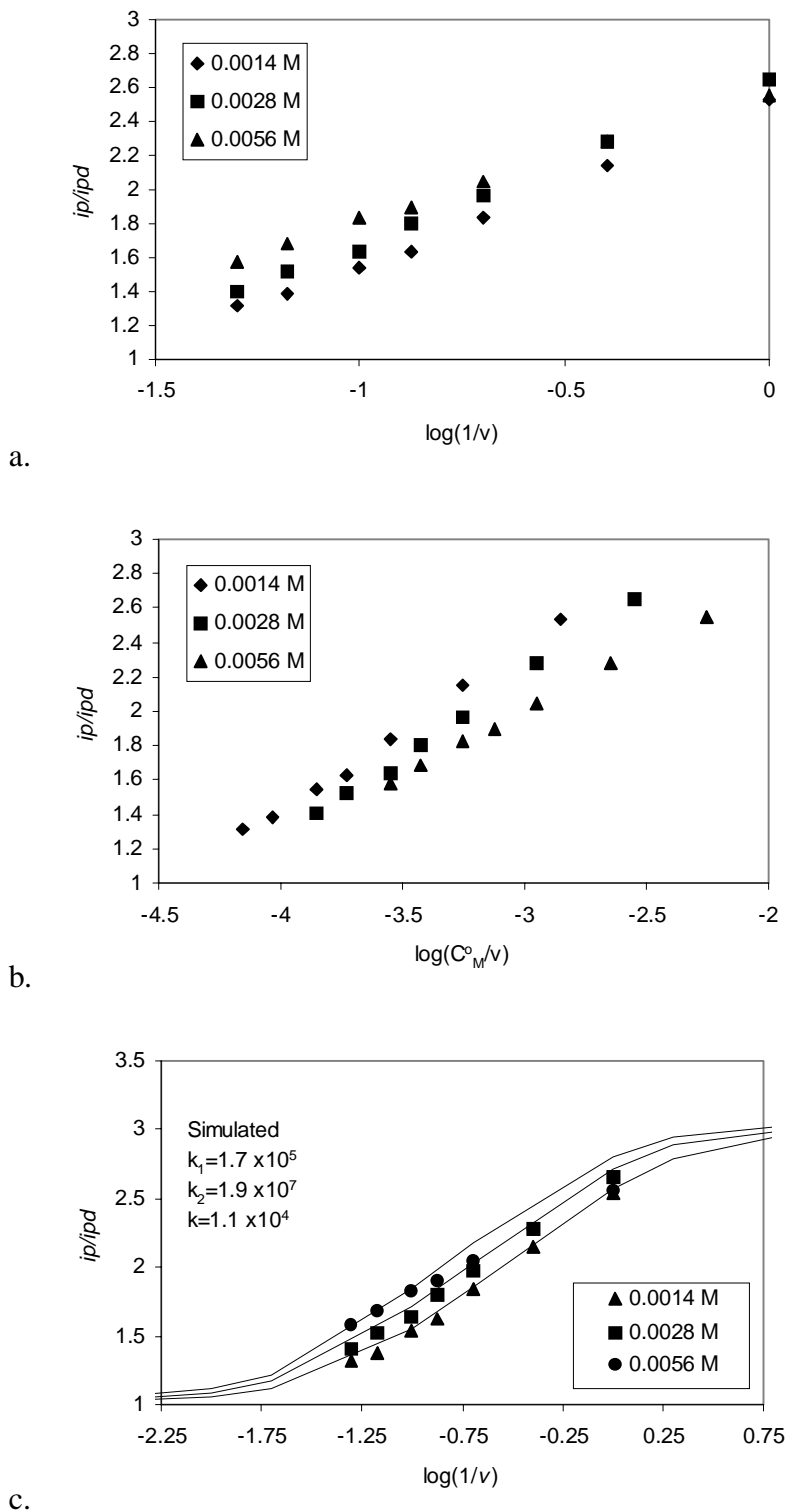
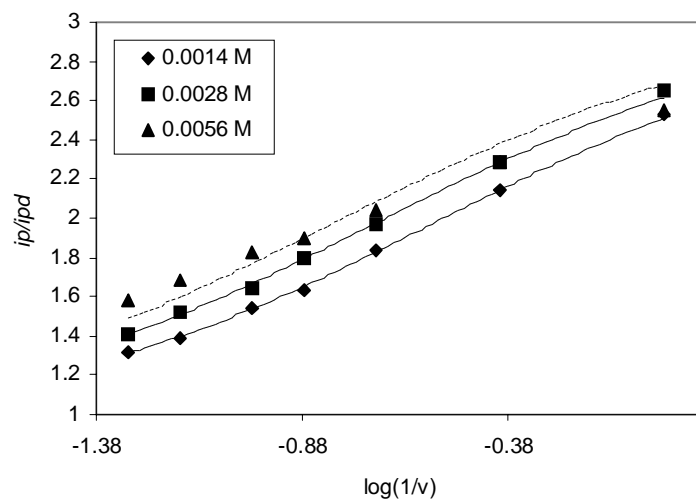


Figure 3.8 Mediated reduction of **29** by o-methoxybiphenyl (DMF, GCE, 0.5 M TBAP, $\nu = 1$ to 20 Vs^{-1} , $\gamma = 1.00$, lines in c. reflect simulated results)

In the event of mixed control, it is possible to extract rate constant information via the forced treatment of the i_p/i_{pd} data to the working curves (from Chapter 2) corresponding to rate limiting electron transfer step and equation 3.9.¹⁰⁰

$$\frac{1}{k_{ap}} = \frac{1}{k_1} + 0.33 \frac{k_2}{k_1 k} [M] \quad (3.9)$$

Experimental fits of $[i_p/i_{pd} \text{ vs } \log(1/v)]$ data are shown in Figure 3.9. This approximation is possible because of the similarity of the working curves from the two extreme rate-limiting conditions. The apparent rate constant, k_{ap} , is determined from x' and $1/k_{ap}$ is plotted vs mediator concentration. A linear relationship was obtained ($(y) = 0.0034(x) + 6 \times 10^{-6}$, $r^2 = 0.9997$, Figure 3.10). The intercept gives k_1 , and assuming $E^{\circ}_{29/29} \bullet^- \cong E^{\circ}_{14/14} \bullet^-$, the slope gives k (Table 3.5). Rate constants obtained in this manner were used in digital simulations and fits of experimental data to simulated results are shown in Figure 3.8.c.



0.0014 M, $r^2 = 0.9989$, $x' = 0.512$ (0.006)

0.0028 M, $r^2 = 0.9980$, $x' = 0.652$ (0.008)

0.0056 M, $r^2 = 0.9275$, $x' = 0.755$ (0.037)

Figure 3.9 Mediated reduction of **29** by 2-methoxybiphenyl. Forced treatment of i_p/i_{pd} vs $\log(1/v)$ data from Figure 3.8 to working curves for rate limiting ET step (lines represent theoretical curves, $\rho = 0.8$).

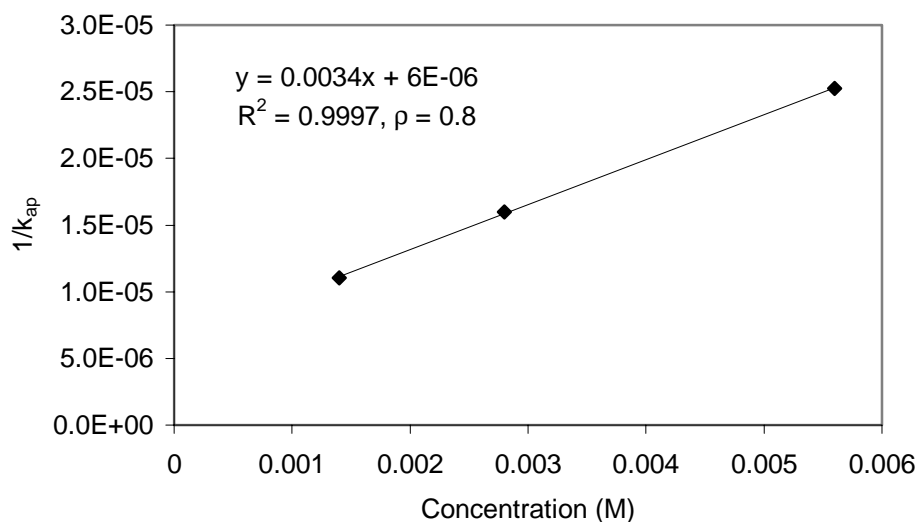


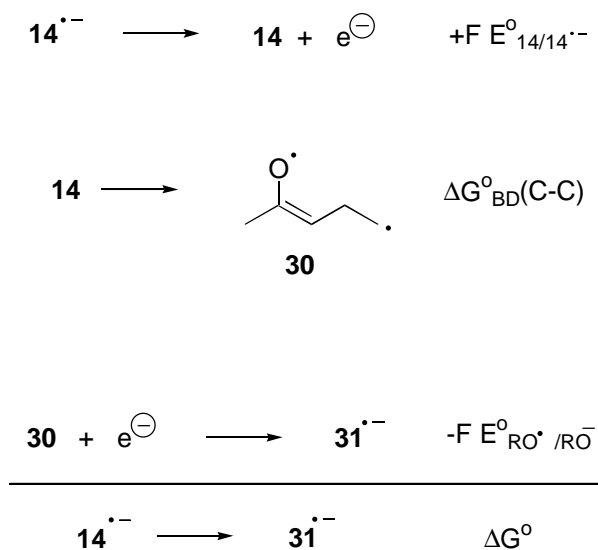
Figure 3.10 Apparent rate constant dependence on mediator concentration for the reduction of **29** by o-methoxybiphenyl.

3.2.7 Thermodynamics of ring opening for **14a^{•-}**, **14b^{•-}** and **29^{•-}**.

ΔG° for ring opening of **14a^{•-}**, **14b^{•-}** and **29^{•-}** were calculated (analogous to **13a^{•-}**, **13b^{•-}** and **13c^{•-}** in section 2.2.5) utilizing the thermochemical cycle depicted in Scheme 3.6 ($\Delta G^\circ = \Delta G^\circ_{\text{BD}(\text{C-C})} + F(E^\circ_{14/14^{\bullet-}} - E^\circ_{\text{RO}^\bullet/\text{RO}^-})$). Three thermodynamic values are needed to solve for ΔG° 1) the standard potential of **14(a,b)** and **29** (median $E^\circ_{\text{A/B}} = -3.2055$ V vs. Ag/Ag⁺ obtained in this study, Table 3.4, assuming $E^\circ_{29/29^{\bullet-}} \cong E^\circ_{14/14^{\bullet-}}$), 2) the standard potential of the RO[•]/RO⁻ couple (estimated to be -0.674 kcal/mole⁷⁹ based upon published results for acetone, this value measured vs. Fc/Fc⁺ (-0.0292 V) and adjusted to Ag/Ag⁺ (-0.1932 V) and 3) the strength of the C-C bond of the cyclopropyl

group ($\Delta G^{\circ}_{\text{BD}}(\text{C-C})$). It is assumed that ΔS for this unimolecular process is small and $\Delta G^{\circ}_{\text{BD}}(\text{C-C}) \approx \text{BDE}_{\text{C-C}}$. This procedure for estimating ΔG° for ring opening is attractive because the pertinent reduction potentials should account for any effect of solvent and/or electrolyte.

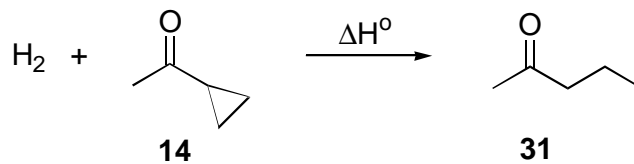
Scheme 3.6



The strength of the cyclopropyl C-C in **14a**, **14b**, and **29** was estimated according to Scheme 3.7, where ΔH_f° 's for the pertinent species were obtained using semi-empirical molecular orbital theory (PM3, details are provided in section 2.4),¹⁰¹ and literature values for the bond dissociation energies: $\text{BDE}(\text{COC-H}) = 94 \text{ kcal/mol}$, $\text{BDE}(1^{\circ}\text{C-H}) = 100.0 \text{ kcal/mol}$, and $\text{BDE}(3^{\circ}\text{C-H}) = 95.6 \text{ kcal/mol}$.¹⁰² We assume that these

calculated values for BDE(C-C) (Table 3.7) are the same in the gas phase and in solution.¹⁰³ Results of this analysis are summarized in Table 3.8.

Scheme 3.7



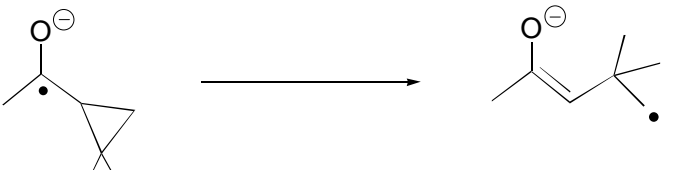
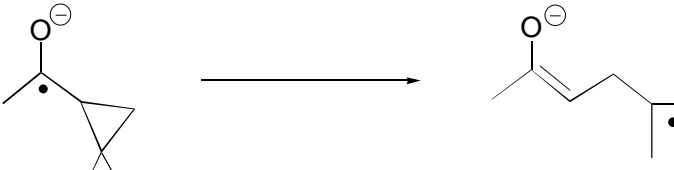
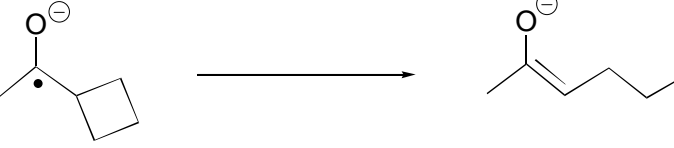
$$\begin{aligned} \Delta H^\circ &= \Delta H_f^\circ(\mathbf{31}) - \Delta H_f^\circ(\mathbf{14}) \\ &= \text{BDE}(\text{H}_2) + \text{BDE}(\text{C-C}) - \text{BDE}(\text{COC-H}) - \text{BDE}(\text{C-H}) \end{aligned}$$

Table 3.7 Calculated BDE(C-C) based upon Scheme 3.7.

Compound	$\Delta H_f^\circ(\text{React.})^a$	$\Delta H_f^\circ(1^\circ\text{-P.})^a$	$\Delta H_f^\circ(3^\circ\text{-P.})^a$	BDE($1^\circ\text{-P.})^a$	BDE($3^\circ\text{-P.})^a$
14a ($R_1=R_2=\text{H}$)	24.85	-62.4	---	52.3	---
14b ($R_1=R_2=\text{CH}_3$)	38.5	-72.8	-73.3	55.5	51.2
29	42.7	-66.6	---	65.9	---

^akcal/mol

Table 3.8. Estimated ΔG° for ring opening of **14a^{•-}**, **14b^{•-}**, and **29^{•-}**

Reaction	ΔH_{ro} (kcal/mol)
	-17
	-14
	-18
	-3

3.3 CONCLUSIONS

Radical anions derived from **14a** and **14b** undergo facile ring opening, with rate constants estimated to be $\geq 10^6 \text{ s}^{-1}$. Based upon the value of α observed in the direct electrochemistry, and more importantly the reorganization energy (λ) derived from the mediated reductions, we conclude that these radical anions have finite lifetimes (*i.e.*, electron transfer and ring opening are not concerted). For unsymmetrical radical anion **14b**, ring opening slightly favored the more substituted (stabilized) distonic radical anion. Standard reduction potentials for aliphatic ketones in aprotic solvents were previously

unknown and this work represents one of the first determinations. Using the homogeneous reduction rate constants (k_1) values obtained in this study and the standard reduction potentials derived for compounds **14a** and **14b**, no evidence could be established for the stabilization of these radical anions via conjugative interactions with the cyclopropyl group. The rate constant for the ring opening of **29** was determined to be on the order of $2.5 \times 10^4 \text{ s}^{-1}$ and can be used in competition experiments with the cyclobutyl cyclopropyl ketone **28** to determine the rates of cyclopropyl ring opening.

3.4 GRAPHICAL ANALYSIS AND SUPPLEMENTAL PLOTS

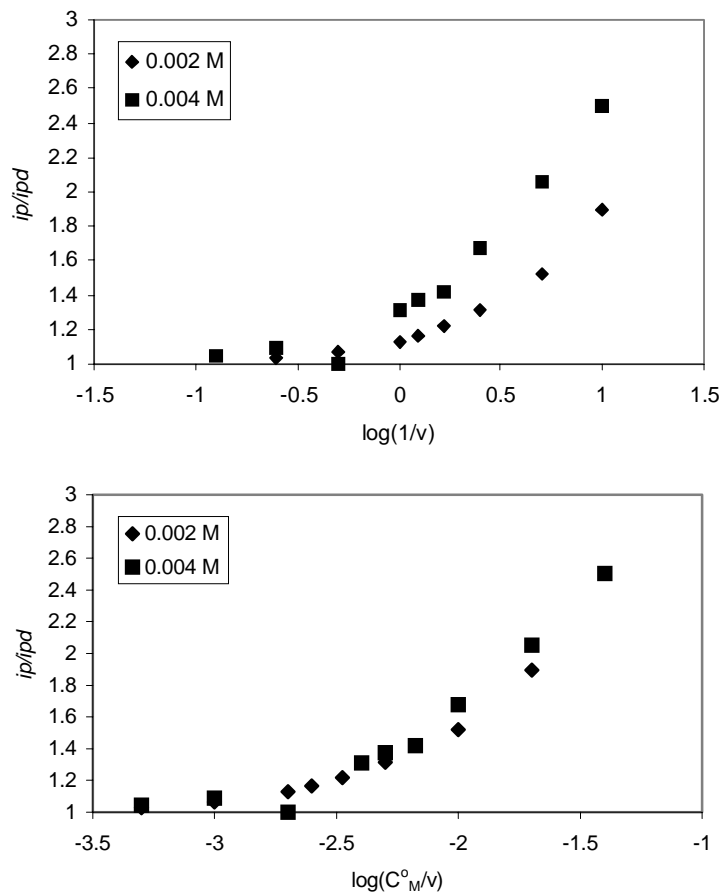


Figure 3.11 Mediated reduction of **14a** with 3,6-dimethylphenanthrene (DMF, GCE, TBAP, $v = 0.1 - 8$ V/s)

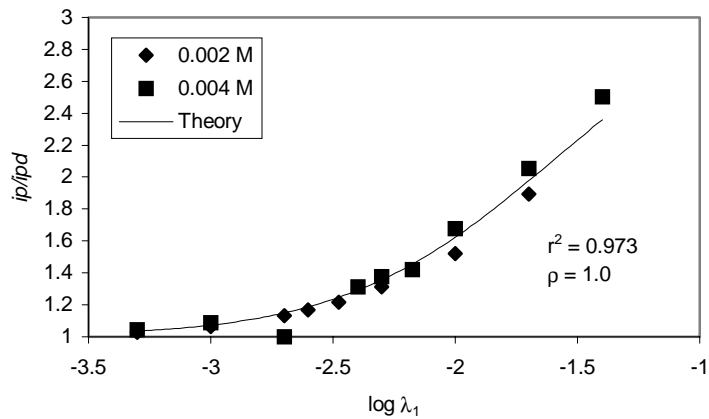


Figure 3.12 Non-linear fitting of results for **14a** + 3,6-dimethylphenanthrene ($x' = 1.5105 \pm 0.022$)

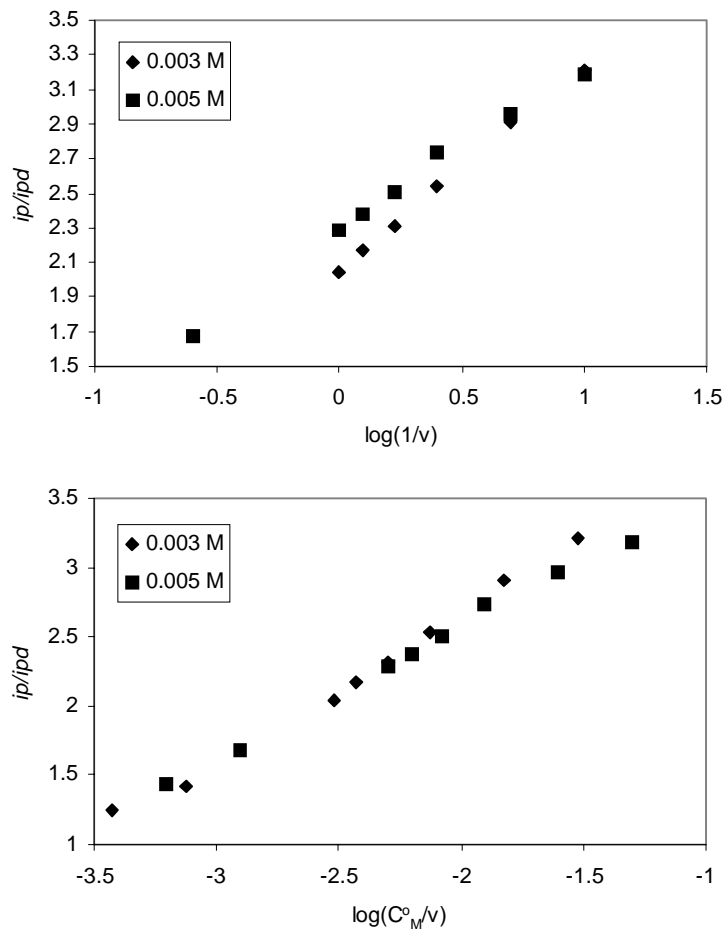


Figure 3.13 Mediated reduction of **14a** with 2,7-dimethoxynaphthalene (DMF, GCE, TBAP, $\nu = 0.1 - 8$ V/s)

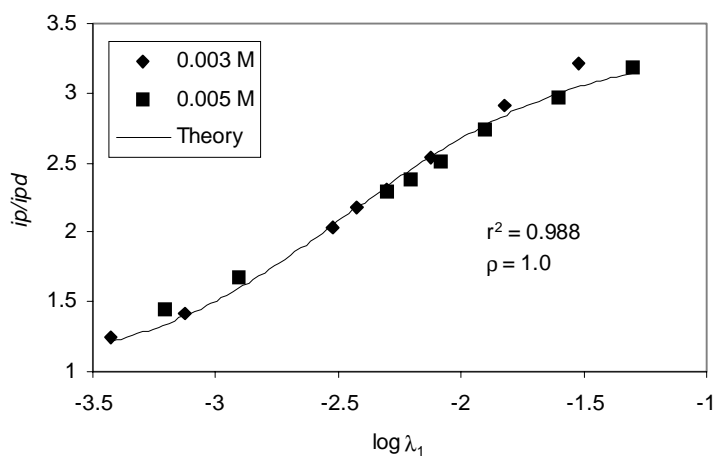


Figure 3.14 Non-linear fitting of results for **14a** + 2,7-dimethoxynaphthalene ($x' = 2.391 \pm 0.018$)

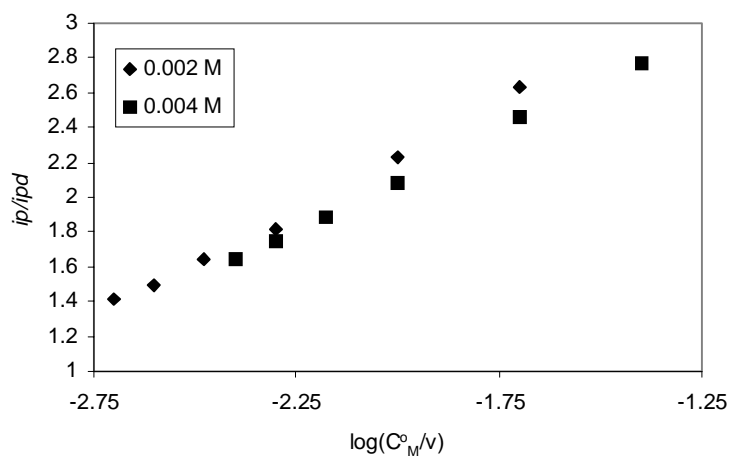
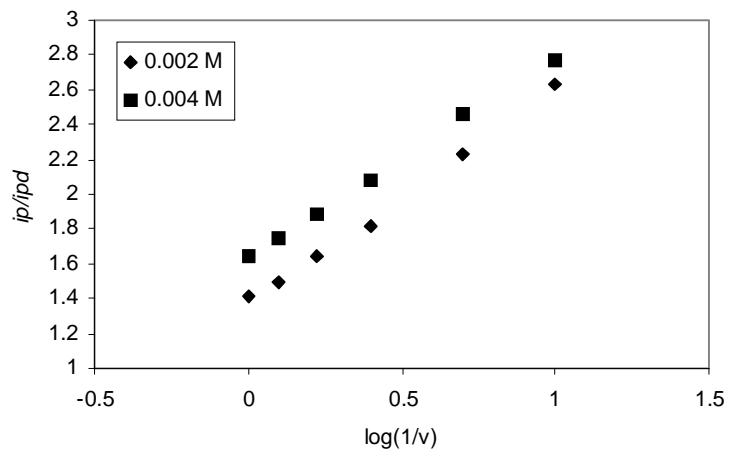


Figure 3.15 Mediated reduction of **14a** with 1,3-dimethylnaphthalene (DMF, GCE, TBAP, $v = 0.1 - 1$ V/s)

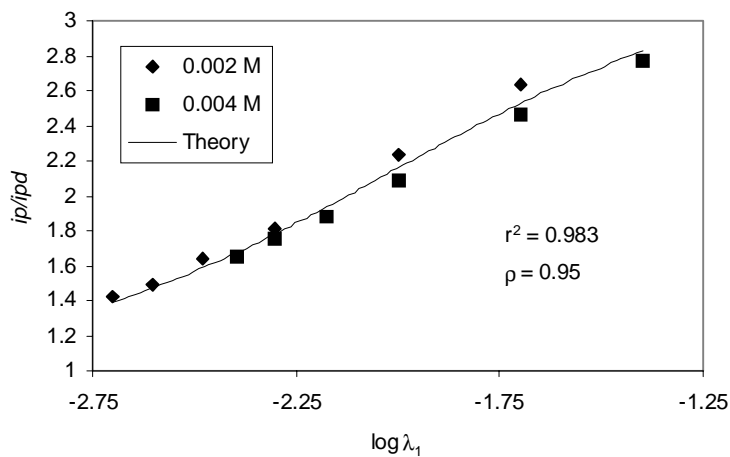


Figure 3.16 Non-linear fitting of results for **14a** + 1,3-dimethylnaphthalene ($x' = 1.957 \pm 0.015$)

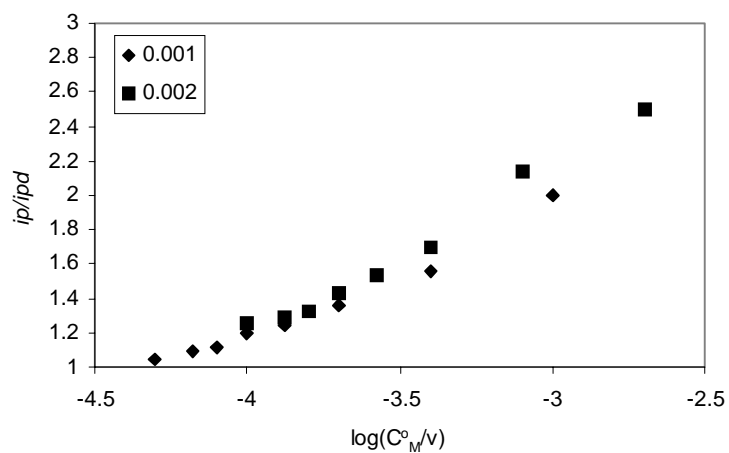
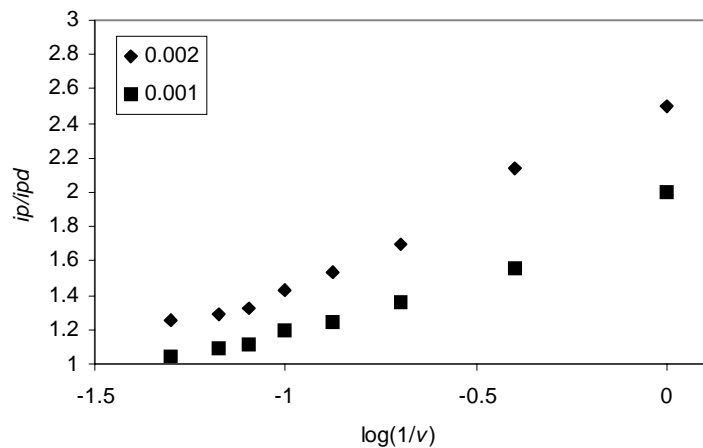


Figure 3.17 Mediated reduction of **14a** with 2-methoxybiphenyl (DMF, GCE, TBAP, $\nu = 1.0 - 20$ V/s)

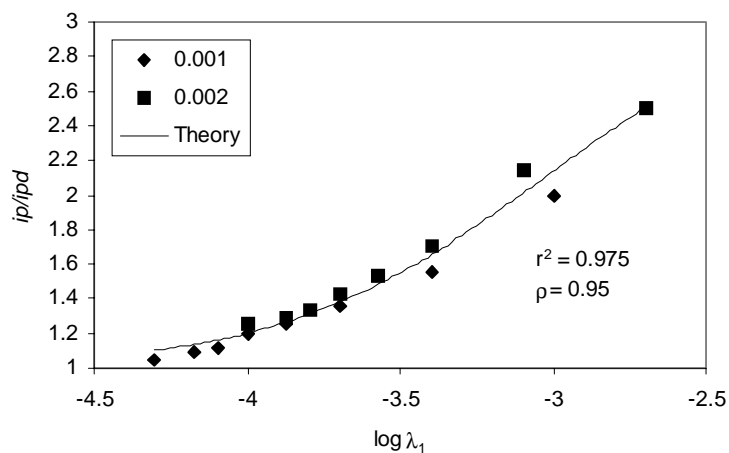


Figure 3.18 Non-linear fitting of results for **14a** + 2-methoxybiphenyl ($x' = 2.940 \pm 0.020$)

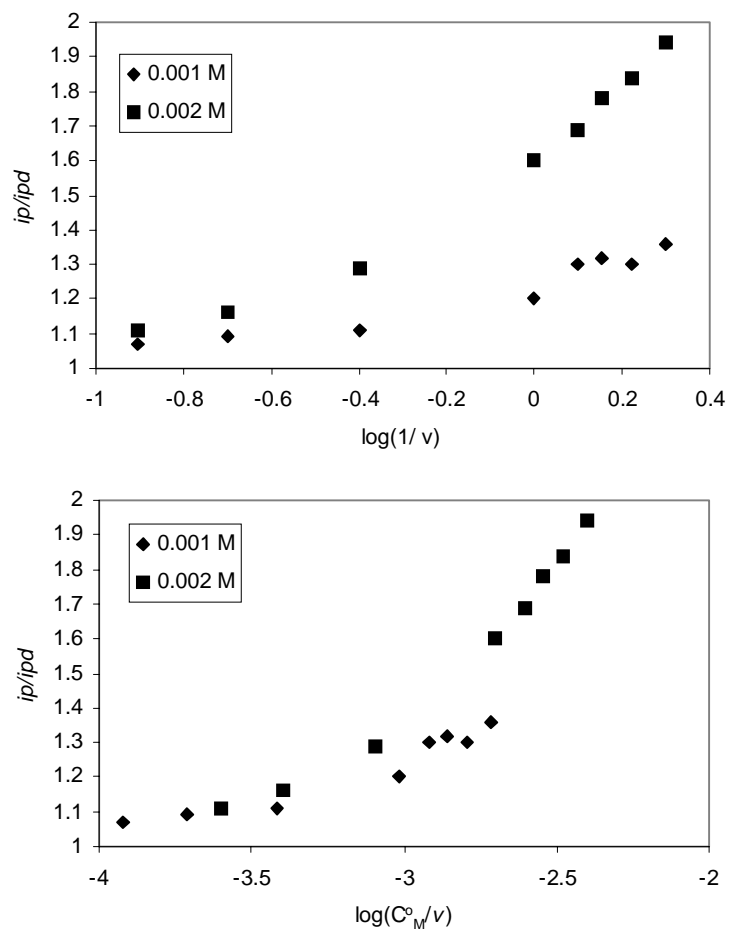


Figure 3.19 Mediated reduction of **14a** with methoxynaphthalene (DMF, GCE, TBAP, $\nu = 0.5 - 8$ V/s)

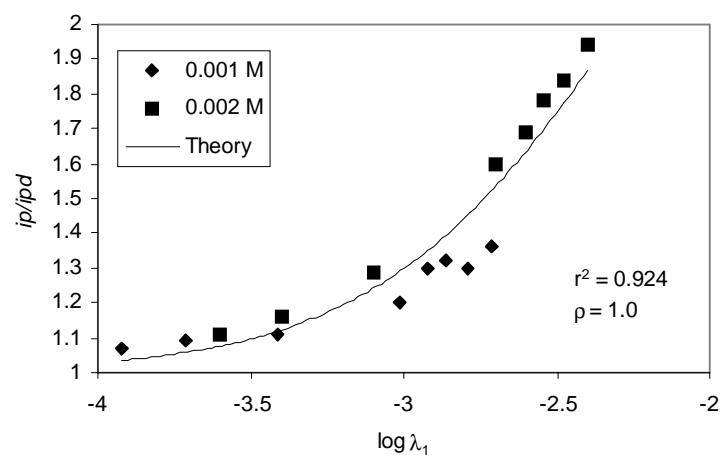


Figure 3.20 Non-linear fitting of results for **14a** + methoxynaphthalene ($x' = 2.123 \pm 0.025$)

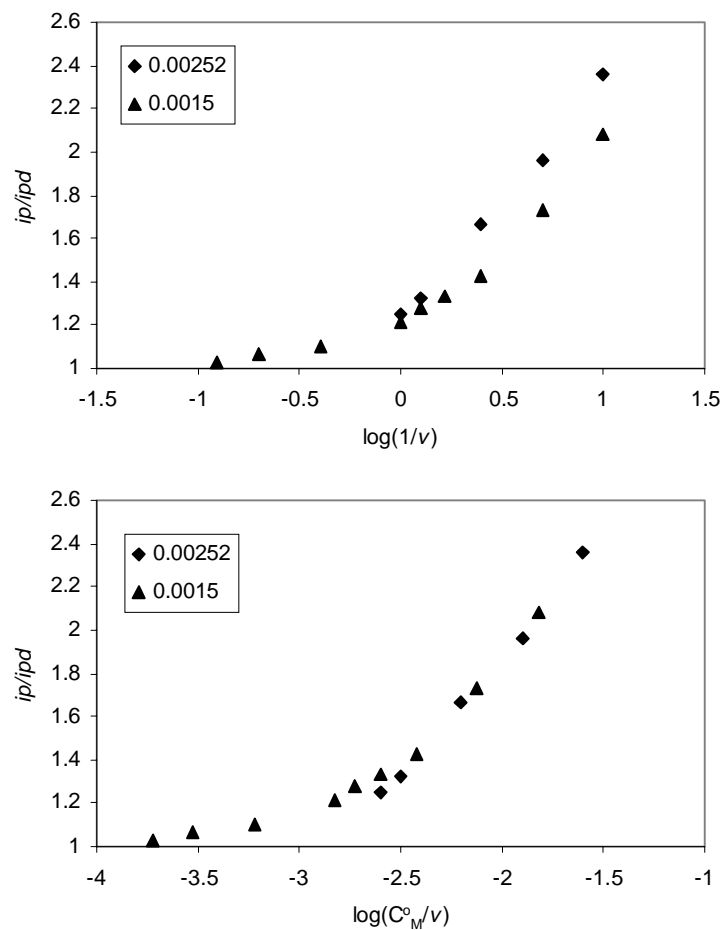


Figure 3.21 Mediated reduction of **14a** with biphenyl (DMF, GCE, TBAP, $\nu = 0.1 - 8$ V/s)

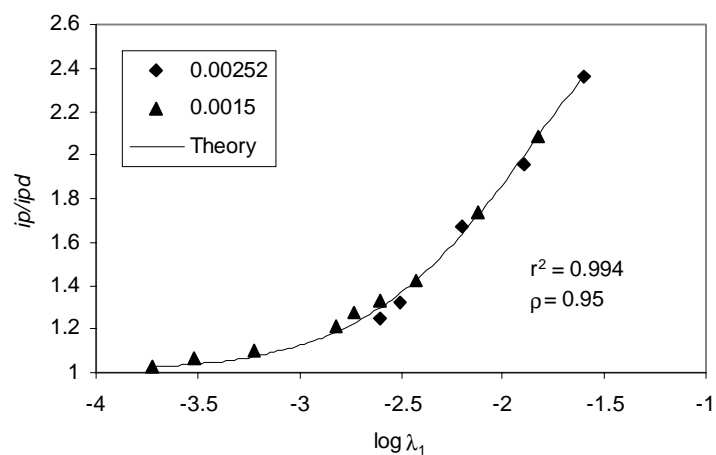


Figure 3.22 Non-linear fitting of results for **14a** + biphenyl ($x' = 1.725 \pm 0.010$)

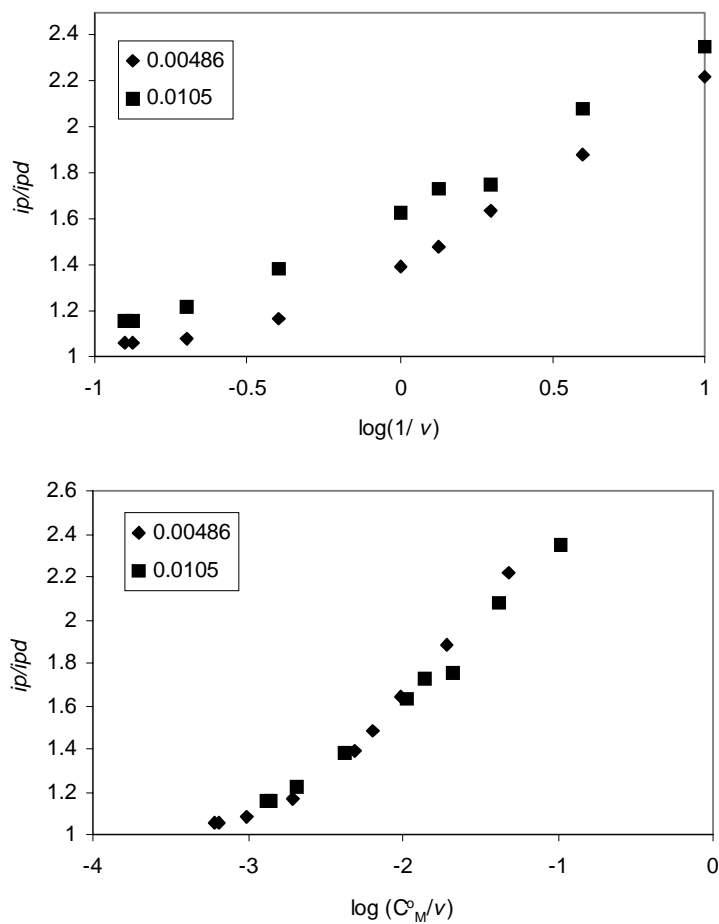


Figure 3.23 Mediated reduction of **14b** with 1,3-dimethylnaphthalene (DMF, GCE, TBAP, $\nu = 0.1 - 8$ V/s)

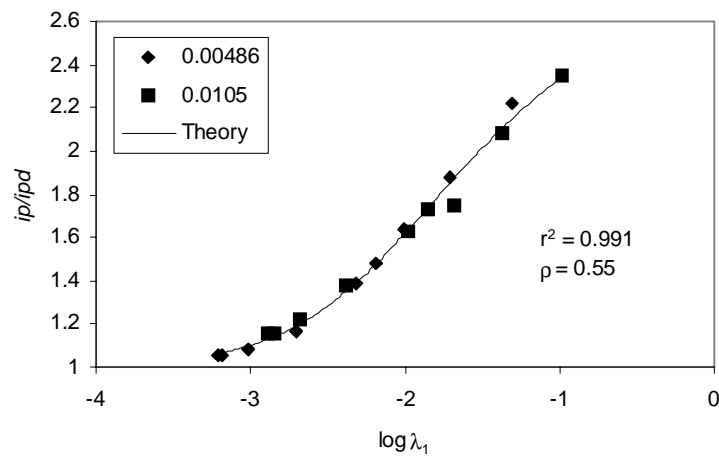


Figure 3.24 Non-linear fitting of results for **14b** + 1,3-dimethylnaphthalene ($x' = 1.752 \pm 0.016$)

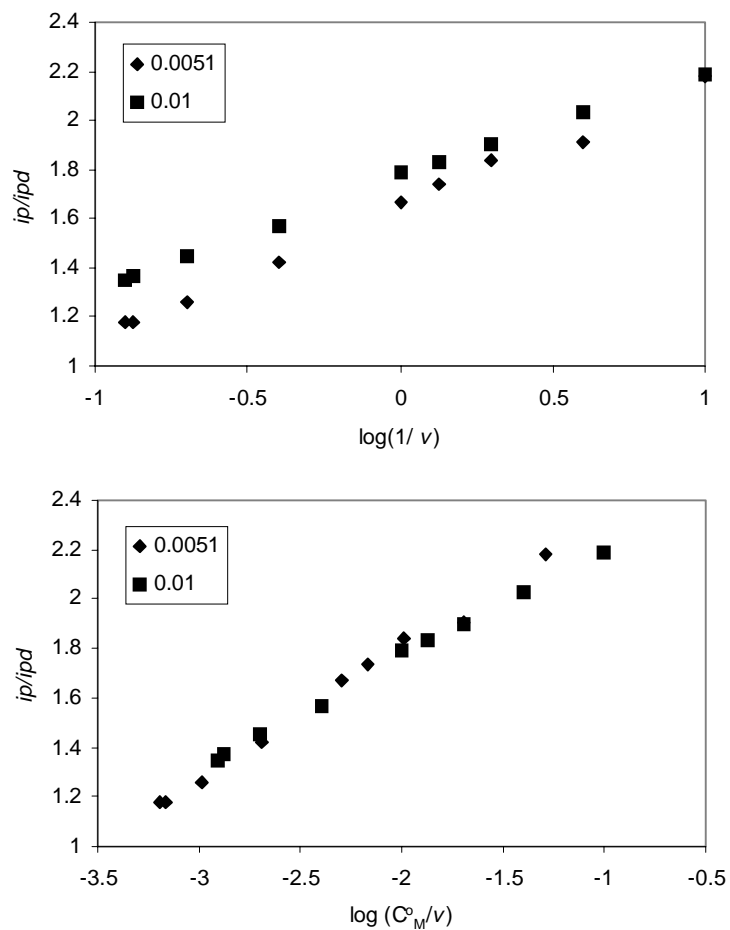


Figure 3.25 Mediated reduction of **14b** with 2,7-dimethoxynaphthalene (DMF, GCE, TBAP, $v = 0.1 - 8$ V/s)

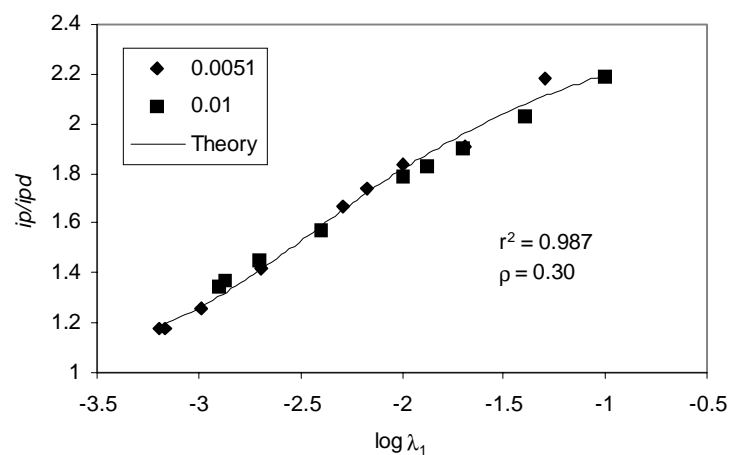


Figure 3.26 Non-linear fitting of results for **14b** + 2,7-dimethoxynaphthalene ($x' = 2.315 \pm 0.019$)

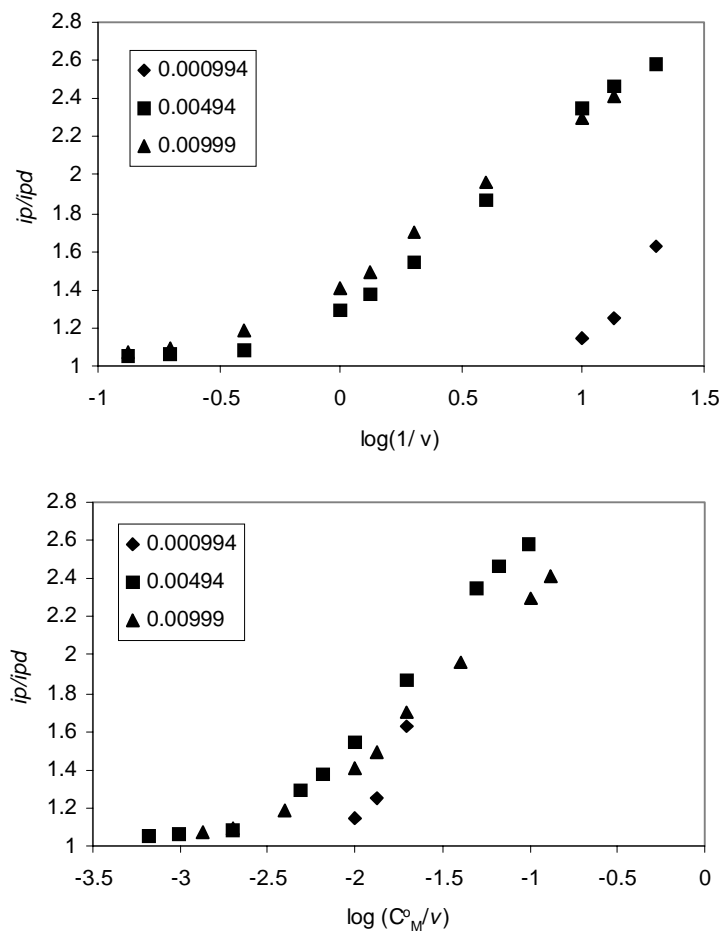


Figure 3.27 Mediated reduction of **14b** with 3,6-dimethylphenanthrene (DMF, GCE, TBAP, $v = 0.05 - 7.5$ V/s)

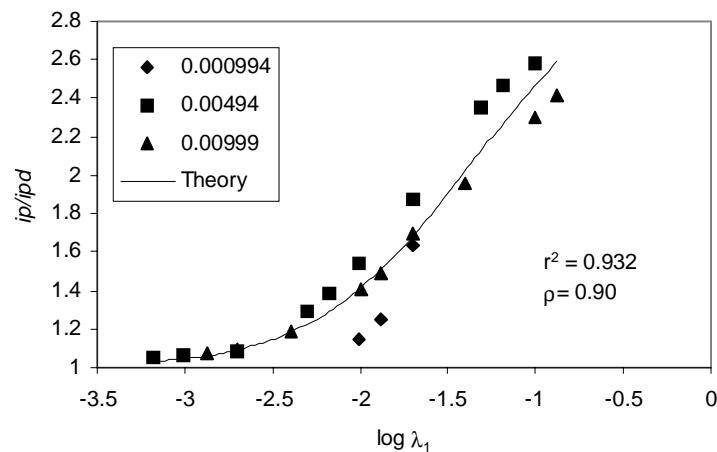


Figure 3.28 Non-linear fitting of results for **14b** + 3,6-dimethylphenanthrene ($x' = 1.316 \pm 0.036$)

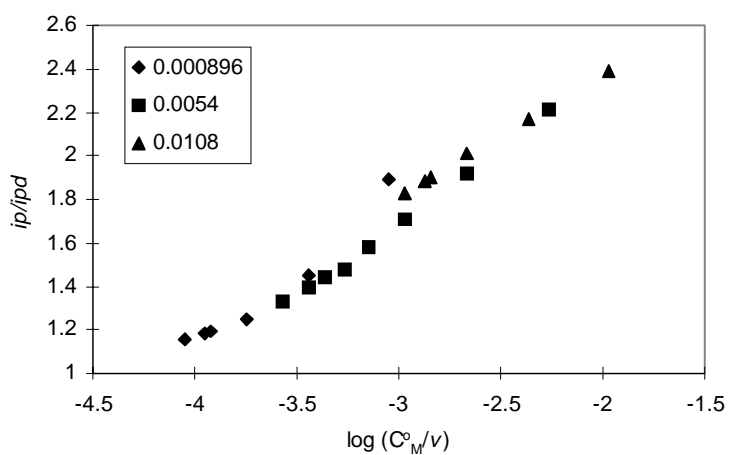
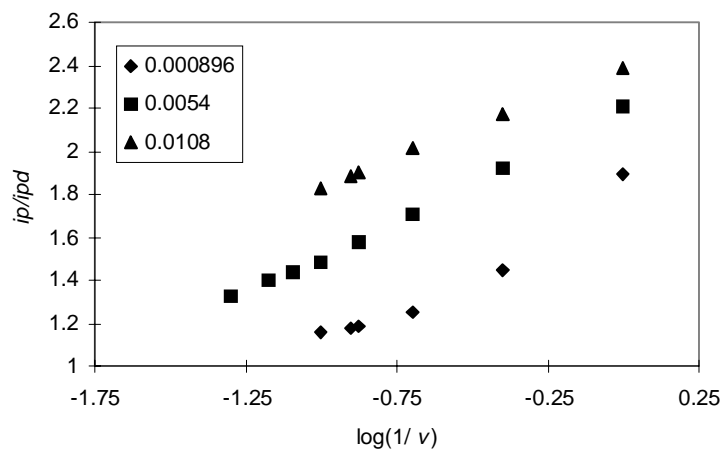


Figure 3.29 Mediated reduction of **14b** with 2-methoxybiphenyl (DMF, GCE, TBAP, $v = 1.0 - 20$ V/s)

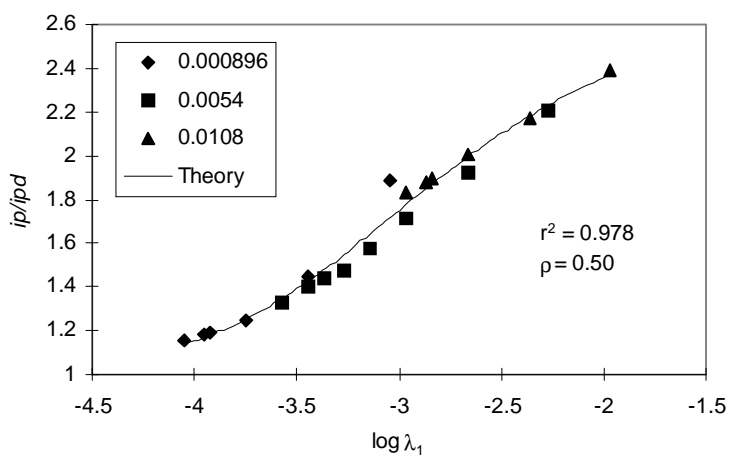


Figure 3.30 Non-linear fitting of results for **14b** + 2-methoxybiphenyl ($x' = 2.960 \pm 0.020$)

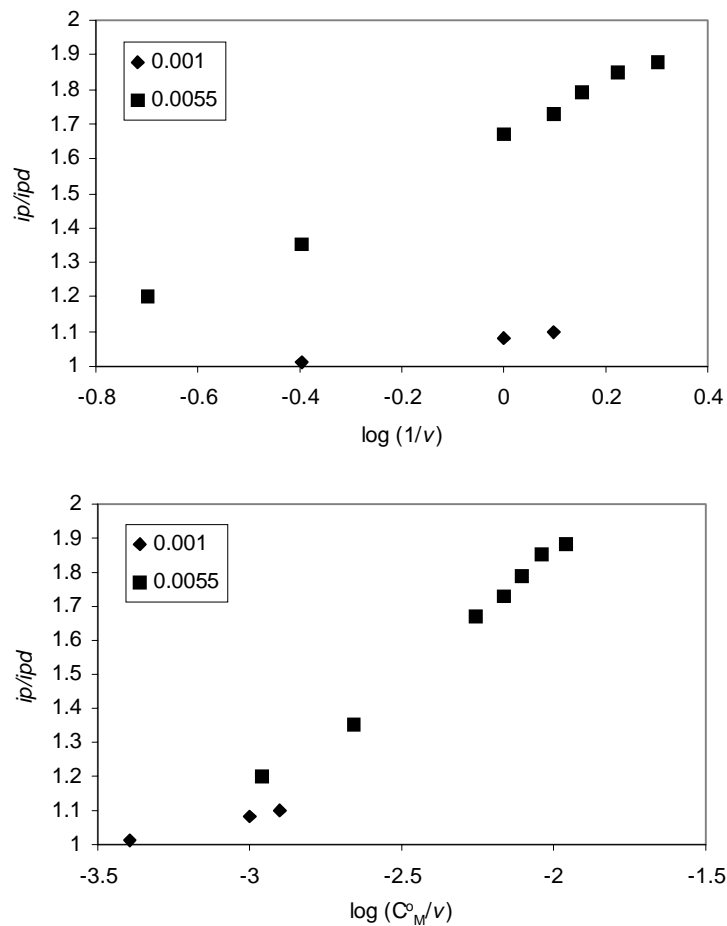


Figure 3.31 Mediated reduction of **14b** with methoxynaphthalene (DMF, GCE, TBAP, $\nu = 0.5 - 5$ V/s)

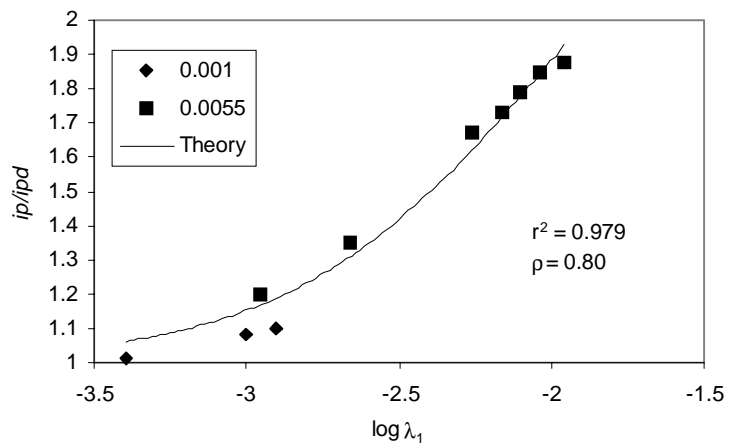


Figure 3.32 Non-linear fitting of results for **14b** + methoxynaphthalene ($x' = 1.864 \pm 0.021$)

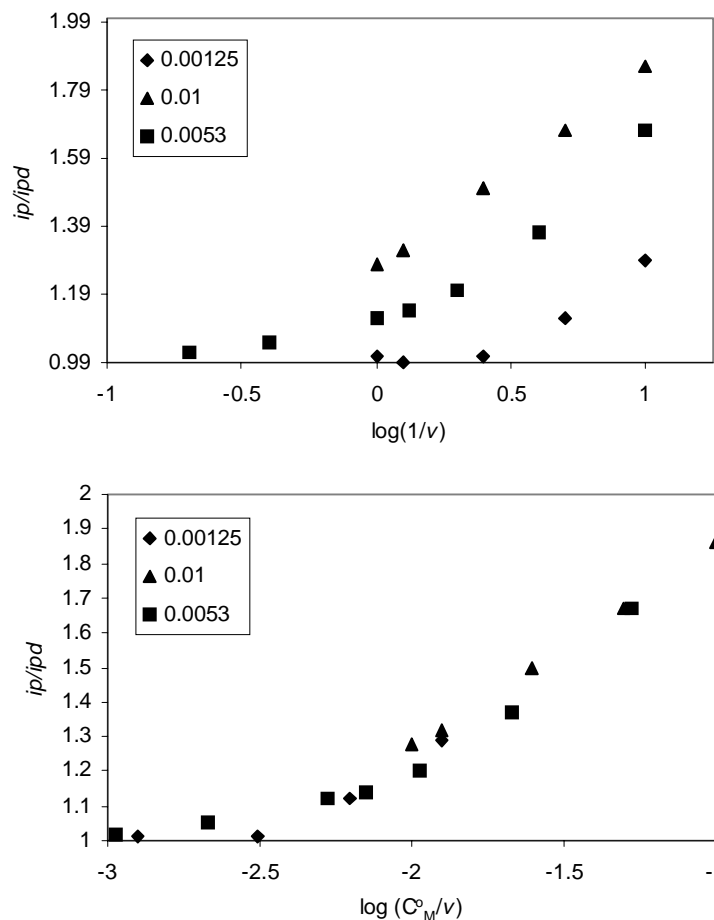


Figure 3.33 Mediated reduction of **14b** with naphthalene (DMF, GCE, TBAP, $v = 0.1 - 5$ V/s)

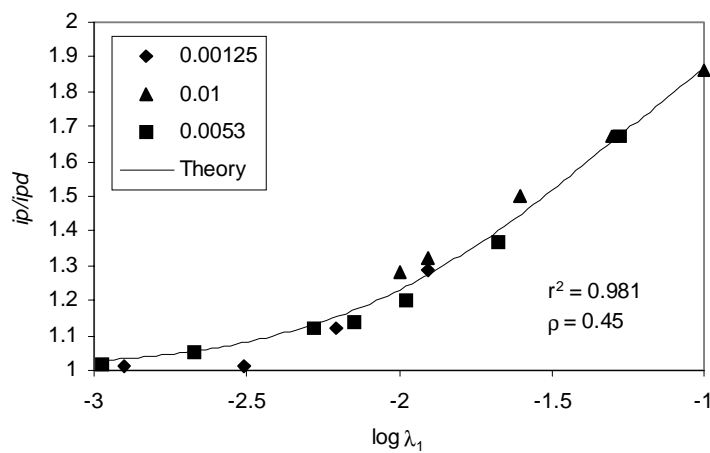


Figure 3.34 Non-linear fitting of results for **14b** + naphthalene ($x^2 = 1.181 \pm 0.019$)

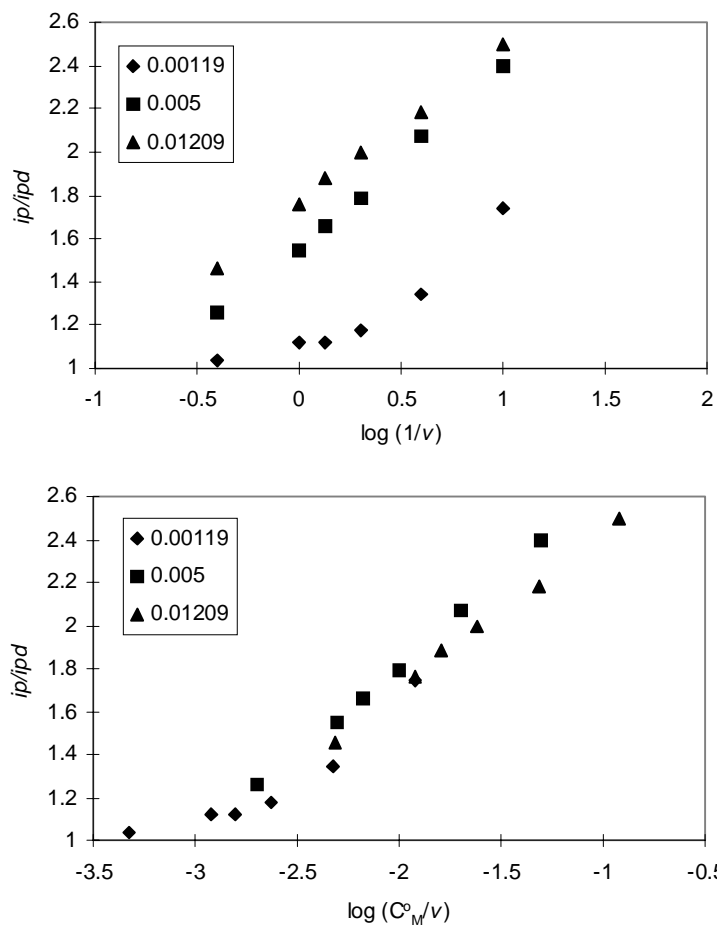


Figure 3.35 Mediated reduction of **14b** with biphenyl (DMF, GCE, TBAP, $v = 0.1 - 2.5$ V/s)

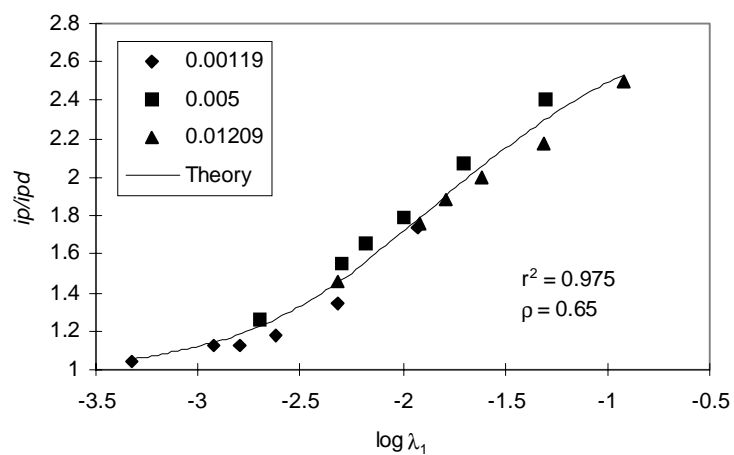


Figure 3.36 Non-linear fitting of results for **14b** + biphenyl ($x' = 1.794 \pm 0.023$)

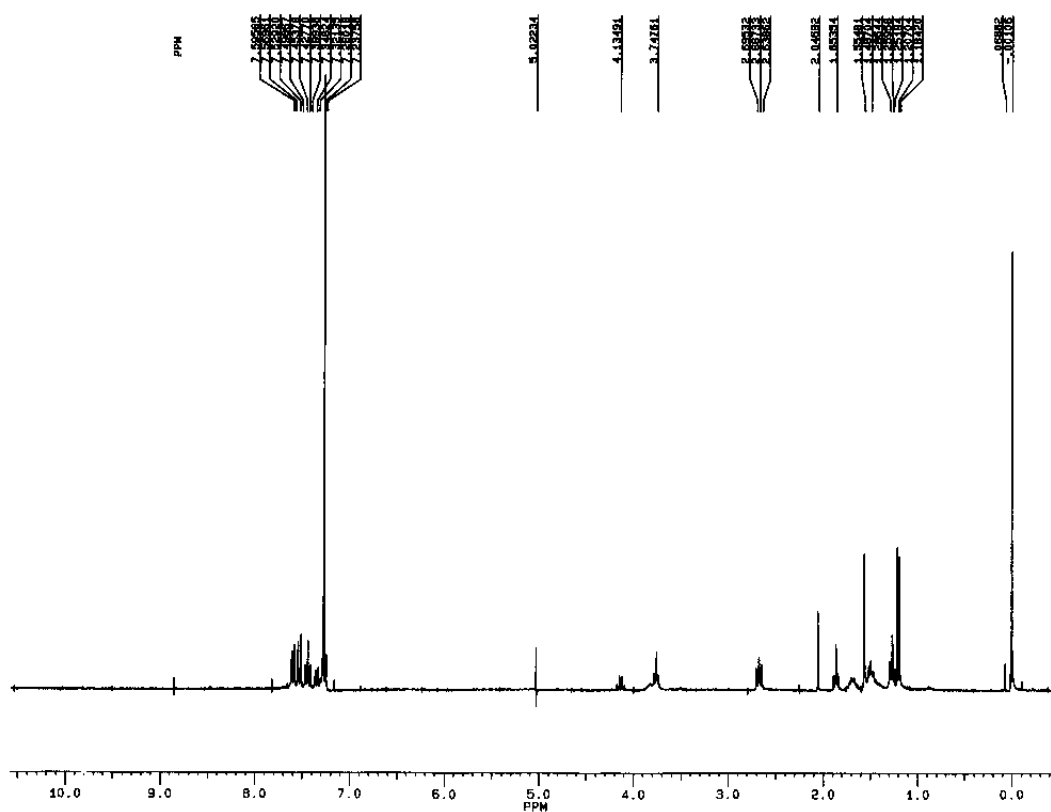


Figure 3.38 ^1H NMR (CHCl_3) of adduct formation in preparative electrolysis of **29**.

GC/MS data for adduct formation in the preparative electrolysis of **29**.

Major adduct: MS(EI) m/e 257 (M+1, 2.4), 256 (M+, 13.0), 157 (22),
129 (79), 115 (65), 91 (100), 83 (54)

Trace adduct 1: MS(EI) m/e 256 (M+, 1.5), 158 (23), 129 (46), 115 (65),
91 (100), 83 (93)

Trace adduct 2: MS(EI) m/e 254 (M+, 5.1), 167 (36), 129 (11), 115 (13),
91 (15), 83 (100)

**CHAPTER 4: CATHODIC REDUCTION OF
3-CYCLOPROPYL-CYCLOHEX-2-ENE-1-ONE**

4.1 INTRODUCTION

Previous systems in this study included highly conjugated cyclohexadieneones **13(a-c)** and aliphatic ketones **14(a, b)**, and **29**. Radical anions generated from α , β -unsaturated ketones offer a good complement to those systems. After one electron reduction, delocalization of spin and/or charge to the β -carbon through resonance (Figure 4.1) gives rise to new reaction pathways. The β -carbon has been shown to react both as a nucleophile and as a radical.

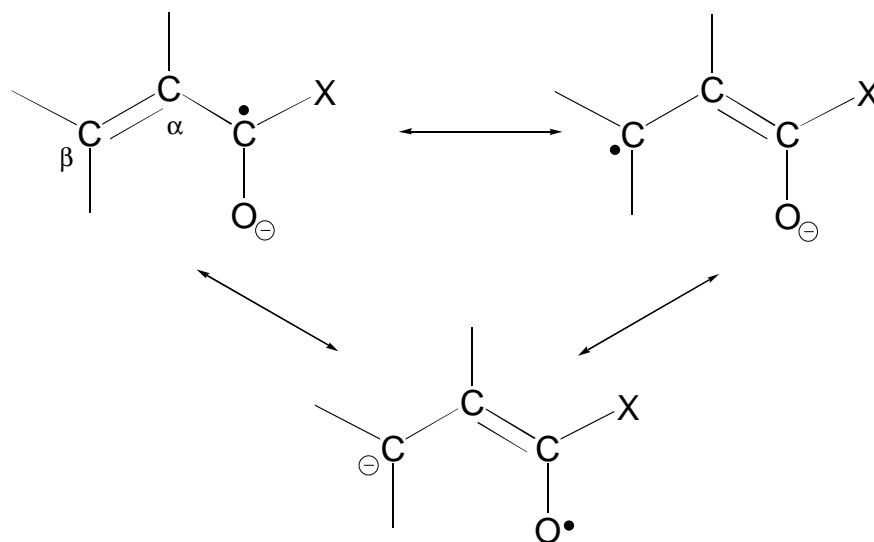
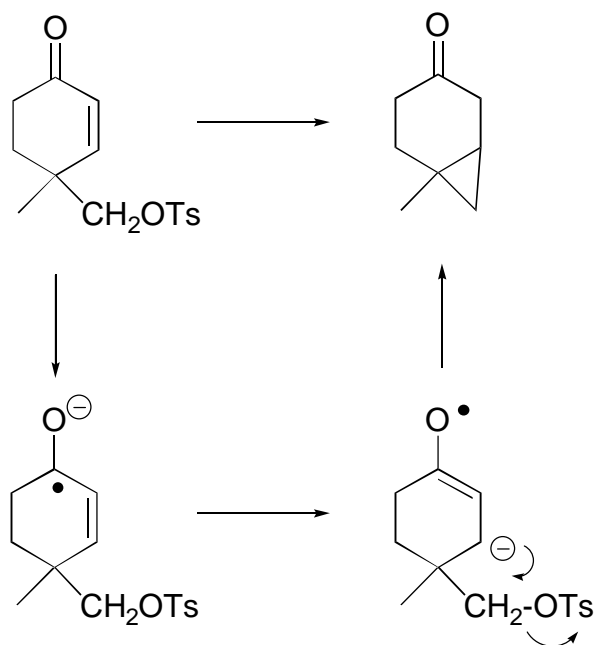


Figure 4.1 Resonance forms of α , β -unsaturated ketones

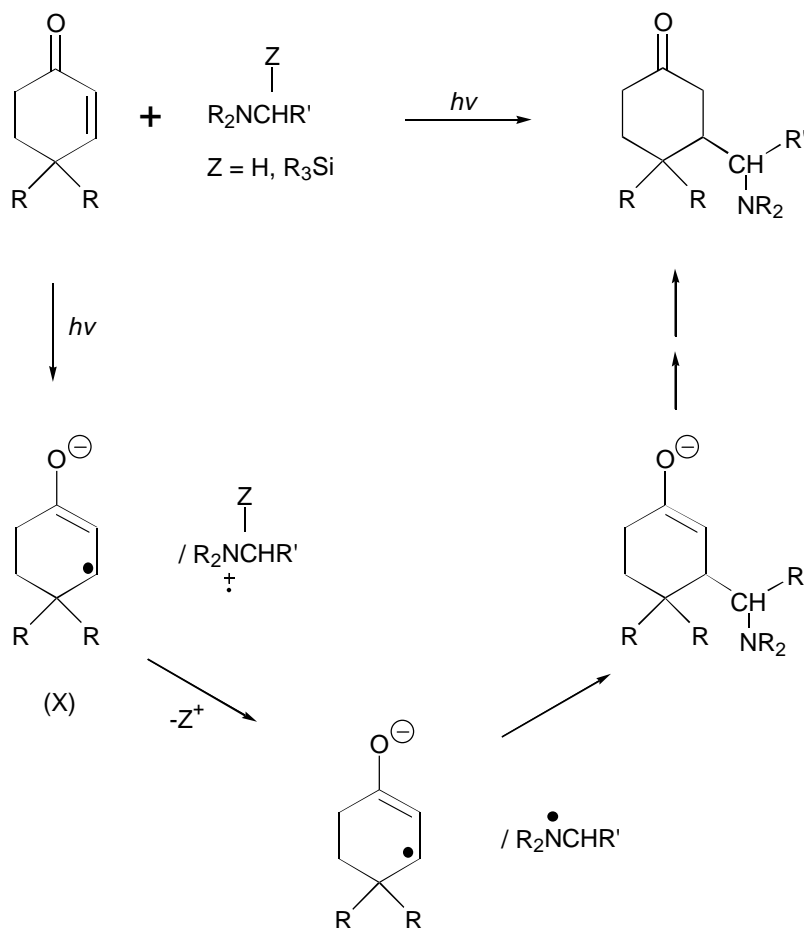
In 1981, Gassman¹⁰⁴ reported that electrochemical reductions of enones possessing a good leaving group at the γ position yield cyclopropanes in excellent (>80%) yields. The mechanism proposed for this reaction is outlined in Scheme 3.1 and illustrates the γ -carbon reacting as a nucleophile. Stork¹⁰⁵ reported similar reductions in 1960 using Li/NH₃.

Scheme 4.1



In contrast, Mariano¹⁰⁶ has reported numerous examples of photochemically-induced inter- and intra-molecular coupling reactions of enones with amines. The γ -carbon is reported to undergo radical anion/radical coupling as described in Scheme 4.2. The radical anion/radical cation pairs are generated by photoinduced electron transfer (PIET). Loss of 'Z⁺' from the ammonium radical cation followed by radical anion/radical coupling generates the final product.

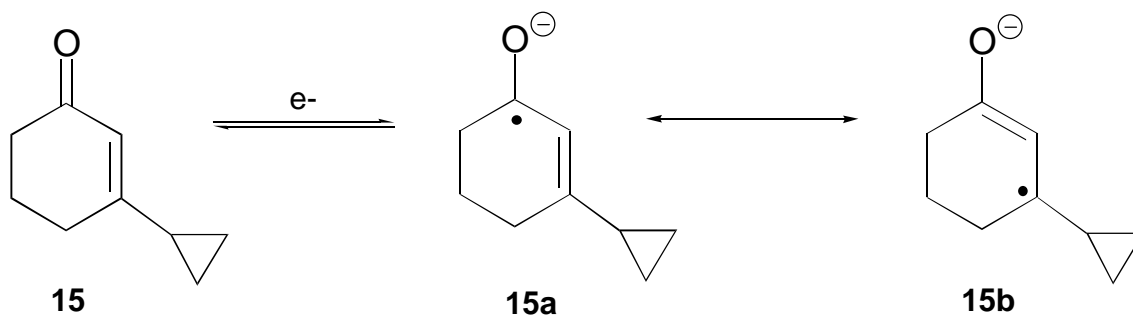
Scheme 4.2



In the context of this study, 3-cyclopropyl-cyclohex-2-ene-1-one offers an interesting extension to the systems previously studied. The thermodynamic driving force for ring opening, and the resonance stabilization gained by generating an aromatic ring, work in concert to make the rearrangements of cyclohexadieneones **13(a-c)** facile and energetically favored. In the aliphatic series compounds (**14a-b**) and **29**, there is little resonance stabilization effect and the relief of cyclopropyl ring strain provides the primary driving force. In the radical anion generated from cyclohexeneone **15**, a resonance form can be drawn that places the radical on the β -carbon next to the

cyclopropane ring. Presumably, this positioning of the radical will lead to ring opening of the cyclopropane ring in analogy to the cyclopropylcarbinyl \rightarrow homoallyl rearrangement. To what extent the resonance stabilization of the radical anion intermediate will be reflected in the rate of the cyclopropane ring opening is uncertain. A thorough linear sweep voltammetry study of **15** ensued.

Scheme 4.3



4.2 RESULTS AND DISCUSSION

4.2.1 Direct electrochemical reduction of **15**.

The cyclic voltammogram of cyclohexeneone **15** is characterized by an irreversible reduction wave at approximately -2.6 V (vs. 0.1 M Ag^+/Ag at 100 mV/s) (Figure 4.2). A linear sweep voltammetry (LSV)¹⁰⁷ study was conducted (Figures 4.3 \rightarrow 4.6) by monitoring the effects of substrate concentration and sweep rate on the peak potential (E_p). In summary: 1) the peak potential of the reduction wave (E_p) varied linearly with log of the sweep rate, 2) E_p was *independent* of substrate concentration, and 3) $E_{p1/2}$ remained constant over the sweep rate studied at $64 (\pm 8)$ mV.

For voltammetric waves in which no reverse current is observed, the variation in the forward peak potential (E_p) as a function of sweep rate and concentration can be related to the individual reaction orders in A and B according to Equations 4.1, 4.2, and Scheme 4.4. Experimental results are then compared to published theoretical responses for several possible mechanisms and results are presented in Table 4.1. Data analysis gives $\delta E_p / \delta \log(\nu) = -31.5 (\pm 4.8)$ mV/decade and $\delta E_p / \delta \log(C_A) = -1.9 (\pm 4.3)$ mV/decade; these values clearly support a mechanism which is first order in radical anion B as shown in Scheme 4.4 (*i.e.*, an EC or ECE type process). The theoretically predicted responses¹⁰⁷ are $\delta E_p / \delta \log(\nu) = -29.6$ mV/decade and $\delta E_p / \delta \log(C_A) = 0$ mV/decade.

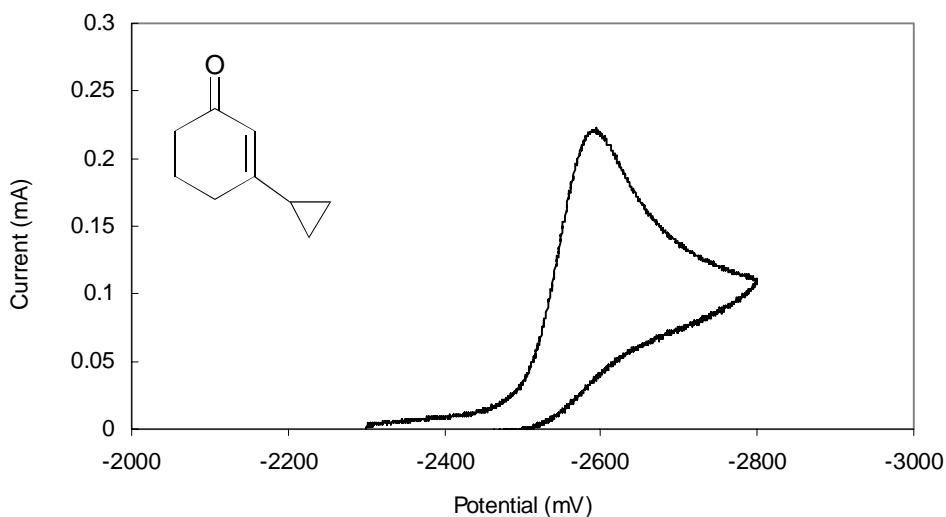


Figure 4.2 Cyclic voltammogram of **15** (0.5 M TBAP in DMF, 0.1 M Ag^+/Ag reference, $\nu = 100$ mV/s, GCE, 0.003 M in substrate)

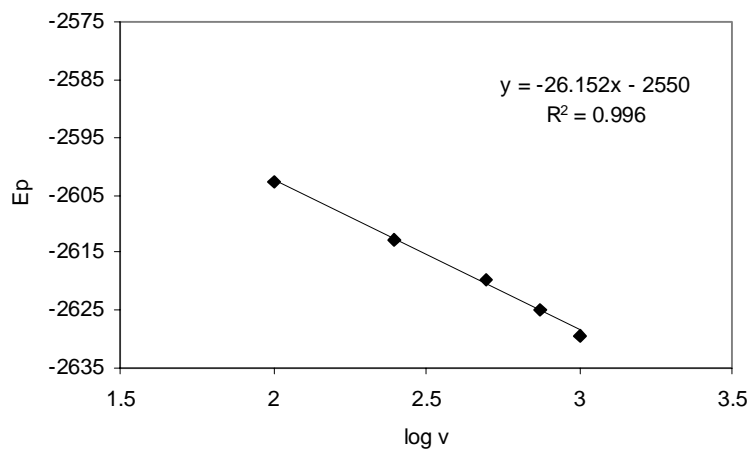


Figure 4.3. LSV analysis of **15**, $\partial E_p/\partial \log v$. (0.0015 M in substrate, 0.5 M TBAP, DMF, $v = 100 - 1000$ mV/s)

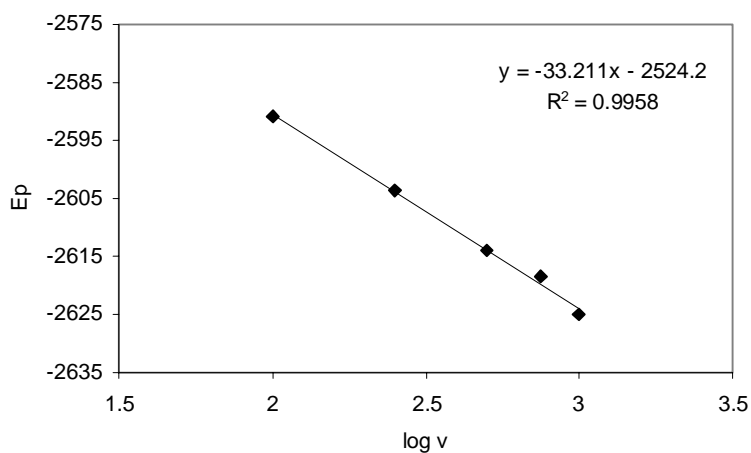


Figure 4.4 LSV analysis of **15**, $\partial E_p/\partial \log v$. (0.0029 M in substrate, 0.5 M TBAP, DMF, $v = 100 - 1000$ mV/s)

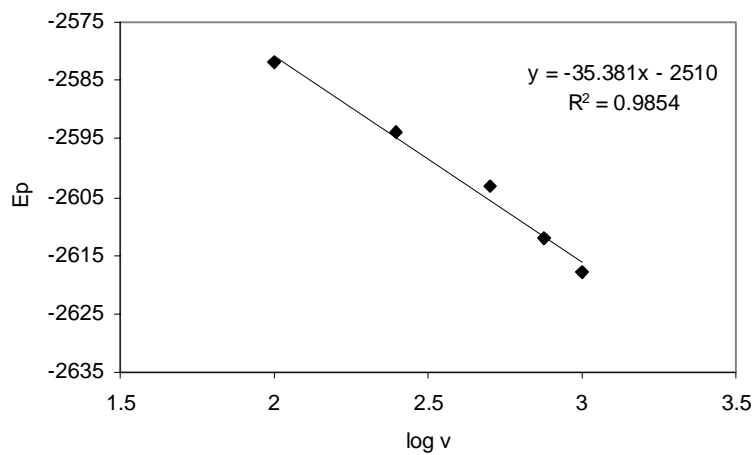


Figure 4.5 LSV analysis of **15**, $\partial E_p / \partial \log v$. (0.0059 M in substrate, 0.5 M TBAP, DMF, $v = 100 - 1000$ mV/s)

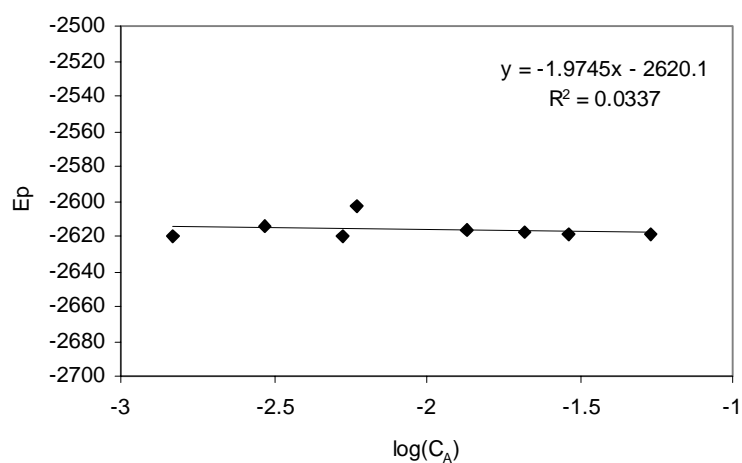


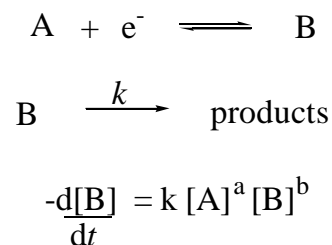
Figure 4.6 LSV analysis of **15**, $\partial E_p / \partial \log (C_A)$. (0.5 M TBAP, DMF, $v = 500$ mV/s)

$$\delta E_p / \delta \log v = -1 / (b + 1) \log (RT / nF) \quad (4.1)$$

$$\delta E_p / \delta \log C_A = (a + b - 1) / (b + 1) \log (RT / nF) \quad (4.2)$$

Table 4.1 LSV analysis of 3-cyclopropyl-cyclohex-2-enone **15**¹⁰⁷.

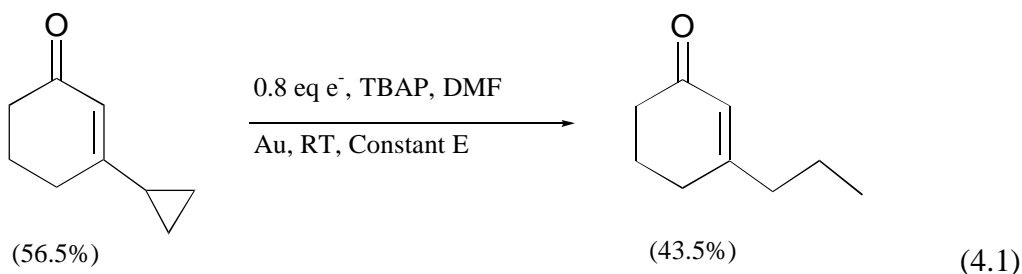
Rate law	$\delta E_p/\delta \log(v)$ (mV/decade)	$\delta E_p/\delta \log(C_A)$ (mV/decade)
$k[B]$	-29.5	0
$k[B]^2$	-19.7	19.7
$k[A][B]$	-29.5	29.5
Obsd	-31.5 ± 4.8	-1.9 ± 4.3

Scheme 4.4

The rate law for decay of the radical anion intermediate was readily determined from published theoretical responses. However, because the cyclic voltammogram produced from **29** is irreversible, the rate constants for cyclopropane ring opening and the standard reduction potential are unavailable.

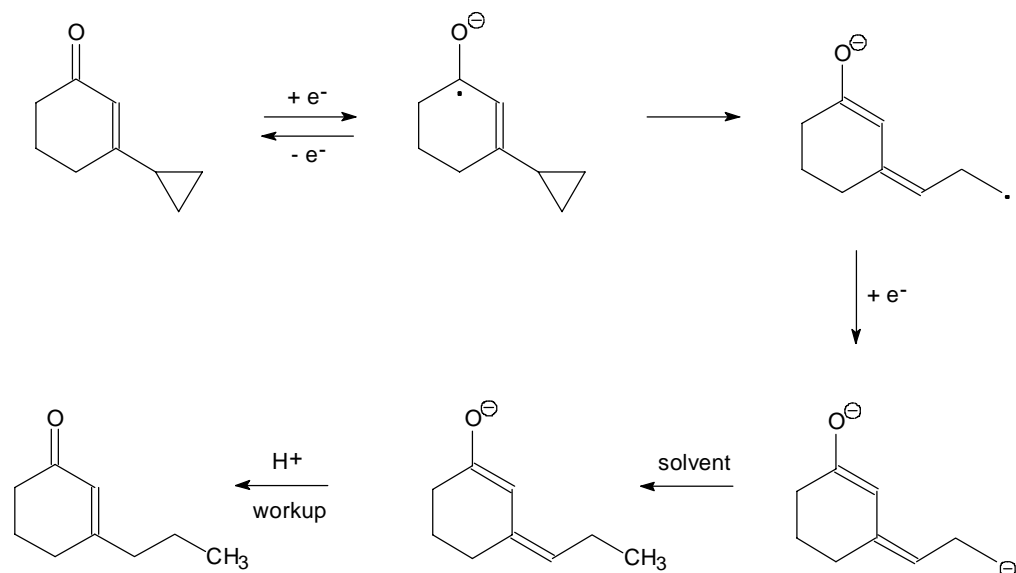
4.2.2 Product analysis from preparative electrolysis of **15**.

Preparative scale reduction of cyclohexenone **15** (Equation 4.1) gave exclusively ring opened product 3-propyl-cyclohex-2-ene-1-one (**30**) in 43.5% yield (56.5% unreacted starting material) after the transfer of 0.8 eq of electrons.

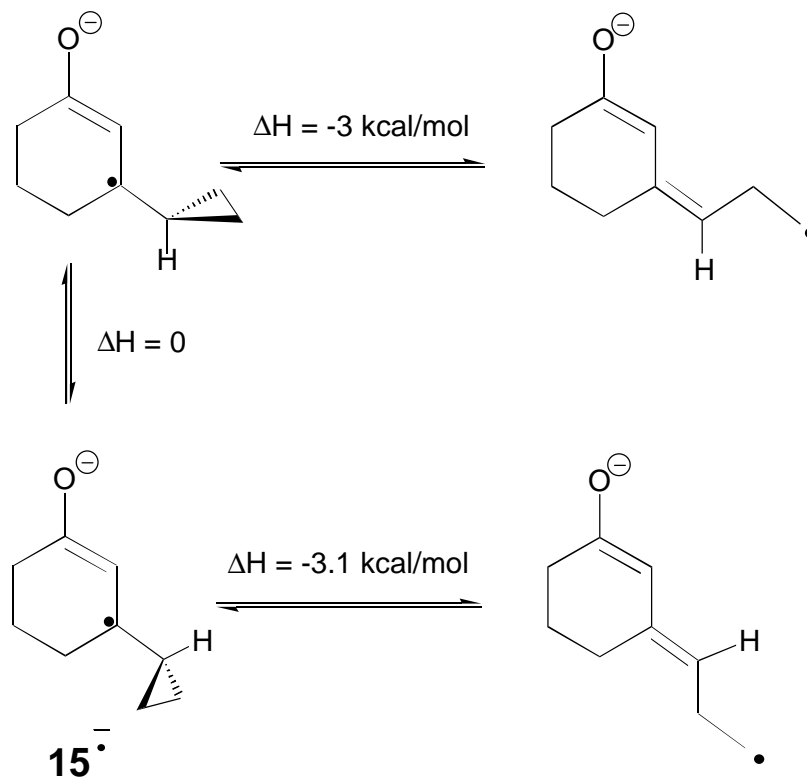


The electrolysis results combined with the rate law determined for the decay of the radical anion support the mechanism described in Scheme 4.5. Cyclohexenone **15** is reduced at the electrode surface to form the radical anion, which upon ring opening is further reduced to the dianion. Abstraction of a proton from the electrolyte solution and acidic work-up yield the final product shown. The radical anion **15^{•-}** can exist in two degenerate bisected conformations, and AM1 calculations suggest that the ring opening is exothermic by ~3 kcal/mol (Scheme 4.6).⁹³

Scheme 4.5



Scheme 4.6

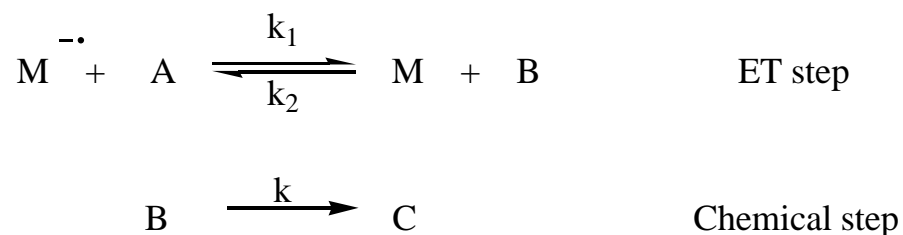


4.2.3 Indirect electrochemistry of **15a**.

The reduction of **15** by two mediators, anthracene and 9-methylantracene, was studied. As in previous experiments, the current ratio i_p/i_{pd} was examined as a function of sweep rate and mediator concentration at constant excess factor γ . However, a $\gamma = 10$ was employed for these reductions. At $\gamma = 1$, these systems were not sufficiently catalytic (no or little increase in current or loss of reversibility was observed upon addition of substrate to mediator).

As described previously (details in section 2.2.3), the discerning characteristic between rate limiting homogenous electron transfer and homogeneous chemical step is the effect of mediator concentration (C_M^0) on i_p/i_{pd} at constant γ and v . Voltammograms of anthracene and 9-methylanthracene in the absence and presence of **15** were obtained. Plots of [i_p/i_{pd} vs $\log(1/v)$] and [i_p/i_{pd} vs $\log(C_M^0/v)$] were obtained at different concentrations of mediator (constant γ) and inspected for a concentration dependence (Figure 4.7 and Figure 4.8). For the reduction of **15** by anthracene and 9-methylanthracene, i_p/i_{pd} was found to vary as a function of mediator concentration. Therefore, electron transfer was the rate limiting step and rate constants for electron transfer from the reduced form of the mediator were determined.

Scheme 4.7



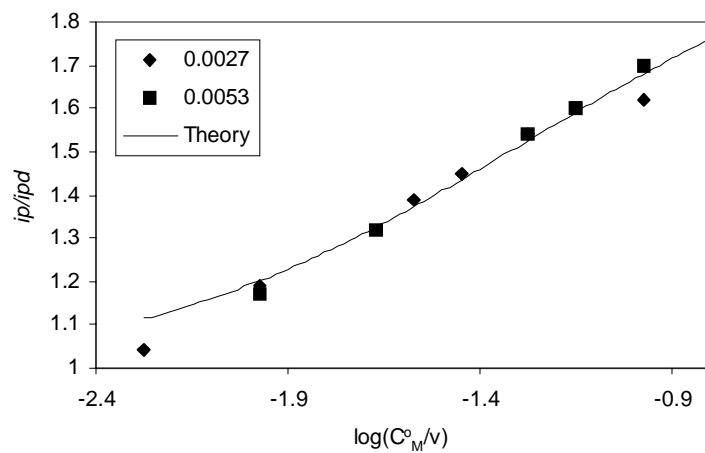
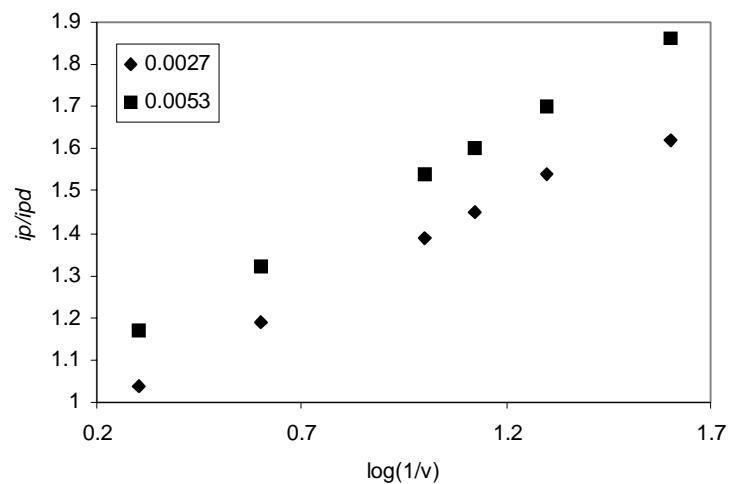


Figure 4.7 Mediated reduction of **15** by anthracene (DMF, GCE, 0.5 M TBAP, $v = 0.025$ - 0.5 Vs^{-1} , $\gamma = 10.0$; line is the working curve for rate-limiting ET, $x' = 1.2443 \pm 0.023$, $\rho = 0$)

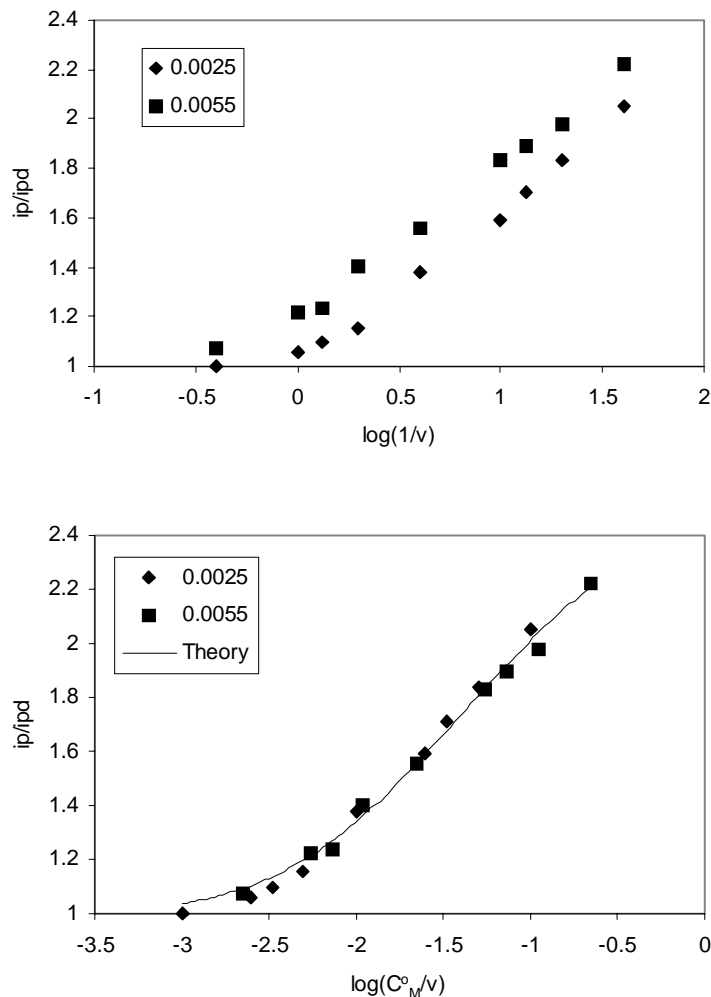


Figure 4.8 Mediated reduction of **15** by 9-methylanthracene (DMF, GCE, 0.5 M TBAP, $v = 0.025\text{-}2.5 \text{ Vs}^{-1}$, $\gamma = 10.0$; line is the working curve for rate-limiting ET, $x' = 1.4558 \pm 0.015$, $\rho = 0.2$)

Previously determined working curves (Chapter 2 and 3) dealing with rate limiting electron transfer and addition to the catalyst express i_p/i_{pd} as a function of $\gamma = 1$. In these experiments, i_p/i_{pd} was measured at various sweep rates at $\gamma = 10$, and it was thus necessary to derive the appropriate working curves (11 plots of i_p/i_{pd} vs $\log(\lambda_1)$ at $\gamma =$

10.00 for $\rho = 0.00$ to 1.00 in 0.10 increments) via digital simulation⁶⁹. These working curves were subsequently fit to a polynomial of the form $y=(a+cx+ex^2)/(1+bx+dx^2+fx^3)$, where the coefficients $a \rightarrow f$ were determined for each working curve. Via non-linear regression,⁶⁹ the experimental data [i_p/i_{pd} vs $\log (C_M^0/\nu)$] were fit to the polynomial form of the working curves, $y = f(x + x')$, and the adjustable parameter $x' = \log (k_1RT/F)$ was determined. The parameter ρ was determined by the working curve which gave the best fit to the experimental data and k_1 was determined from x' . The fits of experimental data to working curves are provided in Figures 4.7 and 4.8. Table 4.2 summarizes the values of k_1 and ρ obtained for reduction of **15** by anthracene and 9-methylanthracene.

Table 4.2. Rate constants for homogeneous electron transfer between the reduced form of the mediator and **15** (0.5 M TBAP/DMF).

Mediator	E^o (V) ^a	k_1 ($M^{-1}s^{-1}$)	ρ
anthracene	-2.337	$6.8 (\pm 0.4) \times 10^2$	$0.0 (\pm 0.1)$
9-methylanthracene	-2.359	$1.1 (\pm 0.1) \times 10^3$	$0.2 (\pm 0.1)$

^avs. 0.1 M $AgNO_3/Ag$

A complete homogeneous catalysis study analogous to that performed for the cyclohexadieneones (Chapter 2) and aliphatic ketones (Chapter 3) could not be performed due to the unavailability of suitable aromatic hydrocarbon mediators. Table 4.3 lists the mediators used in prior studies contained in this dissertation.

Table 4.3. Standard reduction potentials of mediators^{97,98}

Mediator	E ⁰ (vs SCE) ^a	E ⁰ (vs SCE)
fluoranthene	-1.813	-1.715 ^b
4-cyanopyridine	-1.831	-1.730 ^b
cyanonaphthalene	-1.909	-1.810 ^b
9,10-diphenylanthracene	-1.913	-1.840 ^b
9-phenylanthracene	-1.954	
anthracene	-2.000	-1.875 ^b
9-methylanthracene	-2.022	
naphthalene	-2.564	-2.457 ^c
3,6-dimethylphenanthrene	-2.600	
1,3-dimethylnaphthalene	-2.634	
biphenyl	-2.640	-2.519 ^c
methoxynaphthalene	-2.651	-2.537 ^c
2,7-dimethoxynaphthalene	-2.690	
2-methoxybiphenyl	-2.749	

^adetermined in our lab vs AgNO₃/Ag and adjusted to SCE (-0.337 V), GCE, DMF, 0.5 M TBAP; ^bDMF, GCE, 0.1M *n*Bu₄BF₄; ^cDMF, 0.1 M *n*Bu₄BF₄, mercury plated platinum disk electrode.

In Table 4.3 an obvious gap exists between mediators 9-methylanthracene and naphthalene. Suitable substituted aromatic hydrocarbons must be obtained for this potential region before a homogeneous catalysis study can be completed. It is likely that

enough aromatic hydrocarbons will not be available, and other compounds must be investigated. Saveant has employed a series of substituted benzoates for the electrochemical reduction of carbon dioxide with potentials in the range required for this study; these compounds may prove useful here. However, the λ (reorganization energy) obtained is apt to be quite different from that obtained with substituted aromatic hydrocarbons.

If a suitable series of mediators can be obtained for the reduction of **15**, rate constants for electron transfer (k_1) can be used with Marcus theory to obtain the standard reduction potential of $15/15^{\bullet-}$ and the reorganization energy λ . If the rate of the homogeneous catalysis system is found to be controlled by the electron transfer step ($E^{\circ}_{A/B}$ available), as was seen with anthracene and 9-methylanthracene, it will be possible to extract the rate constant for ring opening of radical anion $15^{\bullet-}$ with equation 4.3.¹⁰⁸ This is possible because the rate limiting step in the direct reduction of **15** was found to be the chemical step. The peak potential, E_p , is then a function of the standard potential of the A/B couple, $E^{\circ}_{A/B}$, and of k .

$$E_p = (RT / F)[\ln (RT / F) - 0.78] + E^{\circ}_{AB} + (RT / 2F) \ln(k / \nu) \quad (4.3)$$

4.3 CONCLUSIONS

Upon reduction, the radical anion derived from 3-cyclopropyl-

cyclohex-2-en-1-one undergoes facile ring opening to give exclusively the ring opened product. LSV results indicate the radical anion decays by a first order process, and a rate law ($\text{Rate} = k[\text{B}]$) is obtained. The kinetics of homogeneous catalysis experiments were controlled by the electron transfer step. When a suitable set of mediators can be found, the standard reduction potential of **15** can be determined with Marcus theory. In contrast, the direct reduction (LSV) experiments were controlled by the homogeneous chemical step, not by the heterogeneous electron transfer step. These findings will ultimately allow the extraction of the rate constant for cyclopropyl ring opening.

CHAPTER 5: CONCLUSIONS

In summary, the rearrangements of the radical anions included in this dissertation all yield ring opened products, with rates and selectivities that will prove useful and informative in the design of mechanistic probes based on the cyclopropylcarbinyl \rightarrow homoallyl rearrangement. As more radical ion rearrangements are investigated and the rate constants better defined through these and other analytical techniques, the better we will understand the structural contributions to these rearrangements. The results herein demonstrate that the relationship between rearrangement rates of neutral free radicals and similarly-structured radical ions is not simple. Delocalization of spin is certainly an important consideration affecting the rates of rearrangement of paramagnetic intermediates in general. However, these findings reveal that for radical ions, charge also plays an important role. Stabilization of both charge and spin are important factors to consider when designing electron transfer mechanistic probes. Although this work has focussed specifically on radical anion rearrangements, there is little doubt that the same considerations pertain to the rearrangements of radical cations. In a more general sense, radical ions are an important class of reactive intermediates, with chemistry resulting from their roles as “radicals” and “ions”. If their chemistry can be understood and eventually controlled, new synthetic methodologies may emerge.

CHAPTER 6: EXPERIMENTAL

6.1 General

6.1.1 Instrumentation description

Nuclear magnetic resonance spectra (^1H , ^{13}C) were obtained on either WP 270 MHz Bruker, AM 360 MHz Bruker, or 400 MHz Varian Unity FT NMR spectrometers. All chemical shifts are reported in δ units relative to TMS ($\delta = 0.00$ ppm) in CDCl_3 . Infrared spectra were recorded on a Perkin-Elmer model 1600 FT-IR spectrometer. GC/MS was performed on a Hewlett Packard HP 5890 gas chromatograph interfaced to a HP 5970 low resolution mass spectrometer and a HP series computer. High-resolution mass spectral data were obtained from a VG Analytical model 7070 E-HF double-focusing magnetic sector high-resolution spectrometer using electron impact (70eV) ionization. GC analysis was performed on a Hewlett Packard 5890A gas chromatograph equipped with an FID detector and an HP 3393A reporting integrator. High performance liquid chromatography (preparative and analytical scale) was performed using a Beckman System Gold 128 model solvent pump system with a 166 model UV/VIS detector. Samples were separated using Beckman C-18 reverse phase columns (analytical: 4.6 mm x 250 mm; preparative: 21.2 mm x 150mm) with an 80/20 acetonitrile/water solvent system. Preparative thin layer chromatography separations (PTLC, Whatman, silica gel plates, 250 μm layer, UV₂₅₄) were performed using hexane/ethyl acetate solvent mixtures.

6.1.2 Electrochemical Measurements.

Electrochemical measurements were performed on an EG & G Princeton Applied

Research (EG & G / PAR) model 273 potentiostat/galvanostat interfaced to an MS-DOS computer. The detailed instrumentation employed for cyclic and linear sweep voltammetry as well as cell description and assembly has been described earlier.¹⁰⁹

Voltammetric measurements were performed on solutions which contained 0.5 M tetra-*n*-butyl-ammonium perchlorate (TBAP) in DMF. Solutions were prepared by weighing out 1.71 g TBAP into a 10 mL volumetric flask. The 10 mL flask along with all other voltammetric cell pieces (with the exception of the working electrode) were treated in a Baxter DP-22 vacuum drying oven (30-40 mmHg) at 40° C for 1.5 hours. Voltammetric cell pieces were then placed immediately in a desiccator to cool. The voltammetric cell was assembled under argon/nitrogen flow. The 10 mL flask containing electrolyte was diluted with purified DMF and added to the voltammetric cell. The completed cell assembly was argon (dry, deoxygenated) purged for approximately 15 min. prior to use. The electroactive substance was added to the cell only after clean backgrounds were obtained at each sweep rate used (a maximum cell current < 10 uA at $v = 100$ mV/s over the potential range $-2.7 \rightarrow -3.2$ V was considered acceptable).

A three-electrode voltammetry cell was used. The GCE working electrode (5 mm diameter) was prepared for use by polishing with an alumina slurry to a mirror finish and stored in a desiccator. The Ag/Ag⁺ (0.1 M in CH₃CN, 0.337 V vs SCE, uncalibrated) reference electrode was freshly prepared. A Pt wire coil was used as the auxillary electrode. Mechanical stirring was performed between voltammetric runs to clean the working electrode surface. Positive-feedback iR compensation was set by monitoring the current response. IR compensation was increased until oscillation and then backed off to 90% of that value. All experiments were performed at ambient temperature (23° C).

The GCE working electrodes were prepared as follows. Glassy carbon rod (Alfa Aesar) was cut into several 4-5 mm plugs. Carbon plugs were secured into glass rods with Torrseal – Varian vacuum epoxy resin (Varian vacuum products) being careful not to get epoxy on the reverse of the carbon plug where electrical connection must be made. Rods were left to cure in air for two days. A small amount of silver 2-part conductive adhesive (Alfa Aesar) was placed into the glass rods and a short piece of Cu brazing rod was inserted and allowed to cure for two days. The electrode surface was polished with alumina slurry (Buehler) starting with 1.0 μm grit and decreasing to 0.3 and finally 0.05 μm until a mirror finish was obtained. The surface was maintained by polishing routinely with 0.05 μm grit polish, rinsing with methanol and water, and wiping lightly.

Preparative electrolysis was performed on solutions which contained 0.2 M TBAP in DMF. Solution preparation and cell handling were performed similarly to that for voltammetry. A conventional H-cell with two compartments separated by a medium glass frit was utilized. 50 mL of electrolyte solution was divided equally between the two compartments of the vacuum oven dried H-cell, and the resulting system was purged with dry, deoxygenated argon for > 15 min. before use. The electro-active substrate was placed in the working compartment exclusively and electrolysis was conducted as specified in the specific experiments. For constant potential experiments, iR compensation was set as in voltammetric experiments.

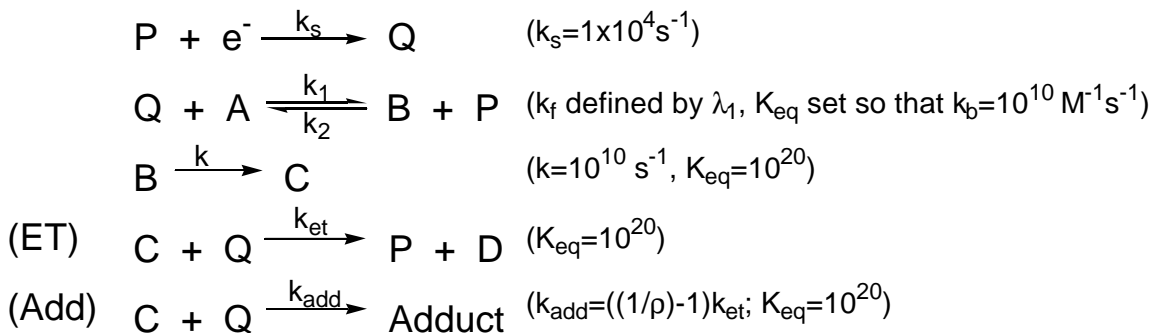
The working electrode was manufactured from gold foil soldered (Ag solder) to a short piece of Ag wire which was in turn soldered to a piece of Cu rod. Coiled Cu wire was used as the auxiliary electrode, and the reference was Ag/Ag⁺ (0.1 M in CH₃CN). All electrolysis experiments were performed at ambient temperature (23° C). Reaction

progress was monitored by GC where necessary. Unless otherwise noted, solution work-up consisted of quenching the cathodic compartment with ca. 1 mL 5% H₂SO₄, adding to ca. 50 mL water, and extracting with 4 x 50 mL ether. Ether layers were combined, washed with water, sat. NaCl, dried over MgSO₄, and concentrated. Product isolations, characterizations, and quantitations were performed as noted.

6.1.3 Digital Simulations

Digital simulations of cyclic voltammograms were performed using Digisim 2.1 (Bioanalytical Systems Inc., 2701 Kent Ave. W. Lafayette, IN 47906) and working curves were generated from simulated responses using TableCurve 2D (Jandel Scientific Software: 2591 Kerner Blvd., San Rafael, CA 94901.). The following assumptions were made in the generation of these curves: 1) the reaction rate constants and mechanism in Scheme 6.1., 2). $k_{\text{et}} + k_{\text{add}} = 1 \times 10^{10} \text{ M}^{-1} \text{ s}^{-1}$, 3) T=298°K, 4) planar electrode geometry with area = 1 cm², 5) semi-infinite diffusion is assumed and the pre-equilibrium is disabled, 6) $\alpha = 0.5$, 7) an average value for the diffusion coefficients of species, $D = 1 \times 10^{-5} \text{ cm}^2/\text{s}$, 8) model parameters: expanding space factor = 0.1, potential step (V) = 0.0025 (or $\leq (\text{sweep rate } (v) / 50)$ at $v < 0.5 \text{ V/s}$), iterations = 2, $D/k = 1 \times 10^{-12}$, $x_{\text{max}}/\text{sqrt}(Dt) = 6$, r0 minimum = 20. Concentration of species, gamma (γ), and sweep rate (v) were varied.

Scheme 6.1



6.1.4 Materials and purification.¹⁰⁹

N,N-dimethylformamide (DMF, EM Science, 98%) was stirred over copper (II) sulfate (Aldrich, 98%) and activated alumina (Aldrich, neutral, Brockman activity I) for > three days and vacuum distilled just prior to use. Alumina was flame dried under vacuum (until evolution of water vapor ceased) prior to use. 1-Methyl-2-pyrrolidinone (NMP) was vacuum distilled and stored over molecular sieves. Dimethylsulfoxide (DMSO) was stirred over CaH₂ for several days and vacuum distilled just prior to use. *Tetra-n*-butylammonium perchlorate (TBAP) was prepared by the method of House¹¹⁰ and recrystallized 4 x from ethyl acetate/hexane and vacuum oven dried before use. 5,7-Di-*t*-butylspiro[2,5]octa-4,7-dien-6-one **13a**,¹¹¹ 1-methyl-5,7-di-*t*-butylspiro[2,5]octa-4,7-dien-6-one **13b**,¹¹¹ 1,1-dimethyl-5,7-di-*t*-butylspiro[2,5]octa-4,7-dien-6-one **13c**,¹¹¹ and 2,6-di-*t*-butyl-4,4-dimethylcyclohexa-2,5-dien-1-one¹¹² were prepared through modification of previously published syntheses. 1-Acetyl-2,2-dimethyl cyclopropane **14b**,^{113,114} and 3-cyclopropyl-cyclohex-2-enone **15**¹¹⁵ were prepared without modification from published synthesis. Cyclopropyl methyl ketone **14a** (Aldrich, 99%), cyclobutyl

methyl ketone **29** (Aldrich, 98%), 2-pentanone (Aldrich, 99+%), 4,4-dimethyl-2-pentanone (Aldrich, 99%), 5-methyl-2-hexanone (Aldrich, 99%), 2-hexanone (Aldrich, 98%), and 4,6-tri-*t*-butylphenol (Aldrich, 96%) were used as received. All catalysts used in this study except fluoranthene (Agros Organics, >98%) and anthracene (Matheson, Coleman & Bell, >98%) were obtained from Aldrich and used as received.

6.2 Electrolysis

Products of bulk electrolysis were all known compounds. Characterization was confirmed as needed for compounds which were not commercially available.

6.2.1 Electrolysis (specific)

5,7-Di-*t*-butylspiro[2,5]octa-4,7-dien-6-one (13a). After electrolysis of 80 mg (0.34 mmol) of **13a** for 37 min at 30 mA (2 equiv. of electrons), subsequent work-up and separation of the crude oil via PTLC (1% EtOAC/Hexane) yielded the following pure compounds: 2,6-di-*t*-butyl-4-ethylphenol¹¹⁶ (35 mg, 43%), 1,4-bis(3',5'-di-*t*-butyl-4'-hydroxybenzyl)butane¹¹⁷ (22 mg, 28%), and unreacted starting material **13a** (10 mg, 11%) quantitated as 2,6-di-*t*-butyl-4-(hydroxy-ethyl)phenol¹¹⁸ generated during the acidic workup.

Cyclopropyl methyl ketone (14a). **14a** (1.28 mmol) and biphenyl (1.27 mmol) were electrolyzed for 60 min (1 eq. e⁻) at -3.0 V (vs Ag/Ag⁺). The electrolytic solution was quenched and analyzed by GC (chlorobenzene as internal standard) to give 2-pentanone (34%) and **14a** (60%). Product retention times were determined by comparison to

authentic samples. Work-up and separation via PTLC (EtOAc/Hexane) yielded 11 mg adduct products (1 major). Mixture characterized by GC/MS and ^1H NMR.

1-Acetyl-2,2-dimethylcyclopropane (14b). **14b** (1.53 mmol) was electrolyzed in NMP at 30 mA until 0.4 eq electrons were transferred. The electrolytic solution was quenched and analyzed by GC (cyclohexane as internal standard) to give a mixture of 4,4-dimethyl-2-pentanone (3%), 5-methyl-2-hexanone (7%), and **14b** (91%). Product retention times were determined by comparison to authentic samples.

Cyclobutyl methyl ketone (29). **29** (2.14 mmol) and biphenyl (1.62 mmol) were electrolyzed at 30 mA until 0.7 eq of electrons were transferred. The electrolytic solution was quenched and analyzed by GC (2,5-dimethylhexane as internal standard) to give 2-hexanone (24%). Product retention times were determined by comparison to authentic samples. Work-up and separation via PTLC (EtOAc/Hexane) gave 7 mg adduct products (1 major). Mixture characterized by GC/MS and ^1H NMR.

3-Cyclopropyl-cyclohex-2-enone (15). **15** (0.3902 mmol) was electrolyzed at -2.62 V (vs Ag/Ag^+) for 60 min. (0.8 eq of electrons). The electrolytic solution was quenched and analyzed by GC (biphenyl as internal standard) to give 3-propyl-cyclohex-2-enone (43.5%). A pure sample of 3-propyl-cyclohex-2-enone was isolated by flash column chromatography (20% ethylacetate/hexane).¹¹⁹

6.2.2 Spectroscopic Data

2,6-di-*t*-butyl-4-ethylphenol: $^1\text{H NMR}$ (CDCl_3) δ 7.02 (s, 2H), 5.04 (s, 1H), 2.59 (q, 2H), 1.45 (s, 18H), 1.23 (t, 3H); $^{13}\text{C NMR}$ (CDCl_3) δ 152, 137, 135, 123, 34, 30, 29, 16; **HRMS** (EI) $\text{C}_{16}\text{H}_{26}\text{O}$, obs'd: 234.198700, calc'd: 234.1983657, error: 1.4 ppm.

1,4-bis(3',5'-di-*t*-butyl-4'-hydroxybenzyl)butane: $^1\text{H NMR}$ (CDCl_3) δ 6.99 (s, 4H), 5.02 (s, 2H), 2.56 (m, 4H), 1.67 (m, 4H), 1.44 (s, 36H); $^{13}\text{C NMR}$ (CDCl_3) δ 152, 136, 133, 124, 36, 34, 32, 30; **HRMS** (EI) $\text{C}_{32}\text{H}_{50}\text{O}_2$, obs'd: 466.382034, calc'd: 466.3810813, error: 2.0 ppm.

2,6-di-*t*-butyl-4-(hydroxy-ethyl)phenol: $^1\text{H NMR}$ (CDCl_3) δ 6.99 (s, 2H), 5.09 (s, 1H), 3.81 (m, 2H), 2.79 (m, 2H), 1.41 (s, 18H); $^{13}\text{C NMR}$ (CDCl_3) δ 152, 136, 129, 126, 64, 39, 34, 30; **HRMS** $\text{C}_{16}\text{H}_{26}\text{O}_2$, obs'd: 250.194077, calc'd: 250.1932803, error: 3.2 ppm.

2,6-di-*t*-butyl-4-isopropyl-phenol: $^1\text{H NMR}$ (CDCl_3) δ 1.63 (d, 3H, $J = 6.9$ Hz), 1.45 (s, 19H), 2.83 (m, 1H), 5.03 (s, 1H), 7.03 (s, 2H).

2,6-di-*t*-butyl-4-prop-2-ene-phenol: $^1\text{H NMR}$ (CDCl_3) δ 0.99 (t, 3H, $J = 7.2$ Hz), 1.46 (s, 19H), 1.63 (m, 2H, $J = 7.5$ Hz), 2.52 (t, 2H, $J = 7.6$ Hz), 5.04 (s, 1H), 7.00 (s, 2H).

2,6-di-*t*-butyl-4-propyl-phenol: $^1\text{H NMR}$ (CDCl_3) δ 1.43 (s, 19H), 3.31 (d, 2H, $J = 6.8$ Hz), 5.02-5.11 (complex, 3H), 5.97 (m, 1H), 6.99 (s, 2H).

2-(3',5'-di-*t*-butyl-4'-hydroxyphenyl)-propan-2-ol: $^1\text{H NMR}$ (CDCl_3) δ 1.43 (s, 6H), 1.48 (s, 19H), 5.85 (s, 1H), 7.85 (s, 2H), 9.35 (s, 1H).

2,6-di-*t*-butyl-4-iso-butyl-phenol: $^1\text{H NMR}$ (CDCl_3) δ 0.91 (d, 6H), 1.43 (s, 18H), 1.78 (m, 1H), 2.37 (d, 2H), 5.00 (s, 1H), 6.92 (s, 2H); $^{13}\text{C NMR}$ (CDCl_3) δ 152, 136, 132, 126, 46, 34, 31, 30, 23; **MS** (EI) m/e 262 (23, M^+), 247 (38), 219 (100), 57 (15); **IR** ν , cm^{-1} 3649, 3074, 2957, 1773, 1600, 1435, 1364, 1315, 1233, 1158, 1121, 1088, 1023, 932, 898, 884, 801, 786, 768, 742, 641

2,6-di-*t*-butyl-4-isoprene-phenol: $^1\text{H NMR}$ (CDCl_3) δ 6.98 (s, 2H), 5.06 (s, 1H), 4.79 (s, 1H), 4.72 (s, 1H), 3.25 (s, 2H), 1.71 (s, 3H), 1.44 (s, 18H); $^{13}\text{C NMR}$ (CDCl_3) δ 153, 146, 136, 131, 126, 112, 45, 35, 30, 23; **HRMS** $\text{C}_{18}\text{H}_{28}\text{O}$, obs'd: 260.214218, calc'd: 260.214016, error: 0.8ppm. **IR** ν , cm^{-1} 3648, 3072, 2955, 1649, 1431, 1390, 1361, 1313, 1232, 1155, 1120, 1026, 932, 885, 808, 791, 767, 709, 638, 615.

2-(3',5'-di-*t*-butyl-4'-hydroxybenzyl)-propan-2-ol: mp 89-93 (92-93 lit.); $^1\text{H NMR}$ (CDCl_3) δ 6.98 (s, 2H), 5.11 (s, 1H), 2.68 (s, 2H), 1.44 (s, 18H), 1.23 (s, 6H); **IR** ν , cm^{-1} 3643, 3364.

2-(3',5'-di-*t*-butyl-4'-hydroxyphenyl)-2-methylpropanol: $^1\text{H NMR}$ (CDCl_3) δ 7.18 (s, 2H), 5.13 (s, 1H), 3.55 (m, 2H), 1.45 (s, 18H), 1.32 (s, 6H); $^{13}\text{C NMR}$ (CDCl_3) δ 152, 136, 135, 123, 73, 40, 35, 30, 25.

3-propyl-cyclohex-2-enone: $^1\text{H NMR}$ (CDCl_3) δ 5.88 (s, 1H), 2.40-2.12 (m, 6H), 2.00 (m, 2H), 1.54 (m, 2H), 0.95 (t, 3H); $^{13}\text{C NMR}$ (CDCl_3) δ 200, 167, 126, 41, 38, 30, 23, 20, 12.

LITERATURE CITED

1. Andrieux, C.; Bouchait, J.; Savéant, J., *J. Electroanal. Chem.*, **1978**, 88, 43.
2. House, H., “*Modern Synthetic Reactions*”, W.A. Benjamin Inc. Philippines, **1972**.
3. Schlesener, C.; Amatore, C.; Kochi, J., *J. Am. Chem. Soc.*, **1984**, 106, 7472.
4. Bordwell, F.; Cheng, J., *J. Am. Chem. Soc.*, **1989**, 111, 1792.
5. (a) Review: Holm, T. *Acta Chem. Scand., Ser. B.* **1983**, 37, 567; See also Holm, T. *Acta Chem. Scand.*, **1991**, 45, 925; Holm T. and Madsen, J., *Acta. Chem. Scand.*, **1992**, 46, 985; Holm, T. *J. Am. Chem. Soc.*, **1993**, 115, 916. (b) Lopp, I.G.; Buhler, J.D. and Ashby, E.C. *J. Am. Chem. Soc.*, **1975**, 97, 17; Ashby, E.C. and Goel, A.B., *J. Am. Chem. Soc.*, **1981**, 103, 4983. (c) Walling, C. *J. Am. Chem. Soc.*, **1988**, 110, 6846. (d) Yamataka, H.; Matsuyama, T. and Hanafusa, T. *J. Am. Chem. Soc.*, **1989**, 111, 4912. (e) Tanko, J.M. and Brammer, L.E. Jr. *J. Chem. Soc., Chem. Commun.*, **1994**, 1165. (f) Lund, T.; Pedersen, M.L. and Frandsen, L.A., *Tetrahedron Lett.*, **1994**, 35, 9225.
6. Vona, M.L.D. and Rosnati, V., *J. Org. Chem.*, **1991**, 56, 4269; Luchetti, L. and Rosnati, V., *J. Org. Chem.*, **1991**, 56, 6836.
7. (a) Ashby, E.C.; Argyropoulos, J.N. *J. Org. Chem.* **1986**, 51, 472. (b) Palmer, C.A.; Ogle, C.A. and Arnett, E.M., *J. Am. Chem. Soc.* **1992**, 114, 5619; Arnett, E.M. and Palmer, C.A., *J. Am. Chem. Soc.*, **1990**, 112, 7354.
8. Yamataka, H.; Nagareda, K.; Takatsuka, T.; Ando, K.; Hanafusa, T. and Nagase, S. *J. Am. Chem. Soc.*, **1993**, 115, 8570.
9. Ashby, E.C.; Goel, A.B. and Argyropoulos, J.N., *Tetrahedron Lett.*, **1982**, 23, 2273; Ashby, E.C. and Argyropoulos, J.N., *J. Org. Chem.* **1986**, 51, 3593.
10. (a) Yamataka, H.; Kawafuji, Y.; Nagareda, K.; Miyano, N. and Hanafusa, T., *J. Org. Chem.*, **1989**, 54, 4706. (b) Rein, K.S.; Chen, Z.H.; Perumal, P.T.; Echegoyen, L. and Gawley, R.E., *Tetrahedron Lett.*, **1991**, 32, 1941.
11. (a) Scott, L.T.; Carlin, J. and Schultz, T.H., *Tetrahedron Lett.*, **1978**, 22, 4637. (b) Ashby, E.C.; Goel, A.B. and Depriest, R.N., *Tetrahedron Lett.*, **1981**, 22, 4355. (c) Newcomb, M. and Burchill, M.T., *J. Am. Chem. Soc.* **1984**, 106, 8276.
12. Tanner, D.D.; Singh, H.K.; Kharrat, A. and Stein A.R., *J. Org. Chem.*, **1987**, 52, 2142; Tanner, D.D. and Stein A.R., *J. Org. Chem.*, **1988**, 53, 1642; Tanner, D.D. and Chen, J.J., *J. Org. Chem.*, **1989**, 54, 3842.
13. Tanner, D.D. and Yang, C.M., *J. Org. Chem.*, **1993**, 58, 5907.
14. Tanner, D.D.; Diaz, G.E. and Potter, A., *J. Org. Chem.*, **1985**, 50, 2149.
15. Yang, D. and Tanner, D.D., *J. Org. Chem.*, **1986**, 51, 2267.
16. Berger, D.J.; Tanko, J.M. in “*Supplement A3: The chemistry of double-bonded functional groups*,” Patai, S., Ed, Wiley: **1997**, pp 1281-1354.
17. Molander, G.A. *Chem Rev.*, **1992**, 92, 29.; Kagan, H.B. and Namy, J.L., *Tetrahedron*, **1986**, 42, 6573.

-
18. (a) Bard, A. and Faulkner, L.; “*Electrochemical Methods*”, Wiley:New York, **1980**; (b) Baizer, M.M. in “*Organic Electrochemistry, An Introduction and a Guide*”, 3rd. ed., Lund, H. and Baizer, M.M. eds., Marcel Decker : New York, **1991**, pp. 433-464.
19. (a) Andrieux, C.P.; Hapiot, P.; and Savéant, J.M., *Chem Rev.* **1990**, *90*, 723. (b) Lund, T. and Lund, H. *Acta Chem Scand., Ser. B*, **1986**, *40*, 470; Daasbjerg, K.; Pedersen, S.U., and Lund, H. *Acta Chem. Scand.*, **1991**, *45*, 424.
20. (a) Ward, H.; Lawler, R. and Cooper, R. *J. Am. Chem. Soc.* **1969**, *91*, 746. (b) Lepley, R. and Landau, R., *J. Am. Chem. Soc.*, **1969**, *91*, 748. (c) Russell, G. and Larson, D., *J. Am. Chem. Soc.* **1969**, *91*, 3967.
21. Russel, G.A.; Janzen, E.G.; Stron, E.T., *J. Am. Chem. Soc.*, **1964**, *64*, 1807.
22. Ashby, E.C.; Goel, A.B.; Depriest, R.N., *J. Am. Chem. Soc.* **1980**, *102*, 7780.
23. House, H.O.; Chu, C.Y., *J. Org. Chem.*, **1976**, *41*, 3083.
24. Okubo, M. *Bull. Chem. Soc. Jpn.*, **1975**, *48*, 1057.
25. Ebersson, L., “*Electron Transfer Reactions in Organic Chemistry.*” Springer-Verlag: **1987**.
26. “*Linear Sweep and Cyclic Voltammetry*”, Parker, V.D., in “*Comprehensive Chemical Kinetics, Vol. 26, Electrode Kinetics: Principles and Methodology*”, Bramford, C.H.; Compton, R.G., Eds. Elsevier:New York **1986**, pp.145-202.
27. Espenson, J. H., “*Chemical Kinetics and Reaction Mechanisms*”, McGraw Hill:New York **1981**, pp-182-190.
28. Gilbert, A.; Baggott, J., “*Essentials of Molecular Photochemistry*”, CRC Press:Boston **1991**, pp.182-188.
29. Newcomb, M.; Burchill, M. *J. Am. Chem. Soc.* **1984**, *106*, 8276.
30. House, H.O.; Prabhu, A.V.; Wilkins, J.M.; Lee, L.F., *J. Org. Chem.*, **1976**, *41*, 3067.
31. Tanner, D.D.; Stein, A.R., *J. Org. Chem.*, **1988**, *40*, 1642.
32. Tanner, D.D.; Chen, J.J.; Chen, L., and Luelo, C., *J. Am. Chem. Soc.*, **1991**, *113*, 8074.
33. Wipf, D.O. and Wightman, R.M., *J. Phys. Chem.*, **1989**, *93*, 4286.
34. Andrieux, C.P.; Savéant, J.M. and Zann, D. *Nouv. J. Chim.* **1984**, *7*, 107.
35. Andrieux, C.P.; Hapiot, P. and Savéant, J.M., *J. Phys. Chem.* **1988**, *92*, 5987.
36. Sucheta, A. and Rusling, J.F. *J. Phys. Chem.* **1989**, *93*, 5796.
37. Aalstad, B. and Parker, V.D. *Acta Chem. Scand.* **1982**, *B36*, 47.
38. Nadjo, L. Savéant, J.M. *J. Electroanal. Chem.* **1971**, *30*, 41.
39. Yamataka, H.; Yamaguchi, K.; Takatsaka, T.; Hanafusa, T. *Bull. Chem. Soc. Jpn.* **1992**, *65*, 1157.
40. (a) Neckers, D.C.; Schaap, A.P.; Hardy, J. *J. Am. Chem. Soc.*, **1966**, *88*, 1265; Neckers, D.C. *Tetrahedron. Lett.* **1965**, 1889. (b) Pereyre, M.; Godet, J.Y. *Tetrahedron Lett.* **1970**, 3653.; Godet,

-
- J.Y.; Pereyre, M. *J. Organomet. Chem.* **1972**, *40*, C23. Godet, J.Y.; Pereyre, M.; Pommier, J.C.; Chevolleau, D., *J. Organomet. Chem.* **1973**, *55*, C15. (c)Shiota, H.; Ohkata, K.; Hanafusa, T. *Chem. Lett.* **1974**, 1153.; (d) Miyaura, N.; Itoh, M.; Sasaki, N.; Suzuki, A. *Synthesis*, **1975**, *5*, 317.; (e) Bagnell, L; Meisters, A.; Mole, T. *Aust. J. Chem.* **1975**, *28*, 821.; (f) House, H.O.; Weeks, P.D. *J. Am. Chem. Soc.* **1975**, *97*, 2778. (g) Loots, M.; Dayrit, F.; Schwartz, J.. *Bull. Soc.Chim Beig.*, **1980**, *89*, 897. (h) Jullien, R.; Stahl-Lariviere, H.; Zann, D.; Nadjjo, L. *Tetrahedron*, **1981**, *37*, 3159.; (i) Chung, S.K. *J.Org. Chem.* **1981**, *46*, 5457.; Chung, S.K. Dunn, L.B., Jr., *J.Org. Chem.* **1984**, *49*, 935.; (j) Hwu, J. *J. Chem Soc., Chem Commun.*, **1985**, *8*, 452.; (k) Russell, G.A.; Dedolph, D.F., *J.Org. Chem.* **1985**, *50*, 2378.; (l) Meinhart, J.; Grubbs, R. *Bull. Chem. Soc. Jpn.* **1988**, *61*, 171. (m) Castellino, A.J.; Bruce, T.C. *J. Am. Chem. Soc.* **1988**, *110*, 1313.; (n) Zelechonok, Y.; Silverman, R.B. *J.Org. Chem.* **1992**, *57*, 5785.; (o) Vedejs, E.; Duncan, S.M.; Haight, A. R. *J.Org. Chem.* **1993**, *58*, 3056.
41. (a) Wilt, J.W. in *“Free Radicals, Vol.I,”* Kochi, J.K., Ed., Wiley: **1973**, pp.334-501. (b) Beckwith, A.L.J.; Ingold, K.U. in *“Rearrangements in Ground and Excited States, Vol. I,”* DeMayo, P., Ed., Academic Press: **1980**, pp. 161-310.
42. Griller, D.; Ingold, K.U. *Acc. Chem. Res.* **1980**, *13*, 317.
43. (a) Neidig, P.; Sun, S. *J. Org. Chem.* **1969**, *34*, 1854.; (b) Breuer, E.; Segall, E.; Stein Y.; Sarel, S. *J. Org. Chem.* **1972**, *37*, 2242.; (c) Blumbergs, P.; LaMontagne, M.; Stevens, J. *J. Org. Chem.* **1972**, *37*, 1248.; (d) Hall, S.; Sha, C.; Jordan, F. *J. Org. Chem.* **1976**, *41*, 1494 ; (e) Nishida, S.; Kataoka, F. *J. Org. Chem.* **1978**, *43*, 1612.; (f) Krapcho, A.; Seidman, D. *Tetrahedron Lett.*, **1981**, 179.; (g) McCormick, J.; Fitterman, A.; Barton, D., *J. Org. Chem.* **1981**, *46*, 4708.; (h) Degueil-castaing, m.; Rahm, A. *J. Org. Chem.* **1986**, *51*, 1672.
44. Tanko, J.M.; Drumright, R.E. *J.Am. Chem. Soc.* **1990**, *112*, 5362.
45. (a) Maillard, B.; Forrest, D.; Ingold, K. U. *J.Am. Chem. Soc.* **1976**, *98*, 7024.; (b) Kinney, R.J.; Jones, R.D.; Bergman, R.G. *J.Am. Chem. Soc.* **1978**, *100*, 7902.; (c) Beckwith, A.L.J.; Moad, G. *J.Chem. Soc., Perkin Trans 2*, **1980**, 1473.; (d) Mathew, L.; Warketin, J. *J.Am. Chem. Soc.* **1986**, *108*, 7981.; (e) Beckwith, A.L.J.; Bowry, V.W.; Moad, G.J. *J. Org.Chem.*, **1988**, *53*, 1632.; (f) Newcomb, M.; Glenn, A.G. *J.Am. Chem. Soc.* **1989**, *111*, 275.; (g) Beckwith, A.L.J.; Bowry, V.W. *J. Org.Chem.*, **1989**, *54*, 2681.
46. Tanko, J.M.; Drumright, R.E. *J.Am. Chem. Soc.* **1992**, *114*, 1844.
47. Tanko, J.M.; Drumright, R.E.; Suleman, N.K.; Brammer, L.E., Jr. *J.Am. Chem. Soc.* **1994**, *116*, 1785.
48. Tanner, D.D.; Chen, J.J.; Luelo, C.; Peters, P.M. *J.Am. Chem. Soc.* **1992**, *114*, 713.
49. Tanko, J.M.; Brammer, L.E., Jr., Hervas', M.; Campos, K. *J. Chem. Soc. Perkin Trans. 2.*, **1994**, 1407.
50. Tanko, J.M.; Brammer, L.E., Jr. *J. Chem. Soc., Chem Commun.* **1994**, 1165.
51. Volkenburg, R.V.; Greenlee, K.W.; Derfer, J.M.; Boord, C.E., *J.Am. Chem. Soc.* **1949**, *71*, 3595.
52. Norin, T. *Acta Chem. Scand.* **1965**, *19*, 1289.
53. Dauben, W.G.; Deviny, E.J., *J. Org. Chem.*, **1966**, *31*, 3794.
54. House, H.O.; Blankley, C.J. *J. Org. Chem.*, **1968**, *33*, 47.
55. Fraisse-Jullien, R.; Frejaville, C. *Bull. Soc. Chim. Fr.* **1968**, 4449.

-
56. Russell, G.A.; Malkus, H. *J. Am. Chem. Soc.*, **1967**, *89*, 160.
57. Mandell, L.; Johnson, J.C.; Day, R.A., Jr., *J. Org. Chem.*, **1978**, *43*, 1616.
58. Andrieux, C. P.; Savéant, J. M. in *Investigations of Rates and Mechanisms of Reactions, Part II*; Bernasconi, C., Ed.; Wiley, New York, 1986, pp. 305-390.
59. Saveant, J.M. in "Advances in Electron Transfer Chemistry Vol. 4.," Jai Press:Greenwich, **1994**, pp 53-116.
60. For $1^{\bullet-}$, $k_C = k_1$; $2^{\bullet-}$, $k_C = k_1 + k_2$; $3^{\bullet-}$, $k_C = k_1 + k_3$.
61. Nadjo, L.; Savéant, J. M. *Electroanal. Chem. Interfacial Electrochem.* **1973**, *48*, 113
62. Rosanske, T.W. and Evans, D. H. *J. Electroanal. Chem.* **1976**, *72*, 277.
63. This assignment is supported by the following experiment: The cyclic voltammogram of the phenolate anion derived from 2,4,6-tri-*t*-butylphenol (generated with potassium *t*-butoxide in the presence of 18-crown-6) is characterized by a completely reversible oxidation wave with $E^{\circ} = -680$ mV vs. 0.1 M Ag^+/Ag .
64. Beckwith, A. L. J.; Bowry, V. W. *J. Org. Chem.* **1989**, *54*, 2681.
65. (a) Andrieux, C. P.; Blocman, C.; Dumas-Bouchiat, J. M.; M'Halla, F.; Savéant, J. M. *J. Electroanal. Chem.* **1980**, *113*, 12. (b) Savéant, J. M.; Su, K. B. *J. Electroanal. Chem.* **1985**, *196*, 1. (c) Andrieux, C. P.; Hapiot, P.; Savéant, J. M. *Chem. Rev.* **1990**, *90*, 723.
66. Garst, J. F. In : Kochi, J. K., Ed. *Free Radicals*, Wiley: Chichester **1972**, Vol1, p. 520; Pedersen, S. U.; Lund, T. *Acta Chem. Scand.* **1991**, *45*, 397.
67. Nadjo, L.; Savéant, J. M.; Su, K. B. *J. Electroanal. Chem.* **1985**, *196*, 23.
68. DigiSim 2.1, Bioanalytical Systems Inc., 2701 Kent Avenue, W. Lafayette, IN 47906, USA.
69. TableCurve 2D, Jandel Scientific Software, 2591 Kerner Blvd., San Rafael, CA 94901, USA.
70. (a) Marcus, R. A. *J. Chem. Phys.* **1956**, *24*, 966. (b) Marcus, R. A. *Faraday Discuss. Chem. Soc.* **1960**, *29*, 21. (c) Marcus, R. A. *Ann. Rev. Phys. Chem.* **1964**, *15*, 155. (d) Marcus, R. A. *J. Chem. Phys.* **1965**, *43*, 679. (e) Marcus, R. A. *Faraday Discuss. Chem. Soc.* **1982**, *74*, 7. (f) For an excellent review see ref. 72.
71. Andrieux, C. P.; Savéant, J.-M. *J. Electroanal. Chem.* **1986**, *205*, 43.
72. Ebersson, L. *Electron Transfer Reactions in Organic Chemistry*, Springer-Verlag, Berlin, 1987, pp. 25-34.
73. Phillips, J.P.; Gillmore, J.G.; Swartz, P.; Brammer, L.E. Jr.; Berger, D.J. and Tanko, J.M., *J. Am. Chem. Soc.* **1998**, *120*, 195.
74. (a) Tidwell, T. T. in *The Chemistry of the Cyclopropyl Group*, Rappoport, Z., Ed., Wiley: New York, 1987, pp. 565-632. (b) Clark, T.; Spitznagel, G. W.; Klose, R.; Schleyer, P. v. R. *J. Am. Chem. Soc.* **1984**, *106*, 4412.

-
75. Similar hyperconjugative interactions involving the out-of-plane C-H bonds in the cyclohexadienyl radical manifest themselves as an extraordinarily high a_H of 48 G in the EPR spectrum. (Devolder, P.; Goudmand, P. *C. R. Seances. Acad. Sci. Ser. A* **1975**, 280, 1281.
76. For a series of representative cyclopropane derivatives, PM3 was found to accurately reproduce experimentally determined ΔH_f° 's with an average error of ± 4 kcal/mol. Details are provided in section 2.4.
77. Bordwell, F. G.; Liu, W.-Z. *J. Am. Chem. Soc.* **1996**, 118, 10819.
78. Tsang, W. in *Energetics of Organic Free Radicals*, Simões, J. A. M.; Greenberg, A.; Liebman, J. F., Eds., Blackie Academic and Professional: London, 1996, pp. 22-58.
79. Bordwell, F. G.; Cheng, J.-P.; Ji, G.-Z.; Satish, A. V.; Zhang, X. *J. Am. Chem. Soc.* **1991**, 113, 9790.
Bordwell, F. G.; Zhang, X.-M. *Acc. Chem. Res.* **1993**, 26, 510.
80. Fuchs, R.; Hallman, J. H.; Perlman, M. O. *Can. J. Chem.* **1982**, 60, 1832.
81. Lacher, J. R.; Walden, C. H.; Lea, K. R.; Park, J. D. *J. Am. Chem. Soc.* **1950**, 72, 331.
82. Knowlton, J. W.; Rossini, F. D. *J. Res. NBS* **1949**, 43, 113.
83. Good, W. D.; Moore, R. T.; Osborn, A. G.; Douslin, D. R. *J. Chem. Thermodyn.* **1974**, 6, 303.
84. Kozina, M. P.; Timofeeva, L. P.; Gal'chenko, G. L.; Balenkova, E. S.; Ordubadi, M. D. *Moscow U. Chem. Bull.* **1984**, 25, 41.
85. Roth, W. R.; Adamczak, O.; Breuckmann, R.; Lennartz, H.-W.; Boese, R. *Chem. Ber.* **1991**, 124, 2499.
86. Volkenburg, R. Van; Greenlee, J.M.; Derfer, J.M. and Boord, C.E., *J. Am. Chem. Soc.* **1949**, 71, 3595.
87. Norin, T., *Acta Chem. Scand.*, **1963**, 17, 738.; Norin, T. *Acta Chem. Scand.*, **1965**, 19, 1289.
88. Dauben, W.G. and Deviny, E.J. *J. Org. Chem.*, **1966**, 31, 3794.; Dauben, W.G. and Wolf, R.E. *J. Org. Chem.*, **1970**, 35, 374.
89. Molander G. and McKie, J.A., *J. Org. Chem.*, **1991**, 56, 4112.
90. Batey, R.A. and Motherwell, W.B. *Tetrahedron, Lett.*, **1991**, 32, 6649.
91. Imamoto, T.; Hatajima, T. Yoshizawa, T., *Tetrahedron Lett.*, **1994**, 35, 7805.
92. Mairanovskii, S.G.; Kosycheno, L.I.; Kudryavtsev, R.V. *Elektrokhimiya*, **1979**, 15, 1240.
93. Semiempirical MO calculations were performed using the AM1 approximation (M. J. S. Dewar, E. G. Zoebisch, E.F. Healy and J.J.P. Stewart. *J. Am. Chem. Soc.* **1985**, 105, 3902) and implemented through Mopac 6.0 (QCPE, Program No. 439).
94. Kariv-Miller, E., and Mahachi, T. *J. Org. Chem.*, **1986**, 51, 1041.
95. Andrieux, C.P.; Gallardo, I; Savéant, J.M. *J. Am. Chem. Soc.* **1988**, 111, 1620..
Andrieux, C.P. and Saveant, J.M. *J. Electroanal. Chem.* **1989**, 267, 15.
96. Dauben, W. G. and Wolf, R.E. *J. Org. Chem.*, **1970**, 35, 374.

-
97. Occhialini, D.; Pedersen, S.U. and Lund, H. *Acta, Chem. Scand.*, **1990**, *44*, 715.
98. Andrieux, C.P.; Gallardo, I; Savéant, J.M. and Su, K. *J. Am. Chem. Soc.* **1986**, *108*, 638.
99. (a) Measured by kinetic EPR, $k = 2.2 \times 10^4 \text{ s}^{-1}$ (298 K), Ingold, K.U.; Maillard, B.; Walton, J.C. *J. Chem. Soc. Perkin Trans 2* **1981**, 970; (b) measured by the tin hydride method, $k = 5.0 \times 10^2 \text{ s}^{-1}$ (298 K), Beckwith, A.L.J.; Moad, G. *J. Chem. Soc. Perkin Trans. 2*, **1980**, 1083.
100. Andrieux, C.P.; Combellas, C.; Kanoufi, F.; Savéant, J.M. and Thiebault, A., *J. Am. Chem. Soc.* **1997**, *119*, 9527.
101. For a series of representative cyclopropane derivatives, PM3 was found to accurately reproduce experimentally determined ΔH_f° 's with an average error of ± 4 kcal/mol. Details are provided in section 2.4.
102. Tsang, W. in *Energetics of Organic Free Radicals*, Simões, J. A. M.; Greenberg, A.; Liebman, J. F., Eds., Blackie Academic and Professional: London, 1996, pp. 22-58.
103. Bordwell, F. G.; Cheng, J.-P.; Ji, G.-Z.; Satish, A. V.; Zhang, X. *J. Am. Chem. Soc.* **1991**, *113*, 9790. Bordwell, F. G.; Zhang, X.-M. *Acc. Chem. Res.* **1993**, *26*, 510.
104. Gassman, P.G.; Rasmy, O.M.; Murdock, T.O. and Saito, K. *J. Org. Chem.*, **1981**, *46*, 5457.
105. Stork, G.; Goldman, R.; Coomos, R.V. and Tsuji, J. *J. Am. Chem. Soc.* **1987**, *275*, 1965.
106. Yoon, U.C.; Kim, J.U.; Hasegawa, E. and Mariano, P.S. *J. Am. Chem. Soc.* **1987**, *109*, 442.
107. Parker, V.D. in *Topics in Organic Electrochemistry*; Fry, A.J.; Britton, W. eds. Plenum Press: New York, 1986, pp. 35-79.; Parker, V.D. in *Advances in Physical Organic Chemistry*, Vol.19; Gold, V., Bethell, D., eds, Academic Press: New York, pp.131.
108. Andrieu, C.P.; Blocman, C. Dumas-Bouchiat, M'Halla and Savéant, J.M., *J. Am. Chem. Soc.* **1980**, *102*, 3806.
109. Drumright, R., "Radical Anion Rearrangement. Aryl Cyclopropyl Ketyl Anions", Ph.D. Dissertation, 1991, Chapter 5, Virginia Polytechnic Institute and State University, Blacksburg, Virginia.
110. House, H. O.; Feng, E.; Pert, N. P. *J. Org. Chem.*, **1971**, *36*, 2371.
111. (a) Portnykh, N. V.; Volodkin, A. A.; Ershov, V. V. *Bull. Acad. Sci. USSR, Div. Chem. Sci.* **1966**, 2181. (b) Schwartz, L. H.; Flor, R. V. *J. Org. Chem.* **1969**, *34*, 1499. (c) Volodkin, A. A.; Belostotskaya, I. S.; Ershov, V. V. *Bull. Acad. Sci. USSR, Div. Chem. Sci.* **1967**, 1328. (d) Schwartz, L. H.; Flor, R. V.; Gullo, V. P. *J. Org. Chem.* **1974**, *39*, 219.
112. Tarkhanova, M. V.; Volod'kin, A. A.; Ershov, V. V.; Rasuleva, D. Kh.; Malievskii, A. D. *Bull. Acad. Sci. USSR Div. Chem. Sci. (Engl. Trans.)* **1968**, 2642.
113. Dauben, W.G. and Wolf, R.E. *J. Org. Chem.*, **1970**, *35*, 374.
114. Corey, E.J. and Chaykovsky, M., *J. Am. Chem. Soc.*, **1965**, *87*, 1353.
115. Hahn, R.C. and Jones, G.W. *J. Am. Chem. Soc.*, **1971**, *93*, 4232.

-
116. (a) Ng, Soon. *J. Chem. Soc. Perkin Trans. 2* **1972**, 1514. (b) Stillson, G. H.; Sawyer, D. W.; Hunt, C. K. *J. Am. Chem. Soc.* **1945**, 67, 303.
117. Plekhanova, L. G.; Nikiforov, G. A.; Ershov, V. V.; Zakharov, E. P. *Bull. Acad. Sci. USSR, Div. Chem. Sci.* **1973**, 819.
118. (a) Schwartz, L. H.; Flor, R. V. *J. Chem. Soc. Chem. Commun.* **1968**, 1129. (b) Spectroscopic data compared to those of an authentic sample from synthesis of **13a**.
119. Majetich, G.; Defauw, J. and Ringold, C. *J. Org. Chem.*, **1988**, 53, 50.

VITA

Janice Paige Phillips was born as Janice Paige Lilly on July 4, 1966 in Richmond, Virginia, where she lived until the age of 13. Raised by non-traditional parents, Ralph Henry Lilly (now deceased) and Leeda Grace Harper, she was nurtured and fortified with all those things necessary to succeed in life. At 14, she found herself in the Roanoke Va. area and ultimately graduated from Northside High School in 1983.

Paige briefly attended Towson State University in Maryland, but quickly opted for a working sabbatical. During this time she matured and returned to Roanoke College in 1989 as a more serious and dedicated student. Professor Ben Huddle and other faculty at Roanoke College converted her to chemistry and supported her love of research and other academic interests. At Roanoke College, Paige was the recipient of a scholarship and numerous awards.

During her stay at Roanoke College, Paige Lilly married Randy Phillips in 1990 and was blessed with the birth of her first child, Logan Marie in 1991. With the support of her new family, faculty and friends she graduated from Roanoke College, *cum laude*, in May 1993.

In the summer of 1993, Paige worked in the research group of Prof. James Tanko at Virginia Polytechnic Institute and State University and entered the doctoral program at Virginia Tech in the following fall. Paige continued to work in the area of physical organic chemistry under the supervision of Prof. Tanko and earned her Ph.D. in 1998. During her graduate work, she was blessed with the birth of her second child, Mason Brady. Paige assumed a postdoctoral position in the research labs of Prof. Judy Riffle in polymer synthesis at Virginia Polytechnic Institute and State University.